The Institute of Paper Chemistry

Appleton, Wisconsin

Doctor's Dissertation

The Use of a Char Pile Reactor to Study Char Bed Processes

Gregg W. Aiken

January, 1988

THE USE OF A CHAR PILE REACTOR TO STUDY CHAR BED PROCESSES

A thesis submitted by

Gregg W. Aiken

B.S. 1979, University of Wisconsin - Stevens Point

M.S. 1981, Lawrence University

in partial fulfillment of the requirements
of The Institute of Paper Chemistry
for the degree of Doctor of Philosophy
from Lawrence University
Appleton, Wisconsin

Publication rights reserved by
The Institute of Paper Chemistry

January, 1988

TABLE OF CONTENTS

	Page
ABSTRACT	1
INTRODUCTION	3
Background	3
Recovery Boilers	3
Black Liquor Burning in Recovery Boilers	3
Black Liquor Combustion	7
Char Burning	9
Char Composition	9
Potential Char Reactions	11
The Sulfate/Sulfide Cycle	12
Molar Balance of Char Combustion	14
Carbon-Sulfate Reaction	14
Other Sulfate Reduction Pathways	16
Direct Carbon Oxidation Reactions	17
Carbon Oxidation by Carbon Dioxide	18
Sulfide Oxidation Reaction	18
Importance of the CO/CO_2 Ratio	19
Previous Char Combustion Studies	19
Smelt Pool Reactor Studies	19
Single Particle Reactor Studies	20
Char Pile Reactor	20
THESIS OBJECTIVES	22
Research Outline	22
EXPERIMENTAL	24
Experimental Apparatus	24

Description 24

Impingement Geometry Characteristics 26

Data Collected 28

Temperature 28

Exhaust Gas CO, CO_2 and O_2 Concentrations 29

Supply Gas Flow Rates 30

Set Point Temperature 30

Char Sampling and Analysis 31

Total Elemental Analysis 31

Sulfur-Species Analyses 32

Fixed-Carbon Determination 33

Char Sampling Regions - Char Surface Morphology 34

Preliminary Nitrogen-Atmosphere Experiments 37

Initial Char Preparation Procedure 37

Initial Nitrogen-Atmosphere Experiment 37

Effect of Nitrogen-Atmosphere Handling 42

Effect of Extended Pyrolysis Time 44

Subsequent Pyrolysis Experiments 44

Effect of Sulfate-Loading the Black Liquor 45

Modified Char Preparation Procedure 47

RESULTS AND DISCUSSION 48

The CO/CO_2 Product of the Carbon-Sulfate Reaction 48

Description 48

Results 50

The CO/CO_2 Product of Char Burning 53

Gas-Phase Oxidation of Carbon Monoxide 53

Char Burning Experiments 56

Description 56

Examples 57

Results 61

Smelt/Char Wettability 62

Char Burning Rate 64

Description 64

Examples 65

Theoretical Analysis 69

Results 70

Sulfur-Species Analysis Results 70

Char Burning Rates 73

Theoretical Analysis - Kinetic Model 74

Mass Transfer Model 76

Char Burning Rate - Results Summary 78

Conceptual Model of Char Pile Burning 82

Implications 84

RECOMMENDATIONS 86

CONCLUSIONS 87

ACKNOWLEDGMENTS 89

LITERATURE CITED 90

APPENDIX I. MOLAR BALANCE OF CHAR COMBUSTION 92

APPENDIX II. CALCULATION OF THE RELATIVE SIGNIFICANCE OF CO_2 REDUCTION BY CARBON 94

APPENDIX III. EXPERIMENTAL APPARATUS SPECIFICATIONS 96

APPENDIX IV. REYNOLDS NUMBER CALCULATION 97

APPENDIX V. RADIATION-SHIELDED THERMOCOUPLE 99

APPENDIX VI. RESPONSE TIMES OF GAS ANALYZERS 100

APPENDIX VII. SUPPLY GAS SYSTEM 104

APPENDIX VIII. MASS FLOWMETER CALIBRATIONS 105

APPENDIX IX. DATA MANIPULATION FOR PYROLYSIS EXPERIMENTS 8 AND 15 107

APPENDIX X. CALCULATION OF INITIAL C/SO_4 OF EXPERIMENT 17 110

APPENDIX XI. CALCULATION OF INITIAL C/O FOR CO/CO_2 PRODUCT OF THE CARBON-SULFATE REACTION STUDIES 112

APPENDIX XII. ESTIMATION OF THE PORE SIZE FROM THE PARTICLE SIZE DISTRIBUTION 114

APPENDIX XIII. GRAPHIC RESULTS OF CHAR BURNING RATE EXPERIMENTS 115

APPENDIX XIV. DETERMINATION OF THE CARBON CONCENTRATION UPON WHICH TO BASE THE REACTION RATE CALCULATIONS FOR KINETICALLY-LIMITED CONDITIONS 124

APPENDIX XV. KINETIC MODEL CALCULATIONS 126

APPENDIX XVI. CALCULATION OF THE REDUCTION RATIO AT THE CHAR/SMELT INTERFACE 127

ABSTRACT

A study of pile burning of kraft black liquor char was carried out in a laboratory reactor in which an O_2/N_2 jet impinged vertically on the char surface. All data were consistent with the sulfate/sulfide cycle theory of char burning where the heterogeneous reaction between oxygen and char carbon is achieved by the oxidation of sulfide to sulfate and the reduction of sulfate by carbon.

One major focus of this study was to determine the CO/CO_2 product of char burning. This was approached in two steps: determining the CO/CO_2 product of the carbon-sulfate reaction and determining the CO/CO_2 product of char burning. The CO/CO_2 product of the carbon-sulfate reaction was found to be a linear function of the elemental C/O ratio as represented by:

$$CO/CO_2 = 0.403\ C/O$$

At 1033 to 1113°K, temperature did not affect the CO/CO_2 product. The oxygen of the sulfate supplied at least 88% of the elemental oxygen for carbon oxidation with the remainder supplied by oxygen sorbed by the char during sample preparation.

The CO/CO_2 product of char burning was determined to be principally CO for the impingement of a laminar, oxygen-containing jet on the char surface. The CO/CO_2 ranged from 4 to 24 at 1000 to 1150°K and 2.1 to 10.5% oxygen. In order to determine this CO/CO_2 representative of the heterogeneous reaction between char carbon and oxygen, the contribution of the gas-phase oxidation of CO to CO_2 was quantified. When significant concentrations of CO_2 were measured in the exhaust gases, this gas-phase oxidation reaction was a major source of CO_2.

The char burning rate was found to be controlled by the oxygen mass transfer rate at temperatures > 1150°K with 2.1 to 10.5% O_2. At lower temperatures, both oxygen mass transfer and carbon-sulfate kinetics affected the rate.

The smelt product of char burning accumulated on the char surface; it did not percolate through the char pile. This was apparently caused by the inability of the smelt to wet the char. This may be a general characteristic of char pile burning.

INTRODUCTION

BACKGROUND

Recovery Boilers

The recovery boiler in the kraft recovery process functions as both a steam generator and a chemical recovery unit. The black liquor is burned to recover the heating value of its organic portion. The inorganic compounds that flow out of a recovery boiler as smelt are principally Na_2CO_3 and Na_2S. The Na_2CO_3 requires further processing to regenerate the kraft pulping liquor.

Recovery boilers are very expensive. Economies of scale dictate that new boilers be enormous. Because of these factors, many mills expand all other parts of the operation until production is limited by the size of the boiler. Any research that leads to a better understanding of kraft black liquor burning could result in improved operation of existing, or improved design of future, black liquor combustion systems and thus have a direct impact on paper mill profitability.

Black Liquor Burning in Recovery Boilers

Black liquor burning in recovery boilers is a complex process due to several factors. First of all, the water content of the liquor is typically 30 to 35%. Secondly, the black liquor has a high inorganic salt content. Thirdly, the sulfur species in the inorganic salts flowing out of the recovery boiler as smelt should be obtained in the sulfide form.

Figure 1 is a schematic of a typical recovery boiler. Black liquor is sprayed into a recovery boiler ten to twenty feet above the hearth of the unit. This allows sufficient time for its water content to evaporate before the solids

reach the char bed in the hearth zone. The black liquor solids are then pyrolyzed forming combustible gases and a char residue. This char is then combusted, burning the rest of the organic portion of the black liquor. The remaining inorganic salts flow out of the unit. The split between the in flight versus char bed location for pyrolysis and char burning varies from boiler to boiler depending upon operating conditions.

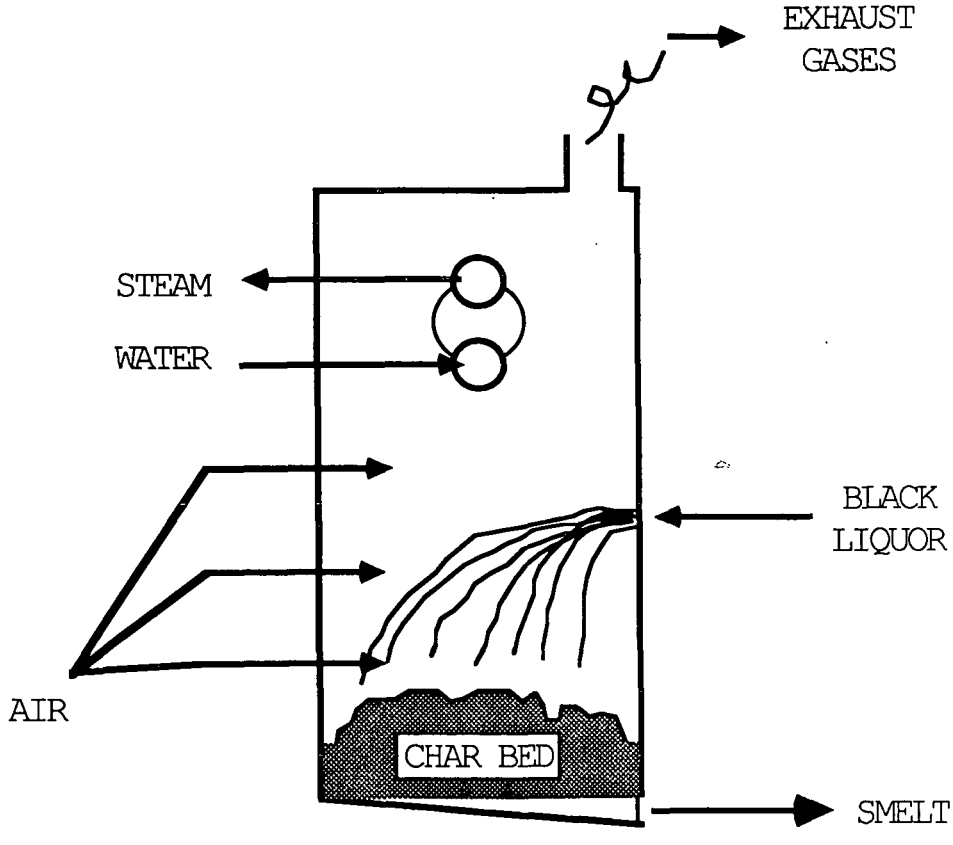

Figure 1. Recovery boiler schematic.

Combustion air is supplied at one or two levels below the liquor guns and at another level above the guns. The strong updraft of combustion gases and inert gas (the nitrogen in the air) entrains a portion of the black liquor. The proportioning of the combustion air affects the location of the exothermic oxidation reactions and thus the temperature distribution in the furnace. The amount of oxygen supplied to the hearth zone may also affect the sulfate/sulfide

split in the smelt flowing out of the recovery boiler. To reduce dead load in the recovery system, it is desirable to have a high level of sulfide in the smelt. The recovery boiler is the only place in the kraft recovery cycle where this active pulping chemical is generated.

The most extensive published char bed sampling data were reported by Richardson.[1,2] He found that the carbon content of the bed surface was in the 5 to 11% range. Borg reported a carbon content of 5%, with 8% measured in cold spots.[3] Compositional analyses of the char beds of two boilers reported by Richardson are given in Table 1.[2] When reviewing these measurements, sampling limitations must be considered.

Table 1. Char bed compositional analyses reported by Richardson[2] (as weight percent).[a]

	Weyerhaeuser (10/12/77)		Westvaco (11/17/77)	
	"Fines"[b]	Bed	"Fines"	Bed
Na_2CO_3	60.3	57.8	80.7	81.7
Na_2SO_4	7.1	1.8	5.6	1.5
Na_2S	7.7	16.7	3.9	6.3
$Na_2S_2O_3$	5.5	2.3	2.6	3.8
Na_2SO_3	0.6	0.3	0.1	0.2
C	10.7	7.5	7.1	6.5
Total accounted	91.9	86.4	100.0	100.0

[a]The values listed are averages of several samples. The Weyerhaeuser fines and bed values and the Westvaco fines and bed values are averages of 7, 3, 3, and 2 different samples, respectively.
[b]The "fines" sample was the material falling on the bed surface.

First, access is only at the periphery of a boiler so sampling in the center of the char bed is quite difficult. Therefore sampling results are skewed toward the composition at the edges of the bed. Since the air ports are located near the periphery of the char bed (in fact, most samples were removed through these air ports), the samples should be more highly oxidized than the average char bed composition. Secondly, long pipes have been used to obtain core samples. It is difficult to ascertain how far into the char bed the sampler has been rammed due to poor visibility and pipe deflection caused by the high temperatures. Thirdly, reactions will continue after a sample has been collected until it has cooled. Therefore, the carbon content of the char sample may be lower than that of the char bed.

Richardson obtained these data using an "inerting" sampler.[2] Nitrogen gas was circulated in the sample chamber as soon as the cover was closed over the sampling apparatus. The purging of nitrogen continued as the apparatus was removed from the furnace. The sample was then placed in a can that was also purged with nitrogen. Char bed samples were obtained at several locations, including "fines" samples. The "fines" were collected by placing the sampler on the char bed surface and allowing the char to rain into the sampler.

I converted the average char bed composition, reported in Table 1, from weight percent to mole percent (Table 2). The molar analysis shows that Na_2CO_3 and fixed-carbon are the main char bed species. The fixed-carbon is the insoluble carbon present in the char. Pyrolysis converts a portion of the organic carbon into this highly-condensed carbon. The carbonate fraction of the carbon is soluble, as are the unpyrolyzed carbonaceous species that have not yet been "fixed." The weight percent did not total 100% for the Weyerhaeuser samples.

This could be due to the presence of unpyrolyzed carbon or perhaps K or Cl. The analyses of the measured compounds may have been inaccurate. The mole percents were calculated assuming the compounds analyzed were the only species present.

Table 2. Char bed relative molar analyses calculated from Richardson's data (mole%).

	Weyerhaeuser (10/12/77)		Westvaco (11/17/77)	
	"Fines"	Bed	" Fines"	Bed
Na_2CO_3	35	39	52	54
Na_2SO_4	3	1	3	1
Na_2S	6	15	3	6
$Na_2S_2O_3$	2	1	1	2
Na_2SO_3	--	--	--	--
C	54	44	41	38
Total	100	100	100	100

There are significant differences between the "fines" samples and the "bed" samples. The carbon content of the "fines" landing on the char bed were higher than those of the char bed samples obtained at the same location. Up to 15.5 wt.% C was reported in the "fines" samples. The sulfur-species of the "fines" were much more oxidized than those of the bed samples. This suggests that a significant amount of sulfate reduction to sulfide is occurring in the bed.

Black Liquor Combustion

Black liquor combustion is the burning of black liquor yielding the combustion gas and inorganic salt products. Three basic stages are involved in black liquor combustion: drying, volatiles burning, and char burning, see Fig. 2.

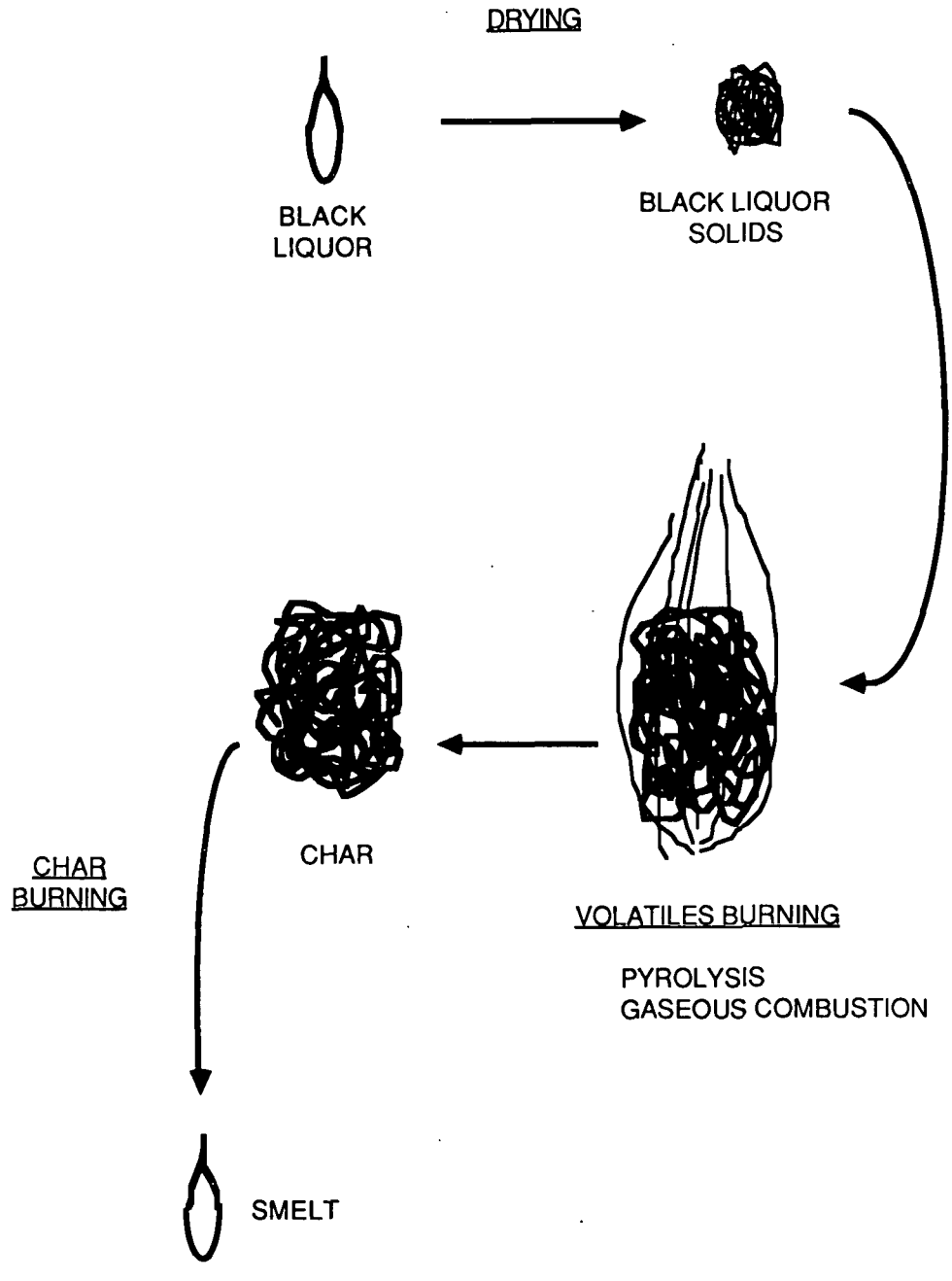

Figure 2. Black liquor combustion steps.

During the drying stage, the water content of the black liquor is evaporated. The volatiles burning stage involves two distinct processes: pyrolysis of the black liquor solids and gaseous combustion of the pyrolytic gases. Pyrolysis reactions are the heat-induced reactions of organic compounds yielding

combustible gases and a char residue. The gaseous combustion of the volatile gases will occur spontaneously if an adequate oxygen supply is available. If sufficient oxygen is not available, the location of volatile combustion can be far-removed from the location of pyrolysis. Char burning is the final stage in black liquor combustion. In this stage, the char residue of pyrolysis is converted to the combustion gases and smelt, the remaining inorganic salts. Char burning will not commence until pyrolysis is nearly complete, because the pyrolytic gases limit oxygen access to the char residue.

Char Burning

Char Composition

Char composition and the composition of the material landing on the char bed are not identical. Char is the product of a fundamental step of black liquor combustion whereas the char bed is simply a physical location in the furnace. Some pyrolysis may be occurring in the char bed as well as char burning. Some char burning may be occurring in flight so the char may be partially combusted when it reaches the char bed. The char compositions presented in this section are for chars produced in the laboratory from commercial black liquor samples.

Cameron reported the kraft char elemental composition listed in Table 3.[4] Grace converted this elemental analysis to the inorganic compound and char carbon compositions given in Table 4 by using the inorganic salt analyses of the char.[5] He assumed that the elements left over after accounting for all the elements in the inorganic salts were part of the "char carbon," the organic component of the char.

Table 3. Char elemental analysis.

	Weight Percent
Carbon, C	29.4
Hydrogen, H	0.7
Oxygen, O	33.8
Sulfur, S	2.1
Chlorine, Cl	0.6
Potassium, K	3.4
Sodium, Na	26.0

Table 4. Calculated relative molar analysis.

Inorganics	Moles/Mole Na_2
Na_2CO_3	0.91
Na_2S	0.045
Na_2SO_4	0.045
K_2CO_3	0.08
Char Carbon	
C	3.34
H	1.15
O	0.59
S	0.03

Grace then used a series of assumptions to obtain the simplified char and smelt compositions in Table 5.[5] Fixed-carbon is the dominant char species.

Table 5. Simplified char and smelt compositions: (moles/mole Na_2).

	Char	Smelt
Na_2S	1/6	19/60
Na_2SO_4	1/6	1/60
Na_2CO_3	2/3	2/3
C	3	1/12
H	1	--

The main difference between the laboratory char and the char bed composition results is that the fixed-carbon concentration is higher in the laboratory samples. There are three possible reasons for this difference:

- The char landing on the char bed is partially combusted in flight.
- The char sample removed from the bed has already been partially combusted in the bed.
- The fixed-carbon was partially combusted while the char cooled after sampling.

All three factors are probably significant.

Potential Char Reactions

There are three potential sources of the oxygen required for fixed-carbon combustion of laboratory chars:

- the oxygen in oxidized sulfur species, such as sulfate ($SO_4^=$), sulfite ($SO_3^=$), thiosulfate ($S_2O_3^=$), and other polysulfates ($S_xO_y^=$)
- the oxygen sorbed by the char during handling
- the oxygen supplied by the combustion air

Char reactions involve either the reaction of these oxygen sources with carbon or the formation of some of these oxygen sources upon exposure to combustion air.

The Sulfate/Sulfide Cycle

Grace suggested that the sulfate/sulfide cycle, shown in Fig. 3, is the primary means of fixed-carbon oxidation for kraft char.[6] Oxygen in the combustion air reacts with the sulfide to form sulfate. The sulfate then reacts with carbon forming sulfide and CO and/or CO_2. A number of different investigations were cited supporting the sulfate/sulfide cycle hypothesis.

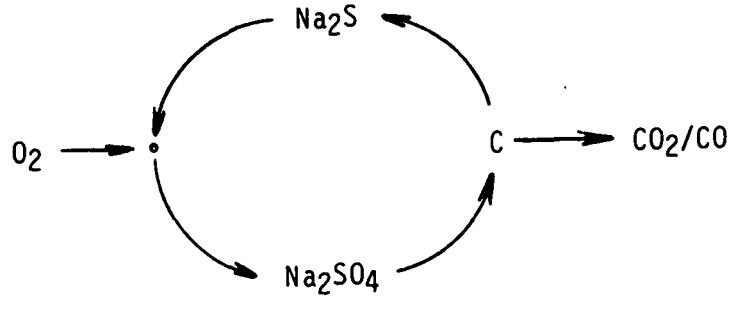

Figure 3. The sulfate/sulfide cycle.

First, the rate of carbon burning for kraft char, soda char, and graphite in a carbonate melt was studied by Cameron.[7] Oxygen/nitrogen mixtures were bubbled through the melt. The reaction was much faster for kraft char, which suggested that the presence of sulfur greatly affected the rate. A comparison of

the rate equation for kraft char burning developed by Cameron in this study to the rate equation he developed for the carbon-sulfate reaction with kraft char as the carbon source revealed that the rate equations were identical. For the smelt pool reactor conditions used, the rate of kraft char burning was controlled by the sulfate/sulfide cycle.

A second experimental observation supporting the sulfate/sulfide cycle hypothesis was obtained using a single particle reactor to study black liquor burning. A dried black liquor sample was pressed onto a microbalance wire then pyrolyzed by directing hot nitrogen gas past the pellet. Char burning commenced when hot O_2/N_2 mixtures replaced the nitrogen flow. The mass of the sample decreased throughout the run as char burning proceeded. At the end of the run, there was an increase in mass for the kraft char but not for the soda char. This mass increase for kraft char was interpreted as sulfide oxidizing to sulfate once the carbon was depleted. An increase in mass at the end of the experiment was not seen for the soda char runs. Soda char does not contain sulfur so the sulfate/sulfide cycle is not operative.

The sulfide oxidation rate was shown by Cameron to be limited only by the rate of oxygen supply.[7] Therefore, the sulfate/sulfide cycle predicts that the char burning rate will be controlled either by oxygen mass transfer to the char or the kinetics of the carbon-sulfate reaction. One of the objectives of recovery boiler operation is to keep the reduction ratio, r, of the smelt flowing out of the unit as high as possible. If oxygen mass transfer is limiting the char burning rate, then fixed-carbon combustion and high reduction ratios can be obtained simultaneously.

$$r = \frac{Na_2S}{Na_2S + Na_2SO_4}$$

Molar Balance of Char Combustion

A molar balance performed on char reactions reveals that 86% of the oxygen required for fixed-carbon oxidation must be supplied by the combustion air with only 14% supplied by the sulfate, assuming:

- The simplified char and smelt compositions suggested by Grace are representative.
- The reduction ratio is 0.50 in the char and 0.95 in the smelt.
- The sodium carbonate is inert.
- The CO/CO_2 ratio in the exhaust gases is 50:50.

See Appendix I for details. The CO/CO_2 ratio in the product gas is an important parameter. The amount of oxygen required by the char reactions is directly related to the CO/CO_2 ratio. Twice as much oxygen is required with CO_2 as the carbonaceous gas product.

Carbon-Sulfate Reaction

The carbon-sulfate reaction is a most important char reaction since it is a significant part of the sulfate/sulfide cycle.[6] This discussion addresses the factors affecting the thermodynamics and the kinetics of the reaction.

The heat of reaction of the carbon-sulfate reaction is strongly dependent on the CO/CO_2 reaction product, as suggested in Table 6. The reaction is three times as endothermic with CO as the reaction product as opposed to CO_2.

Table 6. Heats of reaction for carbon-sulfate reaction.

	ΔH_r: kJ/kg Na_2SO_4 (Btu/lb) 1000°K	1300°K
$Na_2SO_4 + 2\ C \longrightarrow Na_2S + 2\ CO_2$	1261 (542)	1177 (506)
$Na_2SO_4 + 4\ C \longrightarrow Na_2S + 4\ CO$	3667 (1576)	3539 (1521)

The factors affecting the CO/CO_2 product of the reaction are not known. Thorman used activated carbon as the carbon source for his stirred batch reactor studies.[8] He reported a CO/CO_2 ratio ranging from 1:1 to 11:1. Cameron used pulverized graphite, graphite rods, soda char and kraft char as carbon sources in his series of batch reactor studies.[4,8,9] Mixing was achieved in his system by sparging the supply gases through the melt. He reported a CO/CO_2 product ratio of 0.1 or less. The reason why Thorman's and Cameron's CO/CO_2 product results differ is that the carbon-sulfate ratios were probably quite different. This is discussed later in this thesis.

The kinetics of sulfate reduction by carbon are dependent upon the carbon source. Typical Arrhenius behavior has been reported for the reaction.

Thorman suggested that rate Eq. (1) is representative of the carbon-sulfate reaction.[8]

$$-\frac{d[SO_4]}{dt} = A[SO_4]^{0.0 \pm 0.1}\,[C]^{0.31 \pm 0.02}\,\exp\,(-E_a/RT) \qquad (1)$$

where $$-\frac{d[SO_4]}{dt} = \frac{g}{min} \cdot \frac{100\ g}{solution}$$

$$A = 1.67 \pm 0.15 \times 10^8\ \frac{g^{0.69}}{min} \cdot \frac{100\ g^{-0.69}}{solution}$$

$$E_a = 2.04 \pm 0.15 \times 10^5\ J/mole\ (48.7\ kcal/mole)$$

Cameron, in his initial studies using graphite rods as his carbon source, found the reaction to be autocatalytic.[8] This autocatalytic behavior was not exhibited in subsequent studies by Cameron using kraft char, soda char, and pulverized graphite as the carbon source.[4,7] Cameron's rate equations and parameters are given in Table 7.

Table 7. Sulfate reduction by carbon rate equations.[4,7]

$$\frac{d[SO_4]}{dt} = - k_1 \frac{[SO_4]}{1 + k_4 [SO_4]} [C] \exp - (E_a/RT) \qquad (2)$$

Carbon Type	k_1 L/mole-sec	k_4 k:L/mole	E_a:kJ/mole (kcal/mole)
Kraft char	$5.96 \pm 1.86 \times 10^4$	45.6 ± 17.1	122 ± 3 (29.2 ± 1.0)
Pulverized graphite	$1.92 \pm 0.32 \times 10^6$	38.9 ± 7.2	184 ± 5 (44.0 ± 1.2)
Soda char	$7.46 \pm 1.80 \times 10^6$	24.5 ± 7.5	166 ± 6 (39.9 ± 1.5)

Cameron's rate equations are all first order in carbon concentration. The sulfate-dependent terms are significant only at very low sulfate concentrations where a first order sulfate dependence is approached. For higher sulfate concentrations, $k_4 [SO_4] \gg 1$ and thus a zero-order dependence is predicted. Thorman reported a zero-order sulfate dependence and a 0.31 order carbon concentration dependence. The reason for this difference between Cameron's and Thorman's results is not clear. It may be a function of the method of mixing or the carbon source.

Other Sulfate Reduction Pathways

Carbon is not the only potential sulfate reducing agent during char burning. Carbon monoxide and hydrogen gas may also be present in the char and could contribute to sulfate reduction.

Sjoberg studied the sulfate reduction by CO reaction using a batch reactor with mixing achieved by sparging the supply gases through the melt.[10] The rate equation she developed is:

$$\frac{d[SO_4]}{dt} = - k[pCO] \exp (- E_a/RT) \qquad (3)$$

where $k = 1.90 \pm 0.03 \times 10^3 \frac{\text{mole}}{\text{L}\cdot\text{atm}\cdot\text{min}}$

$E_a = 1.15 \pm 0.04 \times 10^5$ J/mole (27.5 ± 0.9 kcal/mole).

The reaction rate is much less than that reported by Cameron for kraft char. Grace compared the two rate equations and determined that at 1200°K (1700°F), a pCO of 0.1 atm and a carbon concentration of 1 mole/L, the relative rate of reaction given in Eq. (4) would apply.[5]

$$\frac{\text{rate of reaction with CO}}{\text{rate of reaction with kraft char}} < 0.005 \qquad (4)$$

Sulfate reduction by CO is probably not a significant sulfate reduction pathway for kraft char.

Atomics International studied the sulfate reduction rate in an alkali carbonate melt using CO and H_2 as the reductant.[11] At 973°K (1291°F) the reaction was 1.9 times greater with H_2 as the reductant. This suggests that sulfate reduction by H_2 is also insignificant in kraft char burning.

Direct Carbon Oxidation Reactions

Direct carbon oxidation refers to either of the following reactions:

$$C + O_2 \longrightarrow CO_2$$

$$C + 1/2\ O_2 \longrightarrow CO$$

These reactions are the rate controlling reactions for coal char combustion when oxygen is present.[12] For kraft char combustion, however, the reported studies suggest that the carbon oxidation rate is controlled by the sulfate/sulfide cycle.[6] This implies that direct carbon oxidation reactions are not significant during kraft char burning.

Carbon Oxidation by Carbon Dioxide

The gasification of the fixed-carbon of kraft char by CO_2 is a reaction that could affect both the rate and the CO/CO_2 product of kraft char burning. Goerg obtained the rate expression of Eq. (5) for the rate of carbon oxidation by CO_2 in an alkali carbonate melt.[13]

$$-\frac{d[C]}{dt} = \frac{k_1\ [pCO_2]}{1 + k_2\ [pCO_2] + k_3\ [pCO]}\ \exp\left(-\frac{E_a}{RT}\right) \qquad (5)$$

where $k_1 = 6.26 \pm 1.82 \times 10^9\ (atm\text{-}min)^{-1}$

$k_2 = 29.0 \pm 8.1\ atm^{-1}$

$k_3 = 45.6 \pm 13.4\ atm^{-1}$

$E_a = 2.27 \pm 0.09 \times 10^5$ J/mole (54.3 ± 2.3 kcal/mole)

The rate of this reaction is much slower than the carbon-sulfate reaction at 1200°K with a pCO at 0.05 atm and a pCO_2 of 0.05 atm.

$$\frac{\text{rate of C oxidation by CO}}{\text{rate of C oxidation by } SO_4} < 0.009 \qquad (6)$$

See Appendix II for the calculation. This suggests that the reaction does not significantly contribute to the gasification of the fixed-carbon content of kraft char nor significantly affect the CO/CO_2 ratio.

Sulfide Oxidation Reaction

The sulfide oxidation reaction is a significant part of the sulfate/sulfide cycle. The sulfide oxidation rate in an alkali carbonate melt was studied by Cameron in his smelt pool reactor:[7]

$$Na_2S + 2\ O_2 \longrightarrow Na_2SO_4$$

O_2/N_2 mixtures were bubbled through a molten carbonate melt that contained Na_2S,

at 1061 to 1144°K (1450 to 1600°F). Cameron found that the reaction rate was limited only by the rate of oxygen supply to the reactor.

Importance of the CO/CO_2 Ratio

The CO/CO_2 ratio is important in kraft char burning for two reasons. First, it dictates the air supply required by the char. Secondly, it has a large effect on the heat of reaction of sulfate reduction by carbon and thus the energy released during kraft char burning.

The gas-phase oxidation of CO complicates CO/CO_2 determinations for studies involving the oxidation of carbon-containing fuels. It is difficult to determine whether CO_2 is a product of the heterogeneous reaction of the gases and the fuel or due to the homogeneous, gas-phase oxidation of CO.

$$CO + 1/2\ O_2 \longrightarrow CO_2$$

Previous Char Combustion Studies

Previous kraft char combustion studies can be categorized into two groups: smelt pool reactor studies and single particle reactor studies. Both types of investigations were used to obtain char burning data with systems that could be well quantified.

Smelt Pool Reactor Studies

The smelt pool reactor used for char burning investigations is a batch reactor into which inorganic salt mixtures are placed along with a small amount of char. If the fixed-carbon in a char bed is completely wetted by the molten salts and the diffusion of gases through the molten salts does not limit the reaction rate then the smelt pool reactor should give results representative of char bed behavior.

An advantage of smelt pool studies is that reactant concentrations, gas flow rates, and temperatures can be precisely controlled and the exhaust gas composition accurately determined. One limiting factor is the maximum carbon concentration that can be used. The melt viscosity increases with carbon concentration, therefore adequate mixing is difficult at high carbon loadings.

Single Particle Reactor Studies

Two types of single particle reactor studies have been reported for kraft char: stagnant atmosphere and convective atmosphere investigations.

Stagnant atmosphere studies were performed by Hupa in a muffle furnace type reactor.[14] A black liquor drop was suspended from a wire attached to a microbalance and lowered into the reactor. The black liquor mass was monitored as a function of time as visual observations were recorded with a camera. For some runs, temperature data were also collected when a thermocouple wire was hung from the microbalance. Hupa was the first researcher to experimentally identify drying, volatiles burning, and char burning as distinct stages.

Convective single particle reactor studies, reported by Grace and coworkers and discussed in the sulfate/sulfide cycle section, are representative of the char burning reactions in flight. They do not address char pile behavior, however. The interaction between particles in a pile may lead to much different results than those obtained for a single particle in a convective flow of gases, because in a char pile, oxygen access is limited.

CHAR PILE REACTOR

The char pile reactor diagrammed in Fig. 4 is a general schematic of the reactor used in my studies. Supply gases are impinged on the surface of the

char in the reactor. Bulk gas CO, CO_2, and O_2 concentrations are monitored in the exhaust gases. The temperature of the reactor is controlled by regulating the current to an induction furnace. The temperature profile of the reactor can be determined by adjusting the position of a series of thermocouples.

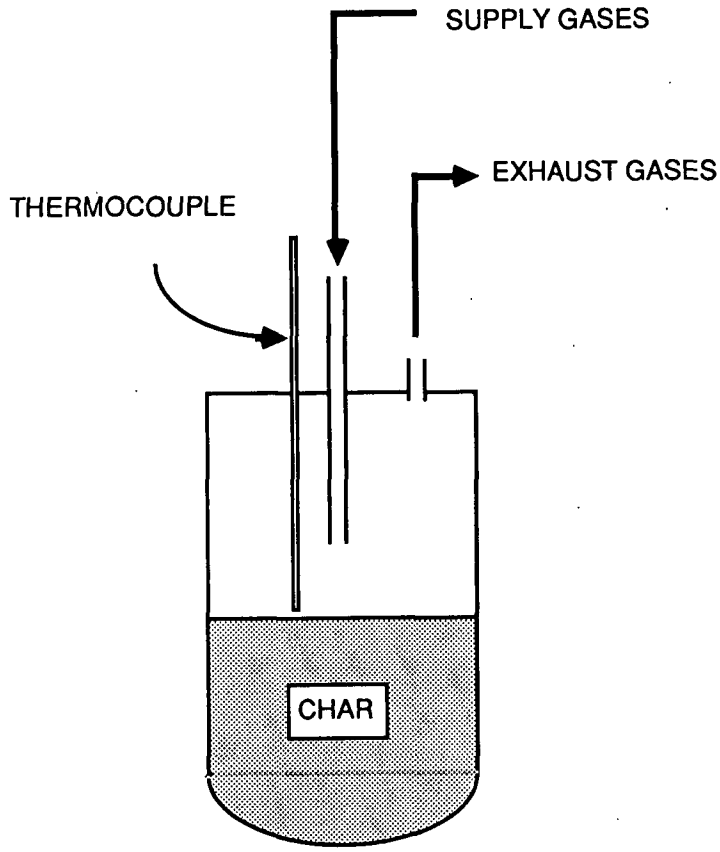

Figure 4. Char pile reactor schematic.

The char pile reactor is an interesting geometry because it is similar to char bed conditions since a supply gas is impinged on the char surface for both. However, the char pile reactor is a batch reactor. Char is continually being deposited on the char bed surface of a recovery boiler. Although the char pile reactor does not exactly duplicate char bed conditions, it was selected since its char pile configuration and impingement geometry should provide valuable insights into char bed behavior.

THESIS OBJECTIVES

The objectives of this thesis were to

- obtain conclusive data on the CO/CO_2 product of the carbon-sulfate reaction
- determine the factors affecting the CO/CO_2 ratios observed during char burning
- determine the factors affecting the char burning rate

RESEARCH OUTLINE

All sources of oxygen for the oxidation of the fixed-carbon of the char required quantification. Only after this was accomplished, could the carbon-sulfate reaction studies and the char burning studies proceed. The preliminary nitrogen-atmosphere studies defined the oxygen sources and suggested the char preparation procedure used for the remainder of the experiments.

Preliminary Nitrogen-Atmosphere Studies

- prepare char and determine whether the carbon-sulfate reaction is responsible for the amount of CO/CO_2 evolved upon heating.
- determine the effect of sorbed oxygen on the amount of CO and CO_2 evolved.
- determine whether continued pyrolysis is a potential oxygen source.
- determine the effect of sulfate-loading the black liquor on the CO/CO_2 product.
- develop a char preparation procedure to be used for the remainder of the experimental program, using these preliminary results as guidelines.

Carbon-Sulfate Reaction Studies

- quantify the factors affecting the CO/CO_2 product with sulfate as the source of oxygen for fixed-carbon oxidation.

CO/CO_2 Product of Char Burning Studies

- determine the temperature-dependence of the gas-phase oxidation of CO to CO_2
- determine the factors affecting the CO/CO_2 product with combustion air as the source of oxygen for fixed-carbon oxidation

Char Burning Rate

- determine whether the char burning rate, with combustion air as the oxygen source for fixed-carbon oxidation, is controlled by carbon-sulfate kinetics, by the rate of oxygen mass transfer, or by a combination of these two mechanisms

EXPERIMENTAL

The apparatus and procedures common to all investigations are included in the Experimental section. Also included are any preliminary studies that helped define the procedures used in the critical experiments of this thesis.

EXPERIMENTAL APPARATUS

Description

The experimental apparatus is diagrammed in Fig. 5. For particulars such as crucible dimensions and equipment manufacturers, see Appendix III.

For most experiments, the char was placed in an alumina crucible secured by a stainless steel retort. A Hastelloy retort was used without the alumina crucible during the pyrolysis portion of char preparation. Ports in the reactor head allowed for the insertion of a supply gas tube and thermocouples, and for the removal of exhaust gases to the gas analyzers.

An induction furnace controlled the temperature of the reactor. An optical pyrometer measured the surface temperature of the stainless steel retort, which was compared to that of the set point and the current supplied to the induction furnace coil was adjusted accordingly.

The supply gas flow rates were monitored by mass flow meters and controlled with appropriate valves. Nitrogen and air were the gases metered into the reactor for most experiments. For the gas phase oxidation of CO studies, CO was also one of the metered gases.

One to four thermocouples were inserted into the reactor to measure temperature. For some experiments, a radiation-shielded thermocouple was used.

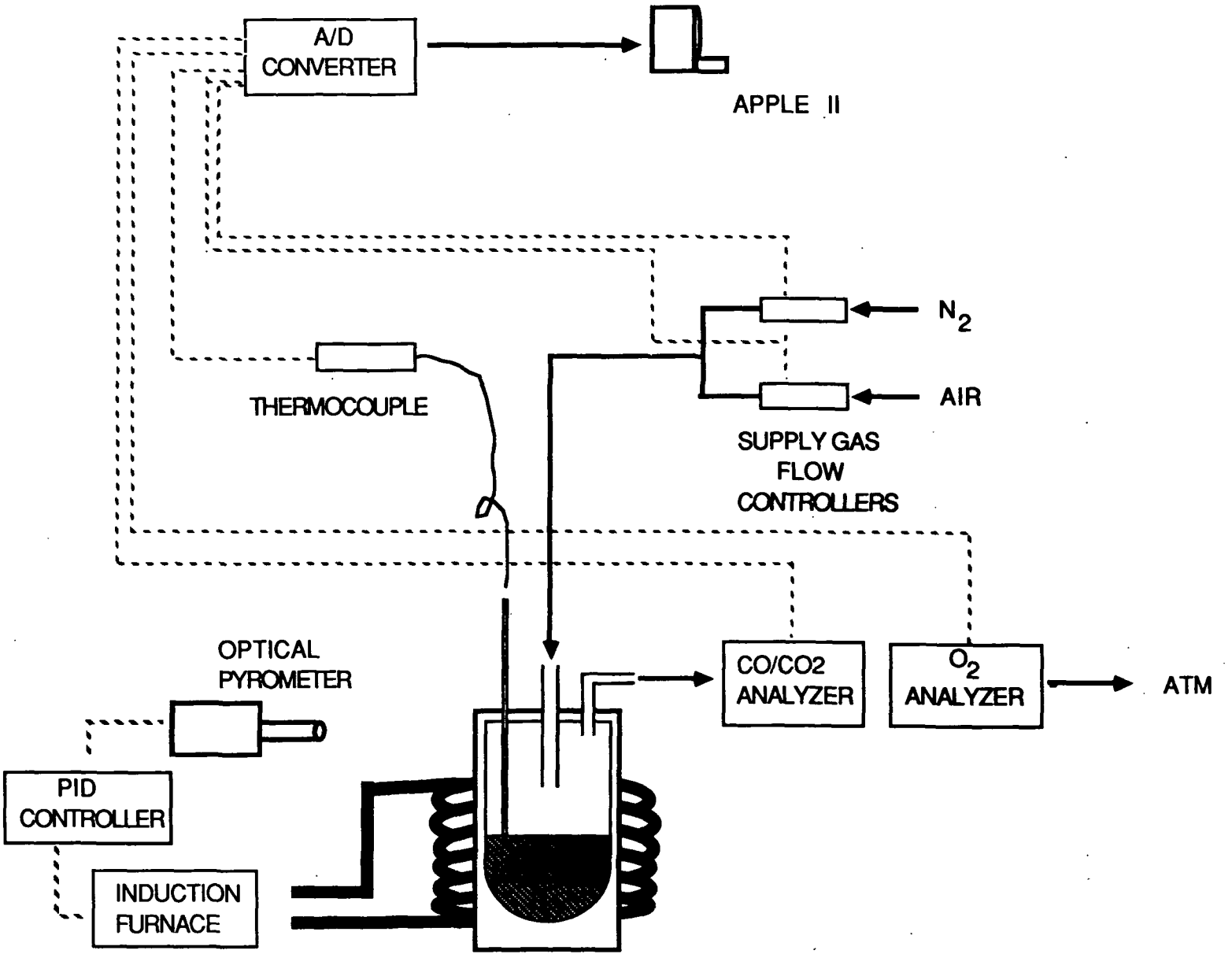

Figure 5. Experimental apparatus.

Temperature measurements, supply gas flow rates and exhaust gas composition data were collected by a data acquisition system attached to an Apple II® computer. The data were displayed on the screen and, at the end of an experiment, a print-out was obtained. The data were also stored on a floppy disk and transferred to an IBM PC® to manipulate the data using Lotus 123® software.

Impingement Geometry Characteristics

The geometry chosen was not altered throughout the char burning experiments. Given in Table 8 and Fig. 6 are the impingement geometry specifics. Since the supply gas was not preheated, the velocity increased as the gas entered the hot reactor. The Reynolds number calculated at 1190°K is 142 (Appendix IV) and at 367°K is 231. Since the Reynolds numbers are less than 2000, the supply gas jet is laminar.[15] Data reported on laminar jets are limited. Turbulent jets expand at a 20° angle.[15] If it is assumed that a laminar jet will behave similarly, the jet should expand to a circle 1.1 cm in diameter upon impingement on the char surface. This is approximately the same diameter as the smelt beads that formed in the impingement region of the high temperature, char burning experiments.

Table 8. Impingement geometry specifics.

Supply gas flow rate	1.0 L/min
Supply gas tube diameter (A)	4.5 mm
Initial height above char surface (B)	2.0 cm
Crucible diameter (C)	4.13 cm
Thermocouple diameter (D)	1.6 mm

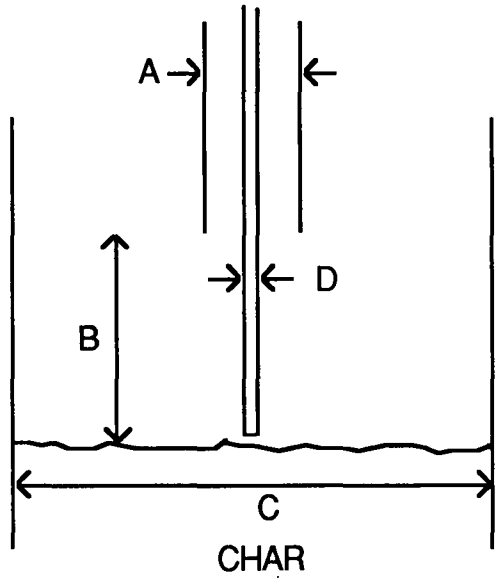

Figure 6. Impingement reactor schematic.

This particular impingement geometry was selected for several reasons:

- The relatively small quantities of char allowed several experiments to be run per batch of char. Since the char preparation procedure was very time consuming, this maximized the number of experiments in a given time period.
- The small reactor diameter minimized the temperature variation in the radial direction.
- The reactor could be easily instrumented by putting access ports in the reactor head.
- The impingement of a gas stream on a small spot in the center of the reactor created different zones that could be studied during a single experiment: an impingement zone where the oxygen concentrations are high in close proximity to the char surface, a nonimpingement zone where the flow is parallel to the char surface, so oxygen access

is more restricted; and a subsurface zone which is oxygen inaccessible at high temperatures.

The disadvantages of this geometry are

- The surface behavior is difficult to model due to the two different surface regions.
- The amount of gas-phase mixing is difficult to quantify and will tend to dampen the transient, exhaust-gas behavior.
- The amount of gas-phase oxidation of CO to CO_2 can be quite significant due to gas-phase mixing.
- The small reactor size limited the amount of sample available from the particular regions.

DATA COLLECTED

Temperature

Standard "Type K" thermocouples, nickel-chromium versus nickel-aluminum, with an ungrounded junction, were used in this study. The claimed accuracy of the thermocouples is ± 0.75% of reading for the temperature range of interest, 922 to 1367°K (1200 to 2000°F). At 1061°K (1450°F), the uncertainty is 5.8°K (10.5°F).

A radiation-shielded thermocouple was constructed (see Appendix V) and placed in the exhaust port to determine whether radiation significantly affected thermocouple readings. Exhaust port placement ensured adequate gas flow rates past the thermocouple and thus improved the accuracy of the reading. A second thermocouple was placed at a similar radial position and height in the reactor. This thermocouple was unshielded. The temperature measured by the unshielded

thermocouple was 14°K (25°F) greater than that of the shielded thermocouple at 1061°K (1450°F, Experiment 35). The unshielded thermocouple was 11°K (20°F) less than the shielded thermocouple reading for a subsequent experiment at a temperature of 1045°K (1425°F, Experiment 37). Gas flow rate had no effect on the readings. From these studies I concluded that radiation shielding did not significantly affect thermocouple readings.

Exhaust Gas Carbon Monoxide, Carbon Dioxide, and Oxygen Concentrations

Exhaust gas CO, CO_2, and O_2 concentrations were measured by a CO/CO_2 analyzer and an O_2 analyzer. A flow rate of 13 to 16 mL/s (1.7 to 2.0 scfh) was maintained by adjusting a bypass valve that vented a portion of the exhaust gas flow.

The CO/CO_2 analyzer and the O_2 analyzer are both claimed accurate to ± 1% of full scale. For most experimental conditions, the lowest range of both instruments was used. The claimed accuracy of the CO/CO_2 readings were ± 0.1%, CO/CO_2; the claimed accuracy of the O_2 readings were ± 0.05% O_2.

The gas analyzers were calibrated with a standard calibration gas before and after each experiment to ensure the most accurate measurements were made. For nearly all experiments, the pre- and postexperiment readings varied less than 0.05% $CO/CO_2/O_2$.

The response times of the gas analyzers were checked for two reasons: to determine the significance of the delay time between the CO/CO_2 analyzer and the O_2 analyzer (since they were connected in series) and to determine whether the responses of the meters were similar when the flows of CO, CO_2, and O_2 were terminated. Details are in Appendix VI. The results indicate that there was a 25-second delay from the time a supply gas valve was adjusted to the time that

the effects were first detected by the CO/CO_2 analyzer. The oxygen analyzer had a 31-second delay. The response curves of the CO/CO_2 and the O_2 analyzers were identical once this difference in delay times was taken into account.

Supply Gas Flow Rates

Supply gas flow rates were measured using two Hastings-Raydist Mass Flowmeters. One was calibrated for the 0.00-1.00 L/min range, a second was calibrated for the 0.0-10.0 L/min range. Appendix VII includes a diagram of the supply gas system.

The flowmeters were factory calibrated for air at 293°K (68°F) and 1 atmosphere. For gases other than air, it was necessary to multiply the flowmeter reading by a gas-specific calibration factor in order to obtain the actual flow rate. Appendix VIII includes a list of the calibration factors used in this study.

The flowmeters were recalibrated using a bubble flowmeter procedure (Appendix VIII). The values were converted to the universal scientific standards of 273°K and 1.0 atm.

Factors accounting for the gas specific calibration factors and the measured differences between the flowmeter readings and the bubble flowmeter values were included in the data manipulation portion of the data acquisition programs.

Set Point Temperature

The temperature of the outside surface of the stainless steel retort was the set point temperature. It was controlled by adjusting the set point of the induction furnace temperature controller. Due to changes in retort positioning, the focal point of the optical pyrometer, the separation of the induction coil

windings and probably several other parameters, the set point temperature did not directly correspond to the temperature inside the crucible.

Char Sampling and Analysis

Total Elemental Analysis

Two char samples were submitted for a total elemental analysis to Huffman Laboratories of Wheat Ridge, Colorado. The elements analyzed included C, H, O, S, Na, K, and Cl. One sample was pyrolyzed for 10 minutes at 1023°K (1381°F); the second was pyrolyzed for 10 minutes at 1223°K (1741°F). Duplicate analyses on samples from the same source were performed by the Analytical Department at IPC for S, Na, K, and Cl. A flame emission after perchlorate digestion technique was used for the Na and K determinations. Total sulfur is discussed in the next section. The chloride determination was made using an ion chromatograph method.[16] The results of these elemental analyses, shown in Table 9, are similar to those reported by Cameron in Table 3. The IPC and the Huffman analyses agreed quite well.

Table 9. Char elemental analyses (weight percent).

	Huffman Laboratories		IPC Analytical Department	
	1023°K Pyrolysis	1223°K Pyrolysis	1023°K Pyrolysis	1223°K Pyrolysis
C	33.1	33.9		
H	0.3	0.1		
O	30.4	30.0		
S	2.3	3.1	2.5	2.8
Cl	0.8	1.0	0.2	0.2
K	2.8	2.7	3.2	3.4
Na	30.6	29.8	29.8	30.0
Total	100.3	100.6		

Sulfur-Species Analyses

The sulfur-species analyses included thiosulfate ($S_2O_3^=$), sulfite ($SO_3^=$), sulfate ($SO_4^=$), sulfide ($S^=$), and total sulfur. Sulfide was determined by potentiometric titration.[17] The thiosulfate, sulfate and sulfite were quantified using an ion chromatograph technique.[16] The total sulfur was determined by first oxidizing all of the sulfur species to the sulfate form via Schoniger flask combustion, then performing a sulfate analysis on the ion chromatograph.

In order to obtain good sulfur species closure, it was necessary to take extreme measures to prevent oxidation of the samples. All sample transfers were made in a nitrogen atmosphere. Any grinding was also done in a nitrogen atmosphere. Samples were stored in vials and placed in a desiccator that was then purged with nitrogen. Samples submitted for analysis were double-bottled in nitrogen gas. Table 10 shows the results of sulfur species analyses of the various samples of Experiments 54-56.

Table 10. Sulfur species analyses.

(% S of each species on a weight basis)

Exp. No.	Location	$SO_3^=$	$SO_4^=$	$S_2O_3^=$	$S^=$	ΣS[a]	Total S
54	Impingement	0.3	2.0	--	3.5	5.8	5.9
54	Surface	0.4	0.1	0.3	5.1	5.9	5.4
55	Impingement	0.3	2.5	--	3.2	6.0	6.4
55	Surface	0.5	0.6	0.4	5.8	7.2	6.6
56	Impingement	0.2	4.8	--	0.9	5.9	6.8
56	Surface	0.4	0.4	0.4	6.7	7.9	7.1

[a] ΣS is the sum total of $SO_3^=$, $SO_4^=$, $S_2O_3^=$, and $S^=$.

Due to the limited amounts of sample available when fractioning the char after an experiment, sufficient quantities were not always obtained to calculate 95% confidence intervals. For experiments where adequate samples were available (at least 3 analyses were made), the confidence interval was ± 5% of reading. For the analyses listed, the value reported is an average of at least two determinations. The fact that the sum total sulfur, "ΣS," and the "Total S" agree quite well suggests that the sulfur-species analyses are reasonable.

Fixed-Carbon Determination

The fixed-carbon is the carbon present in the char that has been pyrolyzed and thus becomes highly-condensed. Since the black liquor solids were pyrolyzed at 1223°K for 10 minutes, the fixed-carbon should be the carbon present that is not in the carbonate form. Fixed-carbon determinations were primarily performed on the char sources for the char burning experiments; but some determinations were made on the various fractions remaining after the char burning experiments. The fixed-carbon concentration of the char sampling regions are presented in the next section.

The fixed-carbon was determined using the induction furnace apparatus. A 0.5 to 1.0 gram sample was placed in the alumina crucible then rapidly heated to 1044°K (1420°F) with a slight nitrogen purge of 0.05 L/min. An air flow of 0.850 to 0.990 L/min was then introduced and the nitrogen flow terminated. The concentrations of CO, CO_2, and O_2 in the exhaust gases and the air flow rate were used to calculate the moles of carbon gases evolved, which is equal to the moles of fixed-carbon in the sample.

The temperature selected was just high enough so that the system became molten with no traces of char remaining in the residual smelt. Excessive

temperature could result in either carbonate decomposition or carbonate reduction by carbon, both of which would lead to measured fixed-carbon concentrations that were greater than the actual values.

Duplicate analyses were performed on only a few samples due to limited sample quantities. Duplicate runs on a char sample resulted in a value of 23.4 ± 1.0% fixed-carbon. The carbon concentrations for the single point analyses should be within ± 1% carbon of the true value.

Char Sampling Regions - Char Surface Morphology

Figure 7 is a picture of the surface of the char pile after Experiment 46. A large smelt bead formed near the center of the reactor in the area of impingement. Samples from this region will be referred to as impingement samples. The rest of the surface of the char will be termed the nonimpingement region, or simply the surface region. Char samples taken below the surface of the char will be called subsurface samples.

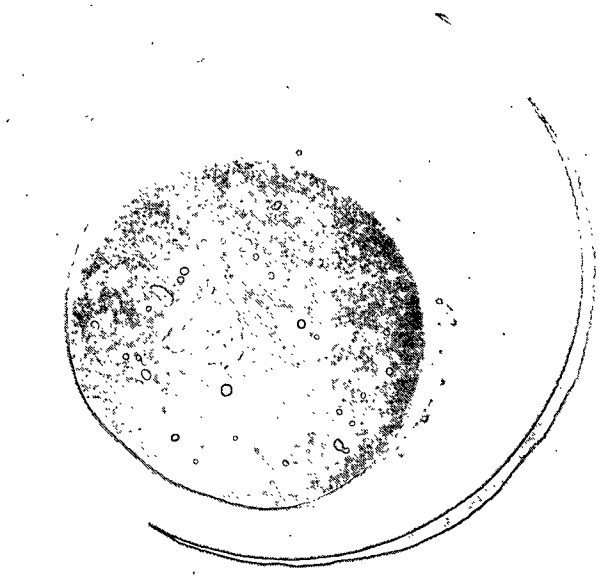

Figure 7. Char surface picture.

Whether the smelt bead was confined to the impingement region or covered a portion or nearly all of the char surface was a function of temperature (Fig. 8). At 1039°K (1410°F), the smelt was wafer-thin, covering nearly the entire surface. At 1083°K (1489°F), the smelt covered the impingement region and a portion of the surface region. At 1139°K (1590°F), the smelt was confined to the impingement region.

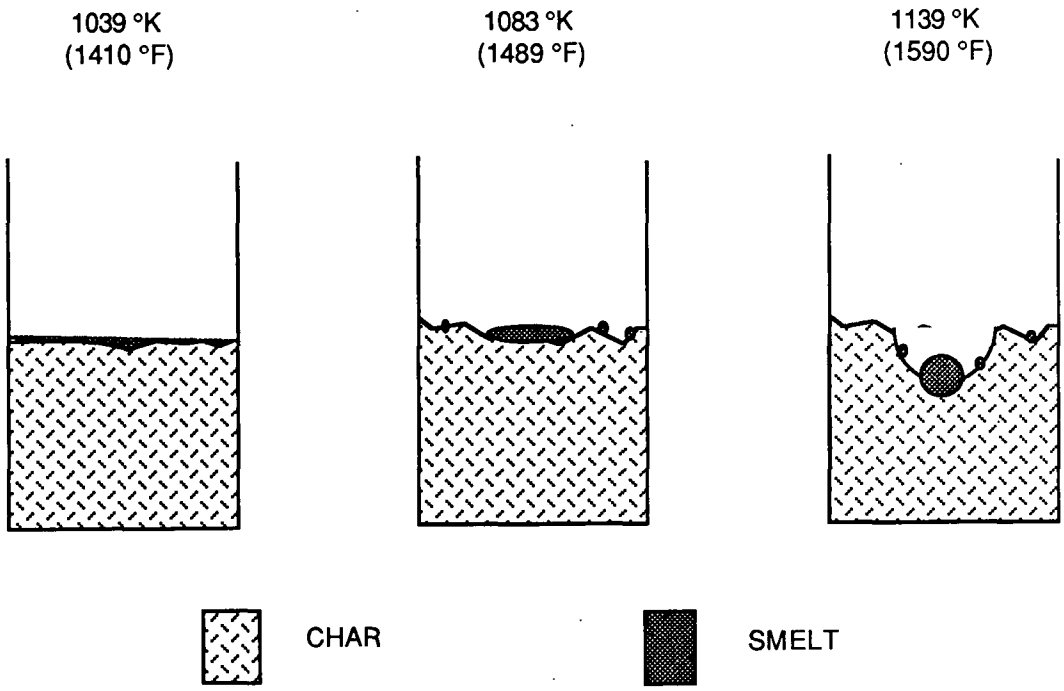

Figure 8. Char surface morphology.

Only one sample was collected for analyses from the surface for the low temperature studies where the smelt layer formed across the entire surface. Both an "impingement" sample and a nonimpingement "surface" sample were collected for the higher temperature studies.

Some problems were encountered when separating the fractions. It was difficult to remove the char particles adhering to the bottom surface of the

impingement region smelt samples. These samples were scraped with a metal spatula to remove the loosely-attached particles. The most difficult separation was between the nonimpingement "surface" samples and the "subsurface" samples. The char particles tended to fuse together slightly during an experiment; a solid rap on the crucible would cause the fused char to separate back into individual particles. Separation was effected by first removing the impingement bead, then lightly scraping the surface region to loosen the char of that region. The loosened char was then poured into a sample vial.

Fixed-carbon concentration results of Experiments 41, 42, and 43 are given in Table 11. The impingement-region smelts measured less than 1% carbon. The samples of the nonimpingement surface region were charlike in appearance and measured between 1.3 and 16.0% carbon. The subsurface results indicate that region is nearly unreactive.

Table 11. Fixed-carbon concentration of sampling regions after char burning experiments.

Sample	Oxygen Partial Pressure (% O_2)	Weight, % C
Source Char	--	23.4 + 1.0
Expt. 41 - Impingement	2.1	0.0
- Surface	2.1	16.0
- Subsurface	2.1	23.0
Expt. 42 - Impingement	4.2	NA[a]
- Surface	4.2	11.9
- Subsurface	4.2	22.2
Expt. 43 - Impingement	10.5	0.7
- Surface	10.5	1.3
- Subsurface	10.5	NA

[a]NA = not available due to either insufficient sample quantities or experimental difficulties.

For subsequent experiments, carbon concentration determinations were made only on the source chars. Since sample quantities were limited, it was deemed more important to obtain sulfur-species analyses on the fractions than carbon concentration analyses.

PRELIMINARY NITROGEN-ATMOSPHERE EXPERIMENTS

A number of interesting results were obtained during the preliminary nitrogen-atmosphere experiments. The initial char preparation procedure was the starting point for this series of experiments. A flow chart of this series is given in Fig. 9.

Initial Char Preparation Procedure

The black liquor was dried under vacuum at 423°K (301°F) with a slow nitrogen purge. The dry black liquor solids were pyrolyzed in an induction furnace reactor at 1223°K (1741°F) for seven minutes with a slow nitrogen purge. The char residue of pyrolysis resembled a brittle black sponge. This material required grinding and screening to obtain a char of uniform particle size.

The char particle size distribution for Char Preparation Experiments 1 through 4 and 29B-2 are given in Table 12. The particle size distribution for the 0 to 0.5 mm fraction of Experiment 29B-2 is listed in Table 13. This was the char source for all experiments discussed in the Results and Discussion.

Initial Nitrogen-Atmosphere Experiment: Experiment 8

Char prepared using the "initial" char preparation procedure was placed in a crucible and heated to 1189°K (1680°F). Figure 10 is a plot of the experimental results. The amount of oxygen under the CO and CO_2 curves was determined by integration to obtain the total amount of oxygen evolved. Even with the most

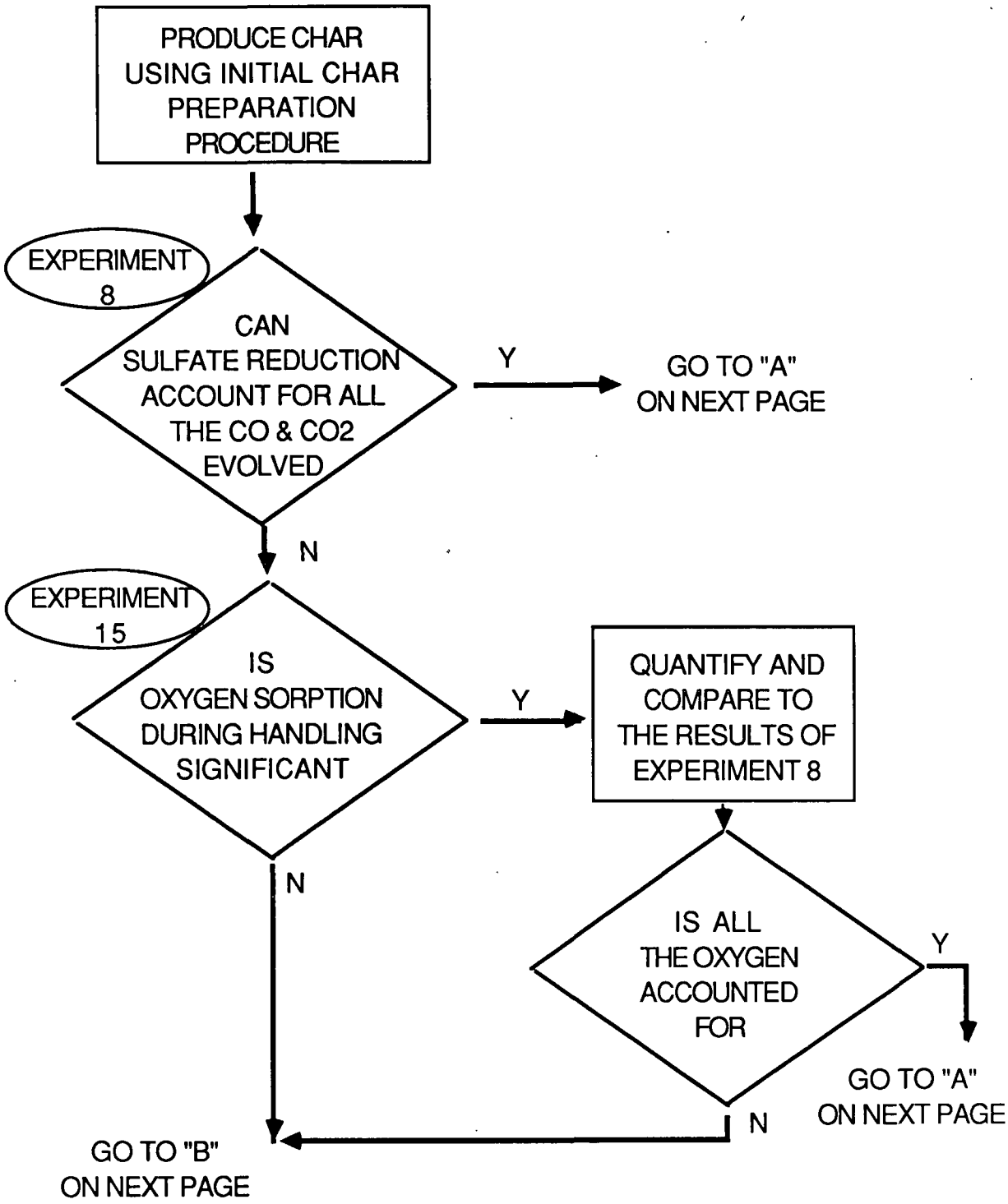

Figure 9. Preliminary nitrogen-atmosphere experimental program.

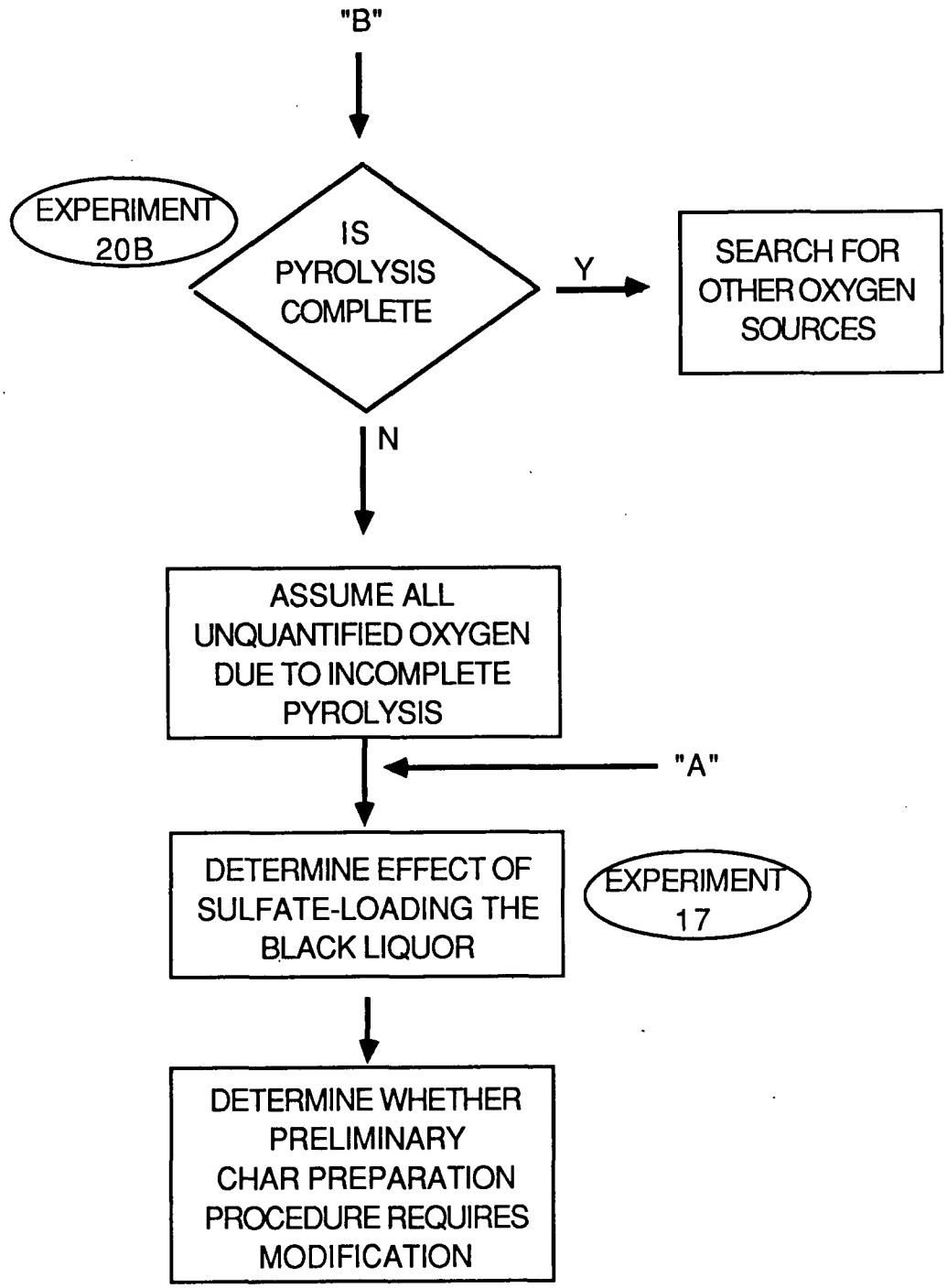

Figure 9 (Continued). Preliminary nitrogen-atmosphere experimental program.

generous estimate of the total sulfate available in the char, only 57% of the oxygen in the CO and CO_2 generated in Experiment 8 can be attributed to sulfate reduction by carbon (Appendix IX). There must be some other source of oxygen in the char besides the oxidized sulfur compounds.

Table 12. Char particle size distribution.[a]

Experiment No.	0 to 0.5 mm, %	0.5 to 1 mm, %	1 to 2 mm, %
1	38	27	35
2	41	22	37
3	51	19	30
4	49	20	31
29B-2	53	19	29

[a]The 1 to 2 mm fraction was retained on an 18-mesh standard sieve, the 0.5 to 1 mm fraction was retained on a 35-mesh standard sieve, and the 0 to 0.5 mm fraction was the catch pan fraction.

Table 13. Particle size distribution for the 0 to 5 mm fraction of Experiment 29B-2.[a]

Fraction (μm)	Weight Percent
250-500	15.8
149-250	13.1
74-149	10.4
62-74	13.4
	52.7

[a]The 250 to 500 μm fraction was retained on a 60-mesh standard sieve, the 149 to 250 μm fraction was retained on a 100-mesh standard sieve, the 74 to 149 μm fraction was retained on a 200-mesh standard sieve and the 62 to 74 μm fraction was retained on a 230-mesh standard sieve.

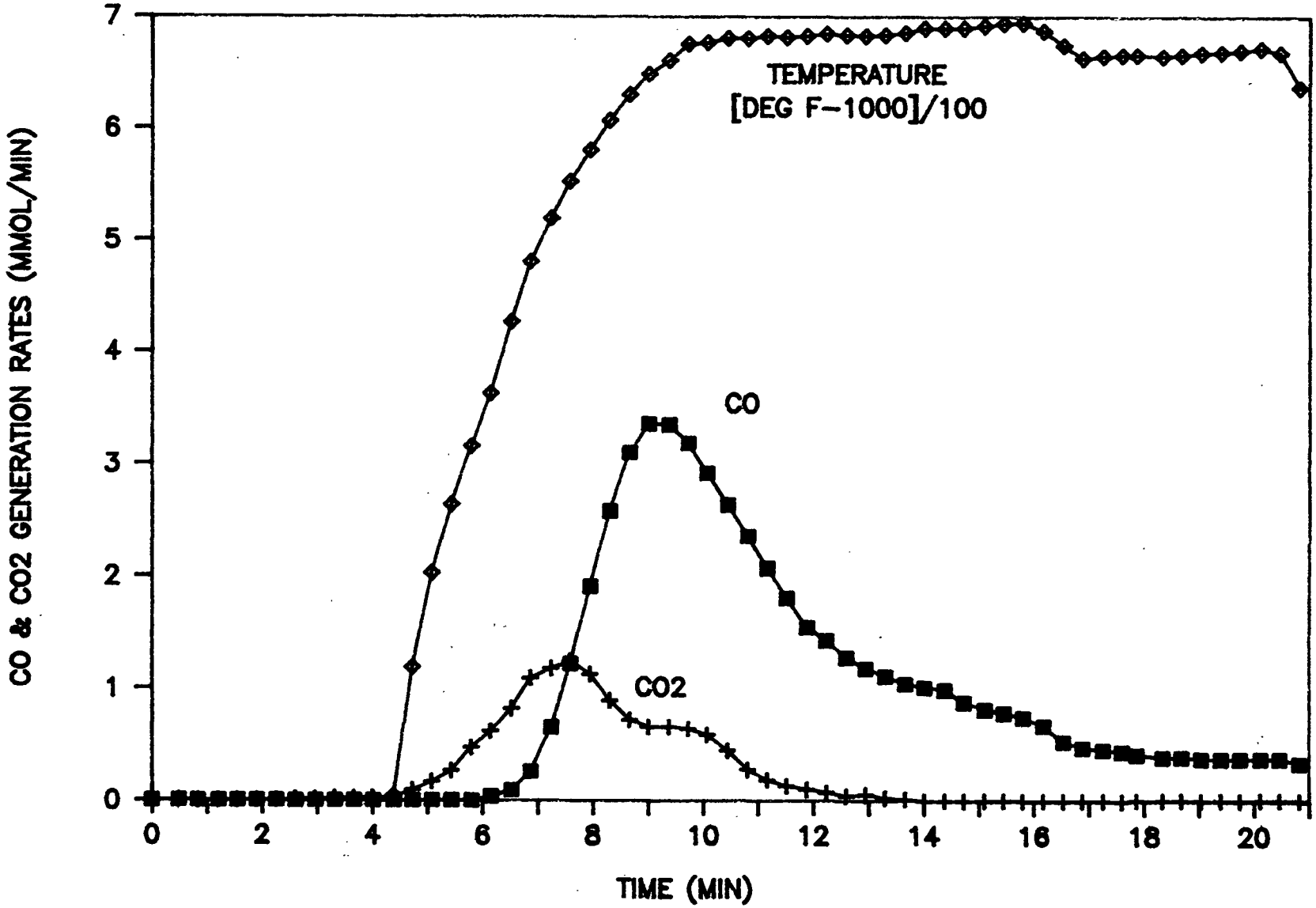

Figure 10. Experiment 8 - initial nitrogen-atmosphere study.

Effect of Nitrogen-Atmosphere Handling: Experiment 15

One potential source of oxygen in the system is oxygen sorbed by the char during the screening and handling. As discussed, 43% of the oxygen generated in the exhaust gases of Experiment 8 could not be attributed to the carbon-sulfate reaction. The sorption of oxygen by the fixed-carbon of the char is a likely mechanism of oxygen pick-up. The following experimental procedure was developed to prevent oxygen exposure of the char.

A custom nitrogen glove bag was constructed to remove the char from the induction furnace reactor. The char was sealed in a mason jar, then transferred to a second nitrogen glove bag that was large enough to perform the grinding and screening operations. The char was sealed in batch-size quantities, 40 mL of char in 60 mL glass jars, while in the nitrogen glove bag. These batch-size jars were then placed in a desiccator purged with nitrogen for storage. The char was transferred into the induction furnace reactor using the custom glove bag prior to the experiment.

These precautions resulted in much reduced CO and CO_2 peaks with nitrogen-atmosphere handling (Experiment 15: Fig. 11). If the difference between the amount of oxygen evolved in this experiment and the amount of oxygen evolved with air-atmosphere handling (Experiment 8) is assumed to be due to oxygen sorption by the char, oxygen sorption is responsible for 27% of the oxygen evolved with air-atmosphere handling (Appendix IX). 1.82×10^{-2} g of O_2 were sorbed per gram of char. The unaccountable oxygen remaining is still 16% of the total oxygen generated. For Experiment 15, where the char was handled in a nitrogen atmosphere, only 43% of the oxygen generated can be attributed to the carbon-sulfate reaction; the unaccountable oxygen is 57% of the total oxygen generated (Appendix IX). There must be additional oxygen sources in the char.

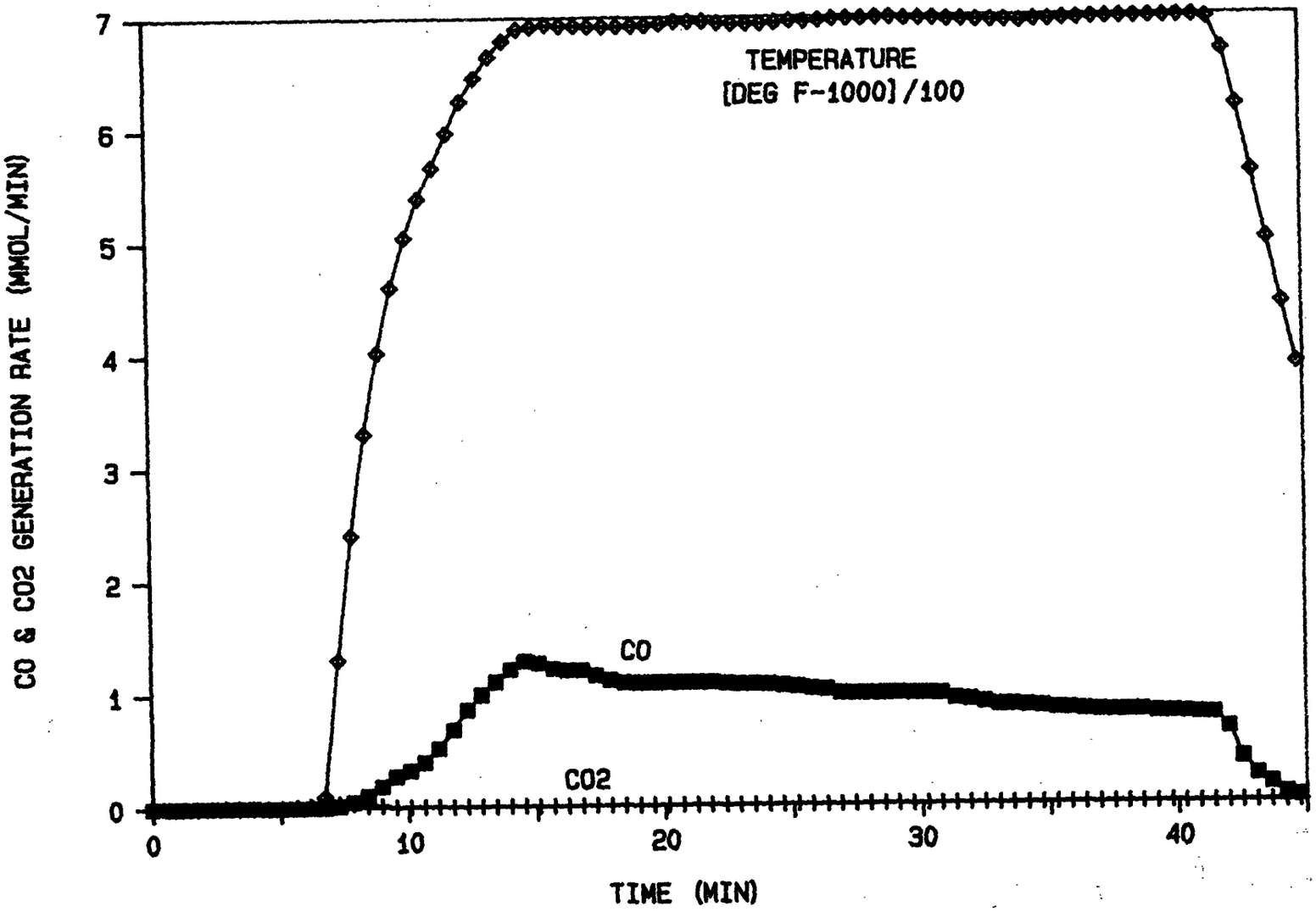

Figure 11. Experiment 15 - air excluded during handling.

Effect of Extended Pyrolysis Time: Experiment 5C4

I suspected that seven minutes at 1223°K (1741°F) was not sufficient to fully pyrolyze the black liquor. To test this hypothesis, the CO/CO_2 gas analyzer was attached to the exhaust gas port of the induction furnace reactor (Experiment 5C4). After seven minutes the CO concentration was 13.4%; after ten minutes the CO concentration was 12.5%. Pyrolysis was not complete after seven minutes at 1223°K.

These data suggest that the unaccountable oxygen of the previous experiments (Experiments 8 and 15) was due to incomplete pyrolysis. If the unaccountable oxygen is assumed to be due to incomplete pyrolysis, then with air-atmosphere handling, 57% of the oxygen in the CO/CO_2 generated was due to the carbon-sulfate reaction, 27% was due to oxygen sorption, and 16% was due to incomplete pyrolysis (Appendix IX).

Subsequent Pyrolysis Experiments: Experiment 20B

Another series of pyrolysis experiments were run to determine the length of time required to ensure complete pyrolysis at a particular temperature. The CO generation rate did not drop to zero at long pyrolysis times but rather leveled at a discrete value that was temperature dependent (Experiment 20B-1). Table 14 shows that the nitrogen flow rate did not affect the CO concentration in the exhaust gases at 1094°K (Experiment 20B-2).

Table 14. The effect of nitrogen flow rate on CO generation during pyrolysis.

Nitrogen Flow Rate	Percent CO
1.00 liters/min	2.1
1.52 liters/min	1.9
1.20 liters/min	1.9

These data suggest that the reaction producing CO was not a pyrolysis reaction but rather a reaction limited by thermodynamic equilibrium. If the reaction was thermodynamically limited, the addition of CO to the supply gas stream should quench the reaction. The results of Experiment 20B-3 indicated that a CO concentration of 3.85% was sufficient to quench the reaction at 1094°K (1509°F). When CO was added to the supply gas, the temperature set point of the reactor was reduced to maintain the 1094°K measured temperature. This indicated that an endothermic reaction was being quenched by the addition of CO. This endothermic reaction could have been carbonate reduction by carbon:

$$Na_2CO_3 + 2C \longrightarrow Na_2 + 3\ CO$$

Effect of Sulfate-Loading the Black Liquor

To determine the effect of the addition of sulfate on the CO/CO_2 product of the carbon-sulfate reaction, 59.8 grams of Na_2SO_4 were added to 583.5 grams of black liquor prior to drying and pyrolysis (Experiment 17). The black liquor solids were pyrolyzed at 1003°K (1345°F) to ensure that the sulfate would not be reduced to sulfide prior to the experiment.

Table 15 gives the sulfur-species analyses of the source char and the postrun char. Figure 12 shows that the CO/CO_2 ratio was approximately 20:1 at 1156°K (1620°F). The carbon/sulfate ratio in the source was approximately 37:1 (Appendix X).

Table 15. Sulfur-species analyses of the sulfate-loaded black liquor char experiment (% S of each species on a weight basis).

	% $SO_3^=$	% $SO_4^=$	% $S_2O_3^=$	% $S^=$	ΣS[a]	Total S
Source char	0.7	1.8	0.6	5.7	8.8	8.7
Postrun char	0.7	0.2	0.8	9.5	11.2	9.9

[a]The ΣS is the sum of % $SO_3^=$, % $SO_4^=$, % $S_2O_3^=$, and % $S^=$.

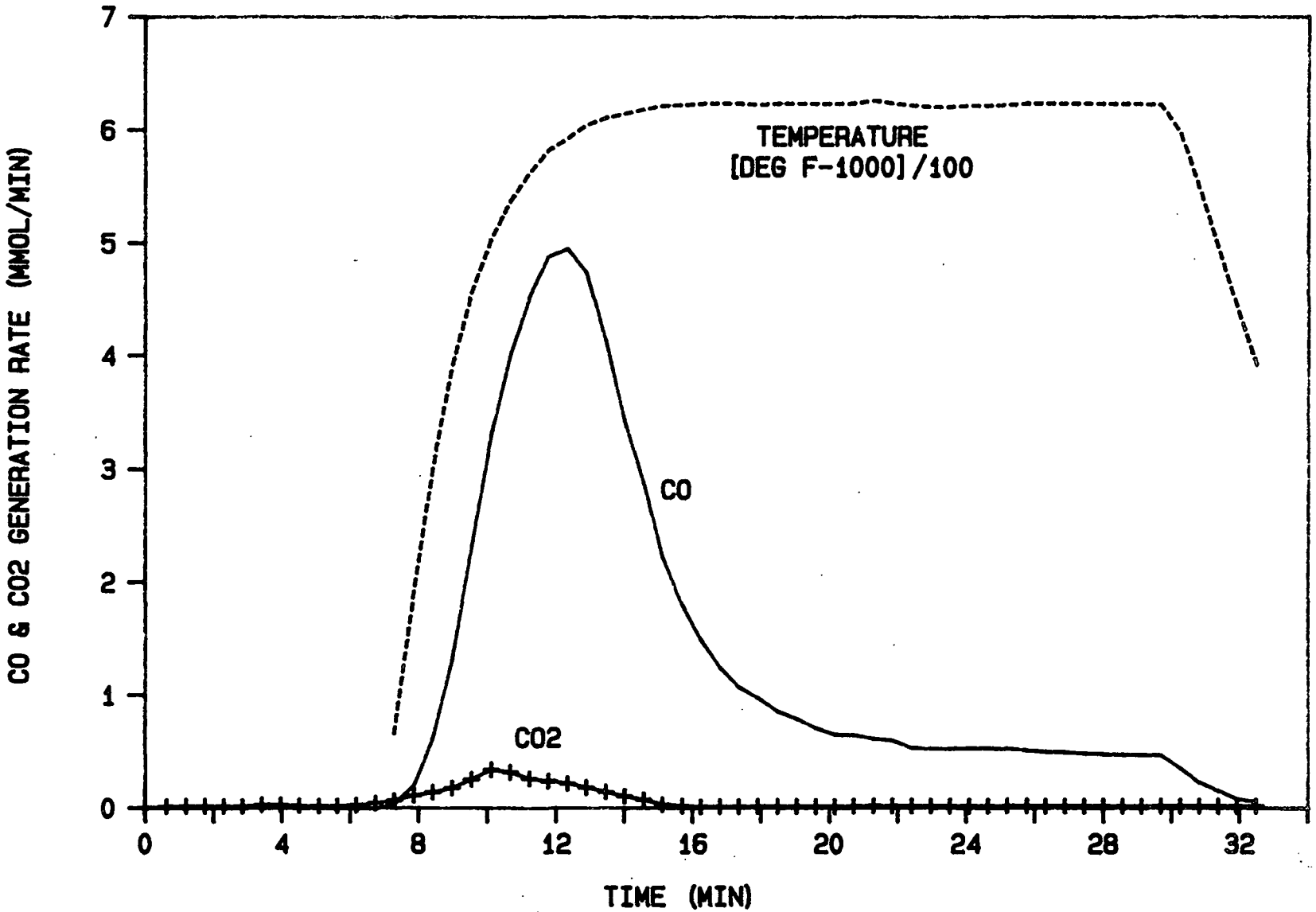

Figure 12. Experiment 17 - sulfate loaded liquor.

Cameron reported a CO/CO_2 of at most 0.1 for his carbon-sulfate reaction studies with much lower carbon concentrations.[4] Quantifying the factors affecting the CO/CO_2 product of the carbon-sulfate reaction is one of the focal points of this thesis addressed in the Results and Discussion section.

Modified Char Preparation Procedure

The modified char preparation procedure was used for the bulk of the char burning experiments, Experiments 46 to 81. The only significant change from the preliminary procedure was that the pyrolysis time was extended from seven to ten minutes at 1223°K (1741°F). This increase in pyrolysis time ensured that the pyrolysis reactions were nearly complete.

Despite the fact that significant amounts of oxygen could be sorbed by air handling, all grinding, screening and transferring of the char was performed in air prior to the char burn experiments. This sorbed oxygen was removed during the warm-up phase prior to the char burning experiments. A slow nitrogen purge of 0.05 L/minute was maintained during heating until the target temperature was attained. The nitrogen flow was then increased so that exhaust gas CO/CO_2 concentrations could be monitored. The supply gases were not admitted until after the CO concentration leveled indicating that all sorbed oxygen was removed.

RESULTS AND DISCUSSION

The first three sections of the Results and Discussion pertain to the three focal points of the experimental program - the CO/CO_2 product of the carbon-sulfate reaction, the CO/CO_2 product of char burning and the char burning rate. A conceptual model of char pile burning is then presented, followed by some implications from this investigation.

THE CO/CO_2 PRODUCT OF THE CARBON-SULFATE REACTION

The primary emphasis of this study was to quantify the factors affecting the CO/CO_2 product of the carbon-sulfate reaction. The results of Cameron's smelt pool reactor studies indicated that CO_2 was the principal product for conditions where the carbon/sulfate ratio was near-stoichiometric (2:1). The CO/CO_2 ratios measured were 0.1 or less. My results for kraft black liquor char spiked with sulfate yielded a CO/CO_2 of 20:1. In this case, there was a stoichiometric excess of carbon to sulfate of about 37:1. One factor that may have a large effect on the CO/CO_2 reaction product is the carbon/sulfate ratio.

Description

These experiments were designed to determine the effects of the carbon/sulfate ratio and temperature on the CO/CO_2 product of the carbon-sulfate reaction. The starting material was a kraft char, sodium sulfate, sodium carbonate mixture that was ground then placed in the induction furnace reactor. Three different initial carbon/sulfate levels were studied: 2/1, 4/1, and 6/1. Temperatures ranged from 1033 to 1113°K (1400 to 1543°F). The temperature was raised to the target and controlled at that temperature for the duration of the experiment. The initial sulfidity, Eq. (7), was 0.33 for all experiments.

$$\text{sulfidity} = \frac{Na_2S + Na_2SO_4}{Na_2S + Na_2SO_4 + Na_2CO_3} \qquad (7)$$

The amounts of carbon and sulfate in the mixture dropped as the reaction proceeded. The relative amounts of carbon and sulfate were monitored as the elemental fixed-carbon to oxygen ratio (the C/O ratio). The C/O ratio was chosen, rather than the C/SO_4, because the sulfate added was not the only oxygen source. Oxygen sorbed by the char was also present.

The C/O level in the mixture, at any time during the run, was calculated by subtracting the total moles of C and O evolved in the exhaust gases up to that time (as CO and CO_2) from the initial moles of C and O, then dividing the moles of C by the moles of O. This technique yields good results when analyzing the results of a particular experiment for if the CO/CO_2 analyzer is slightly out of calibration, it affects the moles of C and O to about the same extent. Comparing the results of different experiments is more difficult, however, because any small inaccuracies in CO/CO_2 concentrations are greatly magnified by the subtraction from initial value technique. This puts a premium on the calibration of the CO/CO_2 analyzer and the estimation of the initial amounts of C and O present.

The initial mass of fixed-carbon is obtained by multiplying the mass of the char by the fixed-carbon concentration. Computation of the initial mass of oxygen is complicated by the fact that kraft char readily sorbs oxygen. The oxygen content of the sulfate and the oxygen content of the char must be taken into account.

The initial moles of oxygen were back-calculated by integrating the total amount of oxygen in the CO and CO_2 generated during the sulfate-limited experiments, with initial carbon/sulfate ratios of 4/1 and 6/1. Since sulfate was the limiting reactant, all the oxygen present in the mixture should have evolved upon heating. The ratio of the oxygen supplied by sulfate to the total amount of oxygen generated was 0.88 and 0.92 for Experiments 77 and 78, respectively (Appendix XI).

The initial moles of oxygen were principally the oxygen content of the sulfate for the four carbon-limited experiments, Experiments 71 to 74, with an initial carbon/sulfate of 2/1. Ninety-five percent of the oxygen was supplied by the sulfate with only 5% supplied by the char (Appendix XI). This assumes that no sorbed oxygen remained at the end of the experiments. Laurendeau suggests that for coal, this assumption is warranted.[12] At temperatures greater than 973°K, all coal chars have similar C, H, O contents, regardless of the methods of pretreatment. In other words, oxygen sorbed by the coal char at ambient conditions is evolved upon heating at less than 973°K. Kraft char should behave similarly. Since temperatures were greater than 1033°K for all experiments, the sorbed oxygen should have been released as CO and CO_2 during heating.

Results

Before presenting the results of the CO/CO_2 product of the carbon-sulfate reaction, it first must be demonstrated that the data obtained using this experimental system were consistent with previous studies and not an artifact of the technique. The activation energy of the carbon-sulfate reaction was calculated to determine whether the data generated were similar to the results obtained by Cameron.[8]

An activation energy of 105 kJ/mole (25.1 kcal/mole) was calculated from the 1033, 1077, and 1113°K (1400, 1479, and 1543°F) experiments, Experiments 71, 72, and 73, respectively, at a time when identical C/O ratios were calculated (Fig. 13). This activation energy is similar to the 122 kJ/mole (29.20 kcal/mole) determined by Cameron using a smelt pool reactor. The fact that the measured activation energy is high suggests that the reaction rate was controlled by chemical kinetics and not mass transfer limited.[17]

I would like to turn to the crux of this portion of my studies - the CO/CO_2 product of the carbon-sulfate reaction. Four experiments were run with different initial C/O ratios at 1077°K (1479°F). Two experiments were run holding the initial C/O constant at 1033 and 1113°K (1400 and 1543°F) to determine the temperature dependence.

Assume that the CO/CO_2 product can be represented by Eq. (8).

$$\frac{CO}{CO_2} = A \left(\frac{C}{O}\right)^n \exp\left(-\frac{E}{RT}\right) \tag{8}$$

Laurendeau reported that an equation of that form, without the C/O term, described the CO/CO_2 product of coal combustion.[12] This equation can also be expressed as Eq. (9).

$$\ln \frac{CO}{CO_2} = n \ln \frac{C}{O} + \ln A - \frac{E}{RT} \tag{9}$$

If the temperature is constant, the temperature-dependent term can be included in A', Eq. (10).

$$\ln CO/CO_2 = n (\ln C/O) + \ln A' \tag{10}$$

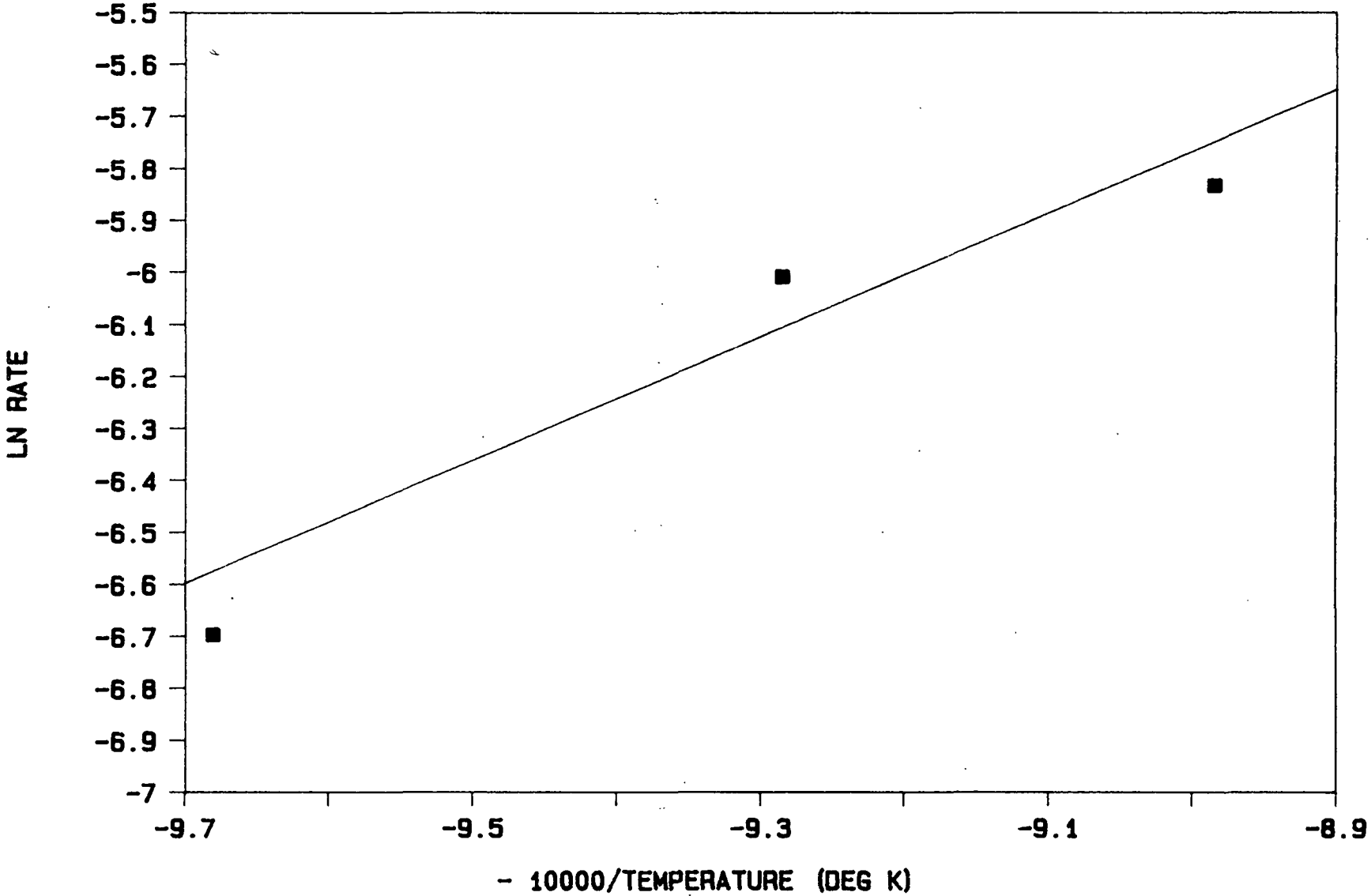

Figure 13. Activation energy of sulfate reduction by carbon.

The ln C/O is plotted versus the ln CO/CO_2 in Fig. 14, for the 1077°K (1479°F) data. A linear regression analysis of the data resulted in Eq. (11).

$$\ln CO/CO_2 = 0.931 \ln C/O - 0.736 \quad (11)$$

The r^2 calculated was 0.94. The CO/CO_2 ratio is a strong function of the C/O ratio of the char. The data suggest that n = 1. A linear regression analysis of the data with n = 1 resulted in Eq. (12), with an r^2 of 0.86.

$$\frac{CO}{CO_2} = 0.403 \frac{C}{O} \quad (12)$$

At low C/O ratios, temperature did not significantly affect the CO/CO_2 ratio. A weak temperature dependence was anticipated from the coal char burning literature. Laurendeau[12] reports an E value in Eq. (8) ranging from 25 to 38 kJ/mole (6 to 9 kcal/mole).

THE CO/CO_2 PRODUCT OF CHAR BURNING

This study was directed at determining the CO/CO_2 ratio in the gases generated by the char pile reactions during char burning. The CO/CO_2 ratio measured by the exhaust gas analyzer may not be indicative of the char pile reaction products due to the gas-phase oxidation of CO. The gas-phase oxidation of CO experiments determined the temperature where this reaction became significant.

Gas-Phase Oxidation of CO

A "placebo reactor" was used to study the gas-phase oxidation of carbon monoxide (Fig. 15). Ceramic chips were placed in the reactor up to the level normally occupied by char in the char burning experiments. Carbon monoxide, air

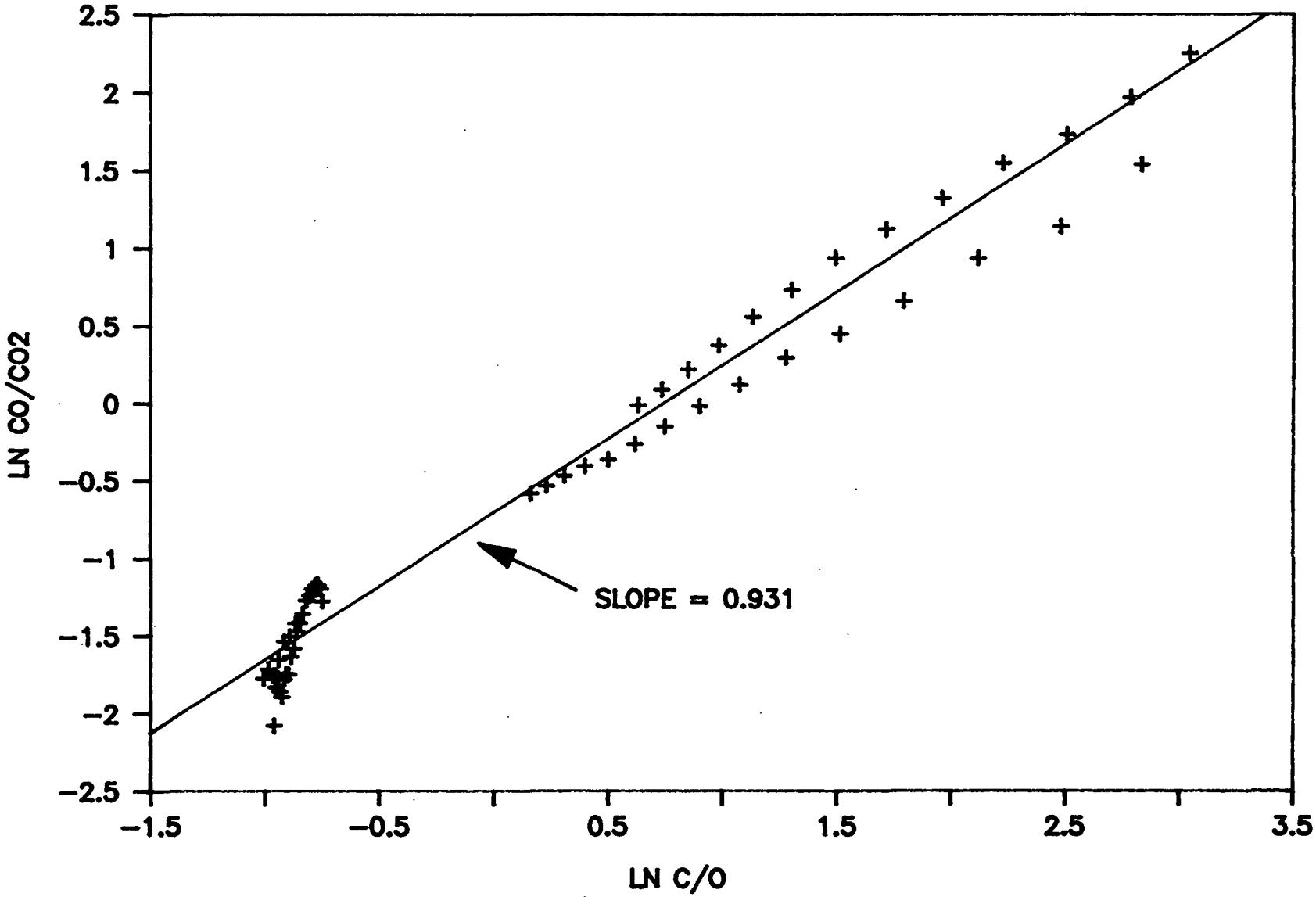

Figure 14. CO/CO_2 product of carbon-sulfate reaction.

and nitrogen were metered into the supply gas line. A radiation-shielded thermocouple measured the gas-phase temperature. Otherwise, the apparatus was identical to that used for the char burning experiments.

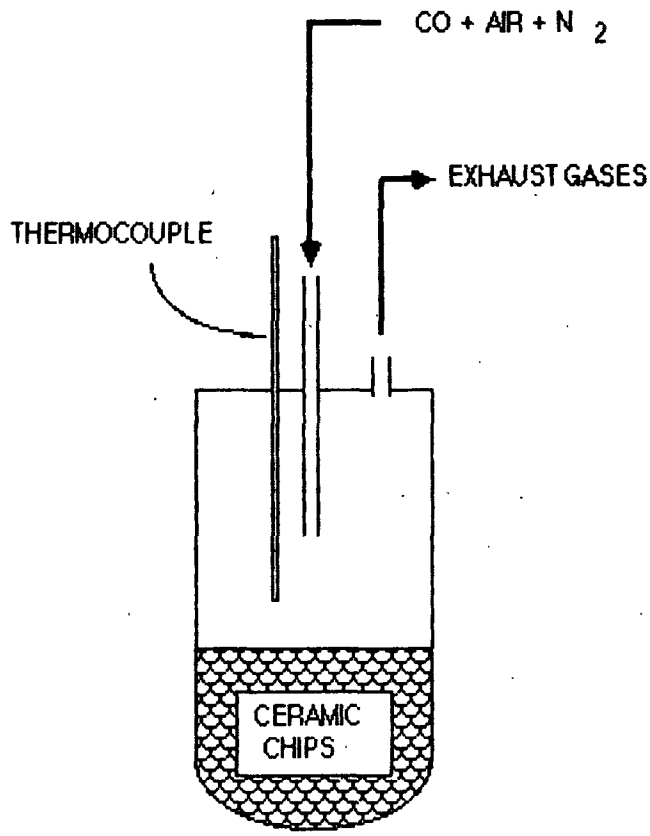

Figure 15. Placebo reactor.

At 1010°K (1359°F) most of the CO did not react with O_2 to form CO_2 whereas at 1050°K (1430°F) the CO_2 product predominated (Table 16, Experiment 37A). There is a sharp break point at approximately 1030°K (1394°F) where the gas-phase oxidation of CO becomes significant. These results were obtained for a hydrogen-free system. The presence of water in the supply gas lowered the transition temperature approximately 111°K (200°F).

Table 16. Gas-phase oxidation of CO results.

Gas Temperature	Exhaust Gas Composition		
	% CO	% CO_2	% O_2
1010°K (1359°F)	2.9	0.9	1.6
1027°K (1389°F)	2.1	1.9	1.0
1050°K (1430°F)	0.9	3.1	0.5

Since temperatures were greater than 1030°K (1394°F) for nearly all char burning experiments, the gas-phase oxidation of CO is a reaction that must be considered when analyzing the char burning data.

Char Burning Experiments

This series of char burning experiments was run to determine the CO/CO_2 product of kraft char burning, when an oxygen/nitrogen supply gas stream was impinged on the char surface. This differs from the previous carbon-sulfate reaction experiments because oxygen in the supply gases is the oxygen source for fixed-carbon combustion, rather than the oxygen in the sulfate.

Description

The fixed-carbon concentration of the char source for this series of experiments was 23.4 ± 1.0%; the total sulfur was 6.8%. Measured temperatures ranged from 1221 to 1420°K (1348 to 1605°F). One 1/16-inch thermocouple was located at a radial position near the crucible wall, a second was in the center of the impingement area; both were positioned 0 to 2 mm above the char surface at the beginning of the experiment.

A nitrogen flow rate of 0.05 L/min was maintained as the reactor was heated. When the temperature stabilized at the target temperature, a supply gas of 2.1,

4.2 or 10.5% O_2 was impinged on the char surface at a total flow rate of about 1.0 L/min. To determine the $CO/(CO + CO_2)$ off the char pile, the air flow was cut and the nitrogen flow simultaneously increased to maintain the 1.0 L/min flow rate. The $CO/(CO + CO_2)$ representative of the off char pile gases for each experimental condition was calculated after the cutting of air flow when oxygen was no longer detected in the exhaust gases.

Examples

Experiments 58 and 59 are chosen as examples because they demonstrate the technique and confirm the validity of the method.

Figure 16 shows the effect of cutting the air flow at 1022°K (1380°F) with 4.2% O_2. Prior to air flow termination, the CO, CO_2, and O_2 concentrations are fairly constant at 2.1, 1.1, and 1.6%, respectively. After air flow termination at the 21.92-minute mark, the CO_2 and O_2 concentrations drop rapidly. The CO concentration, on the other hand, increases before decreasing slowly with time.

I believe that the drop in oxygen concentration, after the air flow was cut, immediately reduces the amount of gas-phase oxidation of CO to CO_2. The char pile reactions, however, are initially less affected by the termination of oxygen in the supply gases than the gas-phase reaction. The termination of air flow therefore results in an increase in CO initially due to the combined effect of the sudden drop in the CO-consuming, gas-phase oxidation reaction and the slow response of the CO-generating char pile reactions. When these char pile reactions eventually respond to the lack of oxygen in the supply gases, the CO concentration gradually decreases with time.

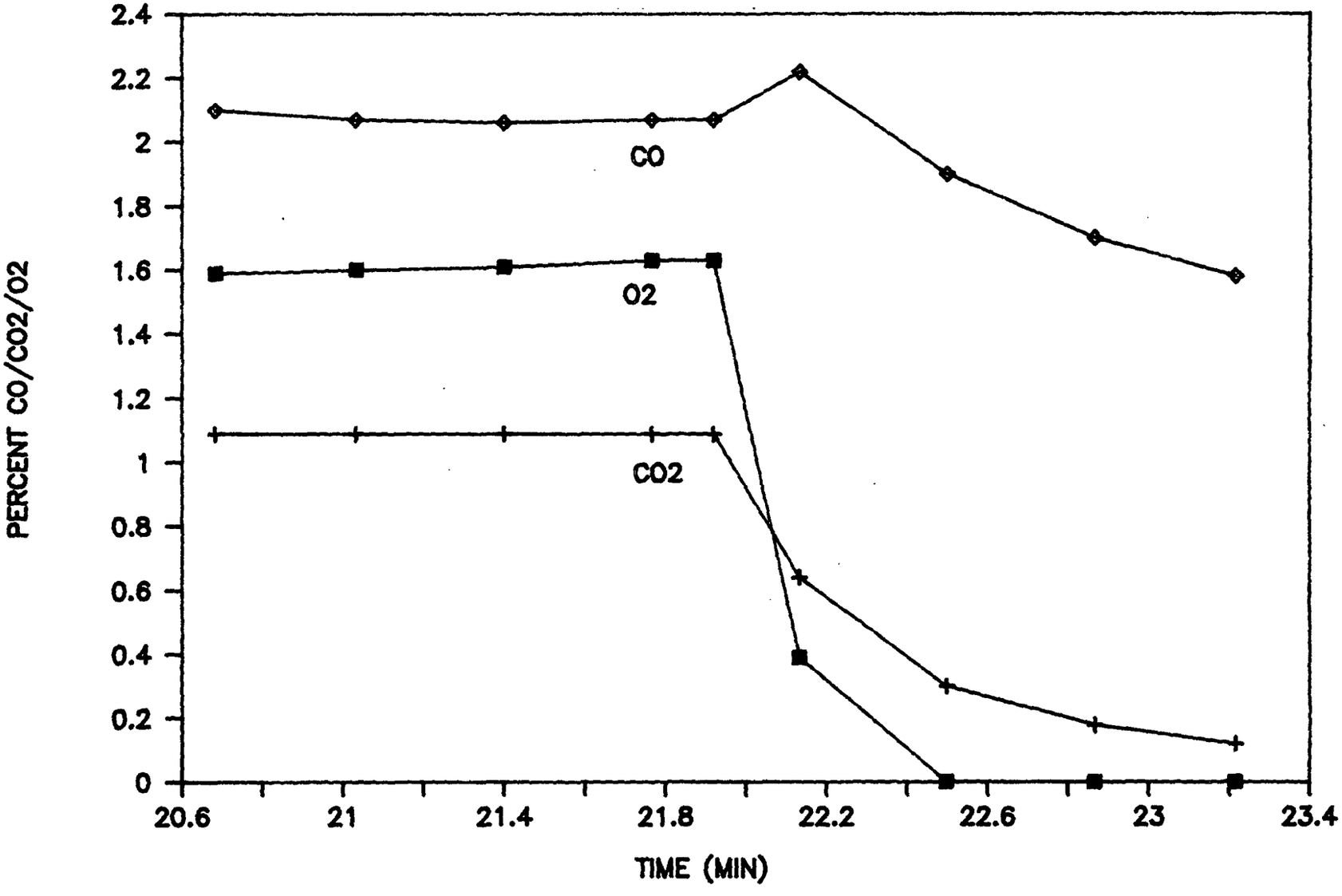

Figure 16. Example 1 - Char pile $CO/(CO + CO_2)$ determination.

The $CO/(CO + CO_2)$ measured at the 22.5-minute mark of Fig. 16 should be representative of the gaseous product of char pile reactions without the complications of the gas-phase oxidation of CO. The $CO/(CO + CO_2)$ just prior to the cutting of air flow was 0.66. The $CO/(CO + CO_2)$ determined at the 22.5-minute mark, after air flow termination, was 0.86. The gas phase oxidation of CO to CO_2 is significant for this example.

Figure 17 shows the effects of cutting the air flow at 1083°K (1490°F) with 10.5% O_2. The termination of air flow at the 9.1-minute mark results in a dramatic flip-flop in CO and CO_2 concentrations.

I believe that this is solid evidence supporting the hypothesis that the rapid drop in CO_2 upon air flow termination is due to the stopping of the gas-phase oxidation of CO. If the CO_2 and CO both dropped after air-flow termination, but at different rates, one could argue that two parallel heterogeneous reactions are responsible for the CO and CO_2 generated. Perhaps the carbon-sulfate reaction produced the CO while direct carbon oxidation produced the CO_2. The fact that the CO <u>increases</u> upon air flow termination refutes this hypothesis. It is difficult to conceive of a plausible mechanism whereby the rate of a heterogeneous oxidation reaction will <u>increase</u> upon the termination of air flow.

The $CO/(CO + CO_2)$ measured in the exhaust gases just prior to air flow termination was 0.06. The off char pile $CO/(CO + CO_2)$ calculated at the 9.8-minute mark in Fig. 14 is 0.82. The amount of gas-phase oxidation of CO to CO_2 was very substantial in this instance. This $CO/(CO + CO_2)$ of 0.80 is nearly identical to the 0.86 determined in Fig. 13.

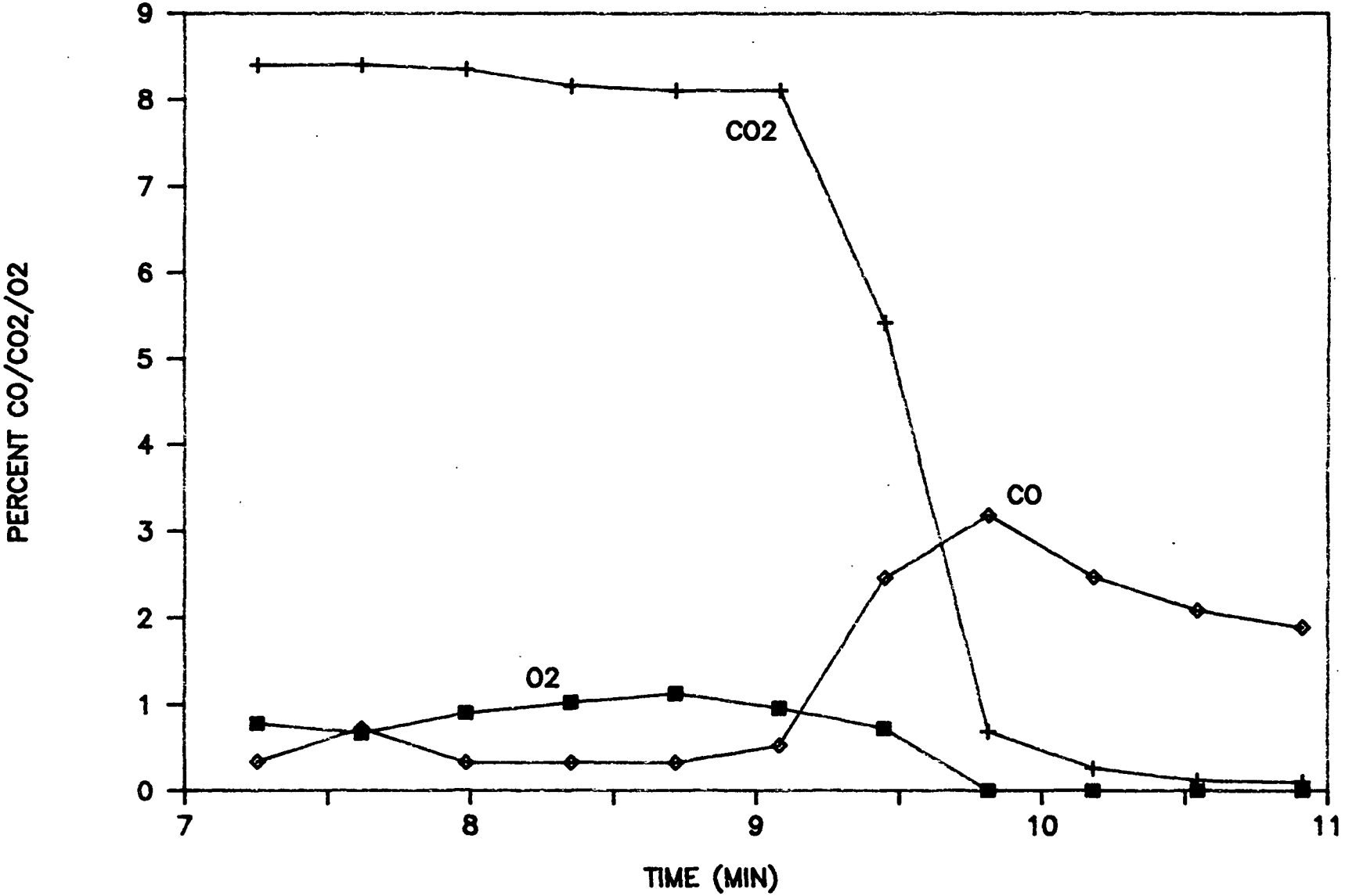

Figure 17. Example 2 - Char pile $CO/(CO + CO_2)$ determination.

Results

The results of all the CO/CO_2 product of char burning experiments are listed in Table 17. The $CO/(CO + CO_2)$ recorded just prior to air flow termination is given as "exhaust gas." The $CO/(CO + CO_2)$ recorded after air flow termination, when the measured O_2 concentration was less than 0.15%, is listed as "off char pile." The ranges listed for each "$CO/(CO + CO_2)$" and "temperature" entry represent the range of values recorded for the four to six times during each experimental run that the air flow was cut. The $CO/(CO + CO_2)$ is listed, rather than the CO/CO_2, because at high CO/CO_2 values a small change in CO_2 results in a dramatic change in the CO/CO_2.

Table 17. Results of CO/CO_2 product of char burning experiments.

Temperature, °K	Percent O_2	$CO/(CO + CO_2)$	
		Exhaust Gas	Off Char Pile
1004-1012	2.1	0.78-0.92	0.88-0.92
1019-1024	4.2	0.65-0.79	0.86-0.90
1049-1083	10.5	0.06-0.71	0.80-0.86
1089-1093	2.1	0.74-0.78	0.83-0.94
1076-1082	4.2	0.77-0.84	0.87-0.90
1097-1100	10.5	0.72-0.80	0.81-0.90
1098-1111	2.1	0.83-0.88	0.96
1108-1116	4.2	0.78-0.82	0.84-0.91
1141-1154	10.5	0.74-0.82	0.83-0.90

The data given in Table 17 suggest that:

- CO is the principal char pile combustion product for all experimental conditions, with the $CO/(CO + CO_2)$ ratio ranging from 0.80 to 0.96.
- The $CO/(CO + CO_2)$ is not dependent upon temperature, time, or supply gas oxygen concentration for all conditions studied.

- The amount of gas-phase oxidation of CO to CO_2 can be quite significant.

SMELT/CHAR WETTABILITY

The smelt product of char burning did not flow through the char and collect in the bottom of the crucible; rather, the smelt beaded on the char surface. The following analysis determined that the beading behavior was due to poor wetting of the char by the smelt and not due to the small char particle sizes.

Whether a liquid "wets" a solid surface is dependent upon the contact angle between the liquid and the solid, Θ, as discussed by Adamson[18] and given in Eq. (13).

$$\cos \Theta = (\gamma_{SV} - \gamma_{SL})/\gamma_{LV} \qquad (13)$$

where: Θ = contact angle

γ_{SV} = solid-vapor surface tension

γ_{SL} = solid-liquid surface tension

γ_{LV} = liquid-vapor surface tension

A contact angle of near zero indicates that the liquid readily wets the solid surface. A contact angle of greater than 90° indicates the liquid is nonwetting. The liquid balls up and easily runs off the solid surface.

Although data are reported for the γ_{LV} term of Eq. (13) for various Na_2CO_3/Na_2S mixtures at 1089 to 1283°K, which should be representative of kraft smelt, the γ_{SV} and γ_{SL} terms are not reported nor easily obtained. Whether the contact angle is suggestive of wetting or nonwetting behavior can be inferred from the Washburn equation, Eq. (14), also discussed by Adamson.[18] This equation

$$v = \frac{r\gamma_{LV} \cos}{4\eta l} \qquad (14)$$

where: v = rate of liquid penetration

r = pore radius

γ_{LV} = liquid-vapor surface tension

η = viscosity

l = length of liquid column

suggests that the velocity of a liquid flowing through a pore can be estimated from the pore radius, the surface tension, the viscosity and the contact angle, when the contact angle is less than 90°. If the contact angle is greater than 90°, the cos Θ is negative and the liquid will not penetrate into the pore.

There are two possible reasons why the smelt collects on the char surface: either the contact angle is greater than 90° or the contact angle is less than 90°, but the rate of smelt penetration is extremely slow, limited by the diameter of the small interparticular pores. Literature reported values of μ_{LV} = 210 dynes/cm and η = 4.5 cp, given by Krause[19] along with a "l" of 0.1 mm and a pore radius of 1.06×10^{-3} cm (see Appendix XII) were used to estimate the rates of smelt penetration into the char at various contact angles (Table 18). This calculation suggests that even for an 89° contact angle, the penetration velocity is significant. Therefore, the small particle sizes and thus the small interparticular pores are not responsible for the smelt beading behavior on the char surface. This suggests that the contact angle is greater than 90° and thus the smelt is "nonwetting."

Table 18. Estimate of smelt penetration rate using Washburn equation.

Contact Angle	Penetration Velocity (cm/s)
0	12.4
45	8.8
89	0.22

CHAR BURNING RATE

This portion of my thesis was directed at determining the factors affecting the char burning rate with combustion air as the oxygen source for fixed-carbon oxidation.

Description

The char source for this series of experiments was from the same batch as the char used for the CO/CO_2 product of char burning studies. The fixed-carbon concentration was 23.4 ± 1.0% and the total sulfur was 6.8%. Temperatures 1 to 2 mm above the char surface ranged from 1029 to 1194°K (1390 to 1690°F). The experiments were grouped into three sets: low temperature (1029 to 1061°K), moderate temperature (1076 to 1108°K) and high temperature (1121 to 1209°K). A set consisted of three different experiments, one with a supply gas of 2.1% O_2, a second with a supply gas of 4.2% O_2 and a third with a supply gas of 10.5% O_2. The supply gases were impinged on the surface of the char at a total flow rate of about 1.0 L/min. A slow nitrogen purge was directed over the char surface until the target temperature was attained, then the O_2/N_2 mixtures were admitted at a total flow rate of 1.0 L/min.

Postrun morphological examination of the char revealed that there were distinct zones in the reactor. Sulfur-species concentration determinations of the samples obtained from the impingement, nonimpingement and subsurface zones aided experimental analysis.

Examples

The results of Experiments 47, 53, and 55 are chosen as examples since they are representative of this series of experiments.

Figure 18 shows the exhaust gas composition results with 2.1% O_2 and temperatures between 1189 and 1194°K (1680 and 1690°F) as measured by the radial thermocouple. For the 18.5 minutes that air was supplied to the reactor, the rates of CO and CO_2 generation were fairly constant.

Figure 19 shows the exhaust gas composition results with 10.5% O_2 and temperatures between 1053 and 1067°K (1435 and 1460°F) as measured by the radial thermocouple and between 1031 to 1052°K (1396 to 1433°F) as measured by the center thermocouple. The rates of CO and CO_2 generation stabilized after about five minutes of air exposure. The CO and CO_2 concentrations remained fairly constant from this point onward; the CO dropped slightly at the 32-minute mark.

Figure 20 shows the exhaust gas composition results with 4.2% O_2 and temperatures between 1098 and 1106°K (1517 and 1530°F) as measured by the radial thermocouple and between 1076 and 1092°K (1476 and 1506°F) as measured by the center thermocouple. The rates of CO and CO_2 generation stabilized within a few minutes and remained extremely constant throughout the thirty-minute experiment.

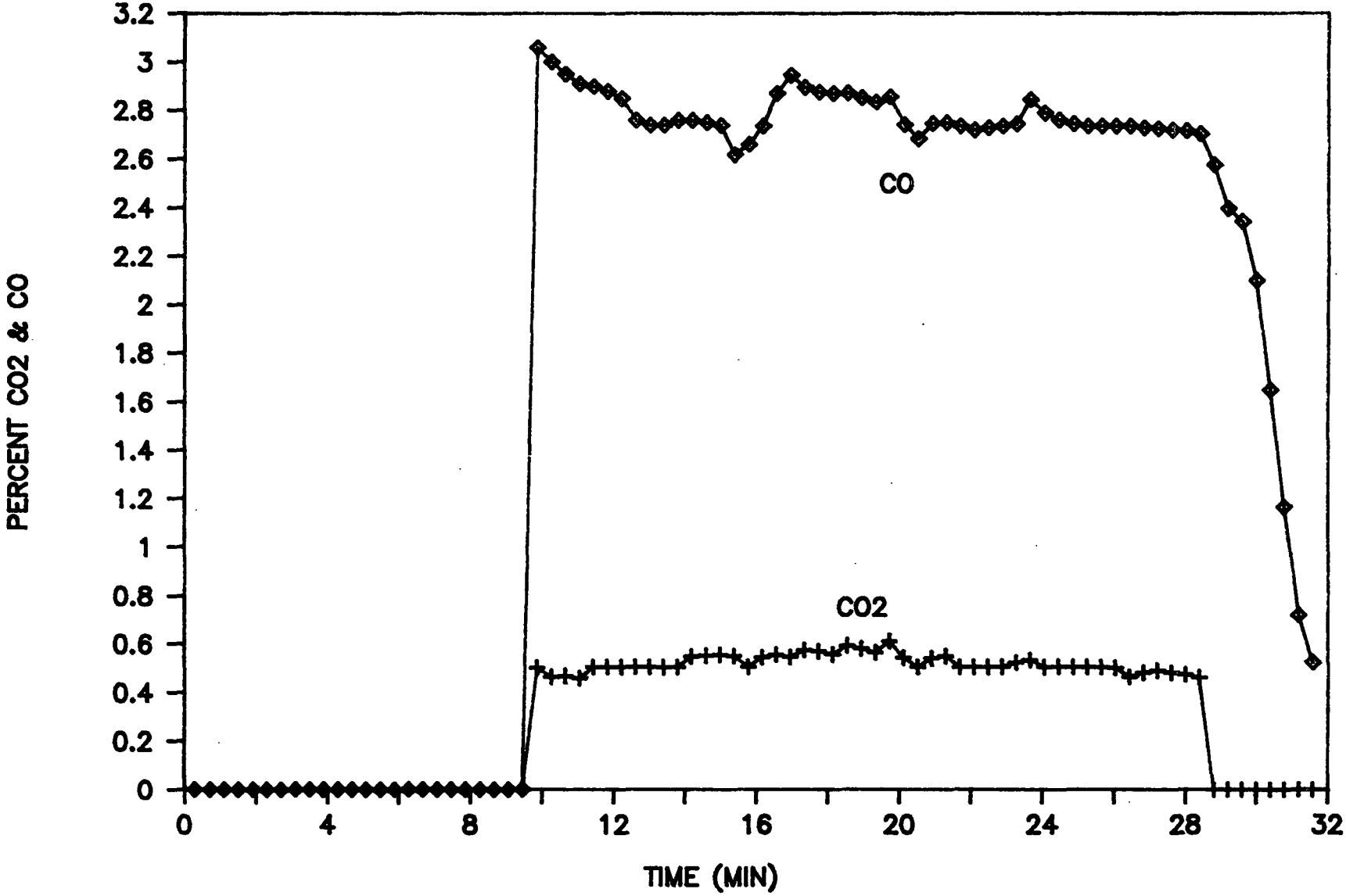

Figure 18. Char burning rate - Example 1: 2.1% O_2, high temperature.

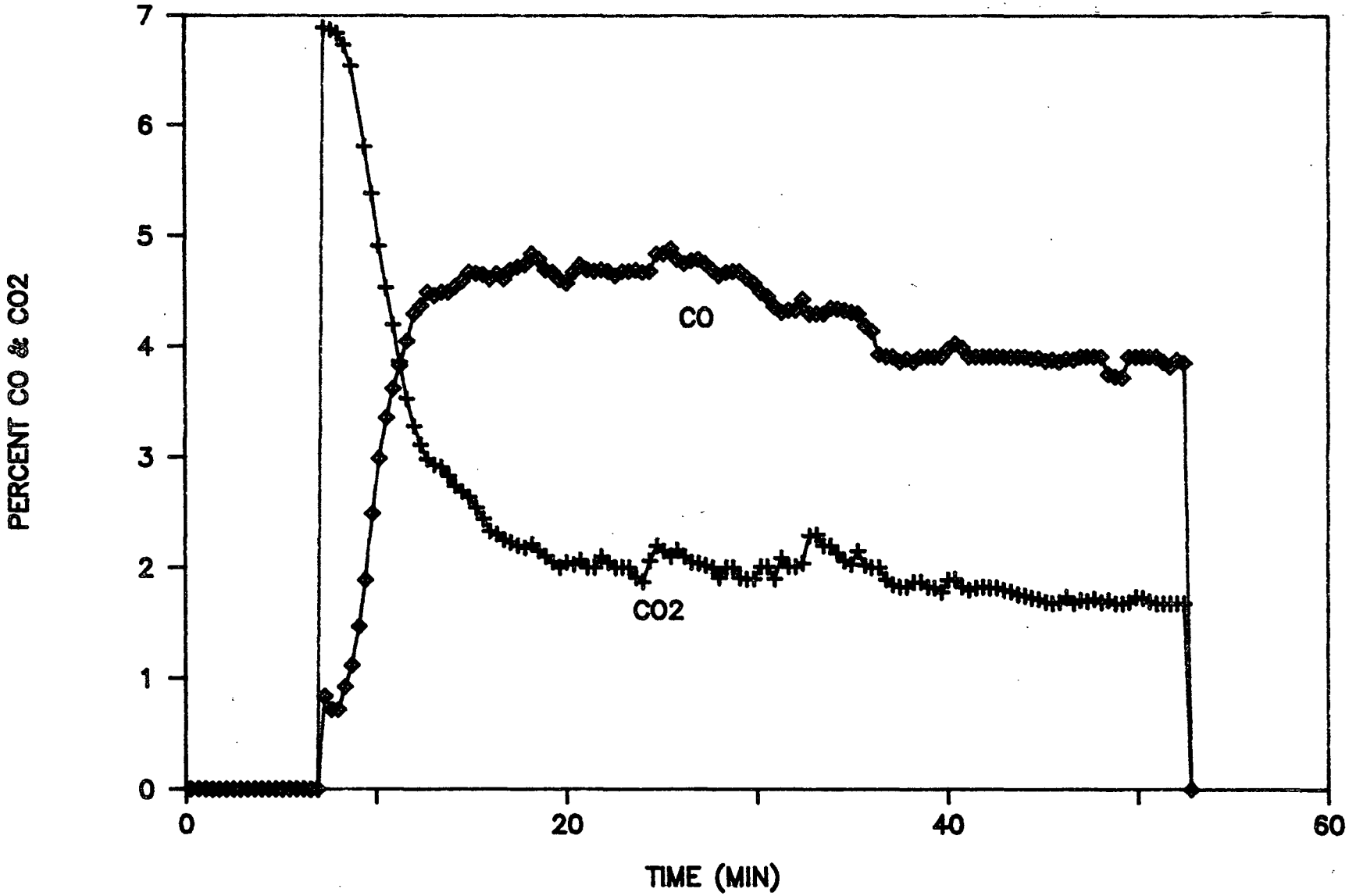

Figure 19. Char burning rate - Example 2: 10.5% O_2, low temperature.

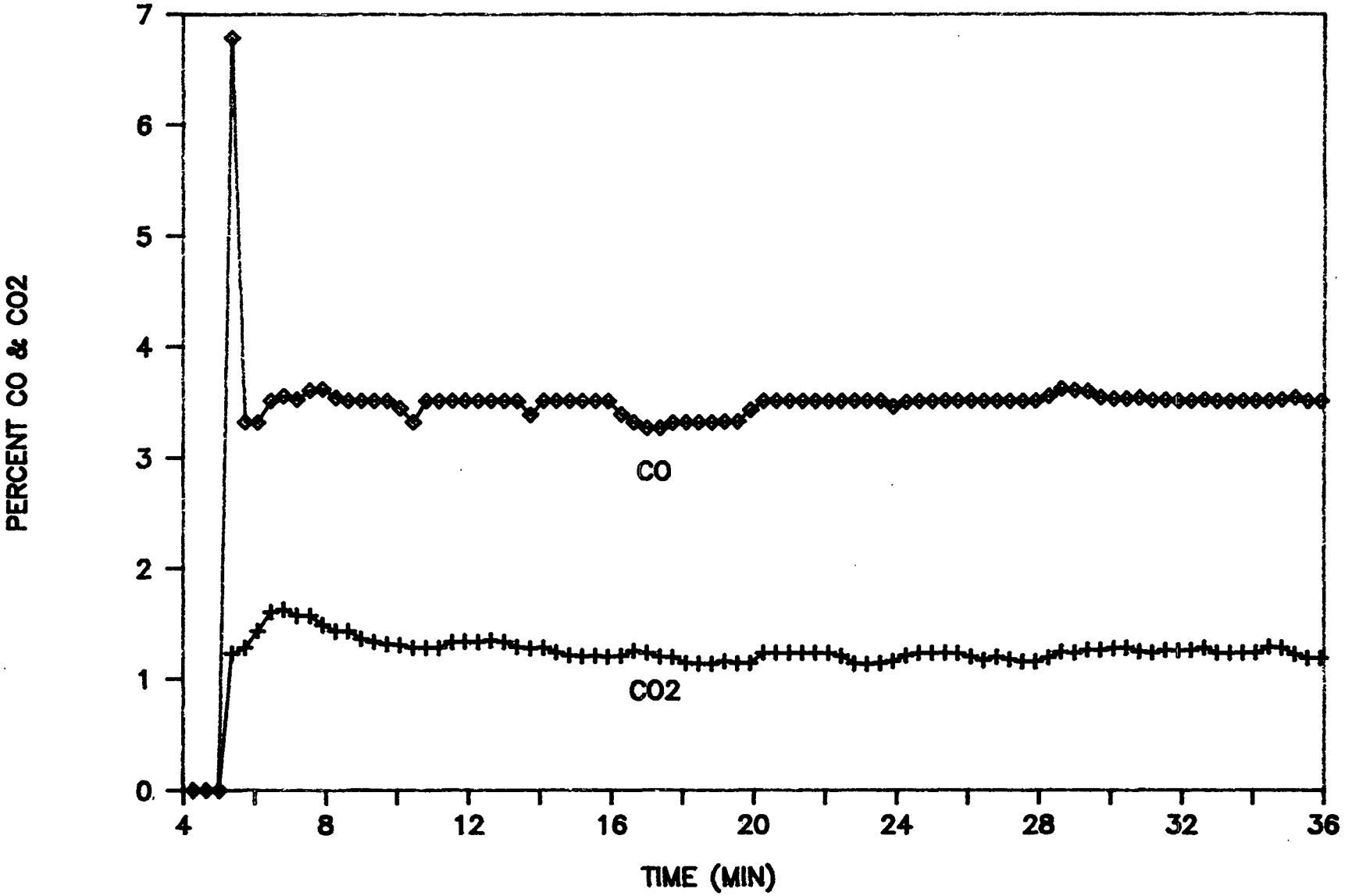

Figure 20. Char burning rate - Example 3: 4.2% O_2, moderate temperature.

The results of these experiments show the rates of CO and CO_2 generation to be fairly constant throughout each experiment, except with 10.5% O_2 at low temperature. The graphical results of the nine experiments of this series, included in Appendix XIII, show that the only other exception was with 10.5% O_2 at moderate temperature. It is surprising that the rates of CO and CO_2 generation remain constant while gross changes in char surface morphology are occurring, as shown in Fig. 7 and 8 earlier.

Theoretical Analysis

When analyzing the factors affecting the rate of heterogeneous reactions, there are two extremes to be considered:

- The rate of diffusion of the gaseous species to the solid may be rate controlling.
- The kinetics of the gas-solid reaction may be rate controlling.

Between these extremes is the transitional regime where the rate is controlled by a combination of mass transfer and chemical kinetics.

The sulfate/sulfide theory of char burning can be analyzed in these terms. Since the oxidation of sulfide to sulfate is a fast reaction, it is an insignificant resistance to the rate of the heterogeneous reaction. Therefore, when studying the char burning rate, the two extremes are:

- The rate of oxygen mass transfer to the char may be rate controlling.
- The kinetics of the carbon-sulfate reaction may be rate controlling.

The rates are controlled by a combination of oxygen mass transfer and carbon-sulfate kinetics for the transitional regime in-between.

Results

Sulfur-Species Analysis Results

The results of the sulfur-species analyses for the samples removed from the reactor after a char burning experiment should provide insights regarding the controlling mechanism:

- The measurement of a high sulfate concentration (or a low reduction ratio) would suggest that the sample was removed from a region where carbon-sulfate kinetics were rate-limiting.

  The measurement of a high sulfide concentration (or a high reduction ratio) would suggest that the sample was removed from a region where the rate of oxygen mass transfer was rate controlling.

  The measurement of a low sulfate concentration for a sample from a low pO_2 experiment, but with increasing sulfate concentrations with increasing pO_2 would suggest that the sample was removed from a region where the rate was controlled by both oxygen mass transfer and carbon-sulfate kinetics.

The sulfur-species analyses of the source char and the various sampling regions after the char burning experiments are given in Table 19. The reduction ratios were calculated assuming that the $SO_3^=$ and $S_2O_3^=$ were insignificant. The low levels reported could have been created during the dilution stage of the ion chromatograph analysis procedure and thus be artifacts of the technique. In most cases, the composition of the surface fractions is much different at the end of the run than that of the source material. As discussed previously, the char surface morphology changed greatly during an experiment. The fact that the compositions vary is not surprising.

Table 19. Sulfur-species analysis results.

(Percent S of each species on a weight basis)

Range	Percent O_2	Location	$SO_3^=$	$S_2O_3^=$	$SO_4^=$	$S^=$	Reduction Ratio
		Source char	0.3	0.3	0.3	5.6	0.95
Low	2.1	Impingement	0.2	--	1.7	2.5	0.60
Temperature	4.2	Impingement	0.2	--	2.7	2.3	0.46
Set	10.5	Impingement	0.2	--	3.5	2.6	0.43
	2.1	Impingement	0.3	--	2.0	3.5	0.64
Moderate		Surface	0.4	0.3	0.1	5.1	0.98
Temperature	4.2	Impingement	0.3	--	2.5	3.2	0.56
Set		Surface	0.5	0.4	0.6	5.8	0.91
	10.5	Impingement	0.2	--	4.8	0.9	0.16
		Surface	0.4	0.4	0.4	6.7	0.94
	2.1	Impingement	0.3	0.3	0.2	3.8	0.95
High		Surface	0.2	0.8	0.1	3.3	0.97
Temperature	4.2	Impingement	0.3	0.2	0.2	5.4	0.96
Set		Surface	0.1	0.3	0.1	3.1	0.97
	10.5	Impingement	0.4	0.3	0.1	6.9	0.99
		Surface	0.3	0.4	0.3	6.3	0.95

The following observations can be made from the data of Table 19:

For all experimental conditions and sample locations at high temperatures (1121 to 1209°K), sulfide was the only significant sulfur species with reduction ratios ranging from 0.95 to 0.99.

For lower temperatures (1029 to 1108°K), the sulfate concentration increased with increasing oxygen concentrations for the samples from the impingement region. In the other regions, sulfide was the only significant sulfur species with reduction ratios ranging from 0.91 to 0.98.

The char surface morphology and sample location must be considered when interpreting the sulfur-species data because they were not identical for each set of experiments. At high temperatures, the smelt was confined to the impingement area. The nonimpingement area, the bulk of the exposed surface that surrounded the smelt pool, was charlike, with some small smelt drops on the surface. At moderate temperatures, the smelt was not confined to the area of supply gas impingement but covered a portion of the nonimpingement surface region. At low temperatures, a thin layer of smelt spread across the entire surface.

At low temperatures, the sulfate concentration of the impingement sample increased directly with pO_2. This suggests that the char burning rate is in the transitional regime where both oxygen mass transfer and carbon-sulfate kinetics are significant. For the 10.5% O_2 case where the measured sulfate is the highest, kinetic control is dominating. Kinetic control is being approached across the entire surface since the smelt was spread uniformly over the char at low temperatures.

At moderate temperatures, the sulfate concentration of the impingement region samples also increases directly with pO_2. This suggests that char burning was also in the transitional regime in the impingement region and approaching kinetic control with 10.5% O_2. However this was not the case across the entire surface because the impingement region smelt covered less than 50% of the char surface. In the nonimpingement surface samples, the sulfide was high, with reduction ratios greater than 0.91. Therefore a mixed-mode char burning rate dependence is anticipated at moderate temperatures since the data suggest

that char burning is approaching kinetic control with 10.5% O_2 in the impingement region whereas in the nonimpingement surface region, char burning is oxygen mass transfer limited.

Analysis of the high temperature samples revealed that the reduction ratio was high in all regions. This suggests that char burning is oxygen mass transfer limited across the entire surface at high temperatures.

Char Burning Rates

The char burning rate was monitored by summing the rates of CO and CO_2 generation. The rate of CO + CO_2 generation results of Experiments 47, and 49 through 56 are summarized in Table 20. For Experiments 53 and 56, the rates of CO generation did not remain constant with time. These are the 10.5% O_2 results at low and moderate temperatures where high sulfate concentrations in the impingement samples suggested kinetic control was being approached. In these experiments, the rates of CO and CO_2 generation were constant for plateaus early and late in the runs. In Table 20, the average rates of CO + CO_2 generation during both constant generation periods are listed. The temperatures are those measured by the center thermocouple, early in the run. This temperature was chosen because the thermocouples should be close to the surface and thus giving the most accurate surface temperature readings. The center temperature was selected since the thermocouple was located in the center of the impingement region, where most of the reactions were occurring, as shown by the postrun morphological examinations.

The char burning rate data can be used to suggest whether the rate is controlled by carbon-sulfate kinetics, oxygen mass transfer, or a transitional regime where both mechanisms are significant.

Table 20. Char burning rate.

Experiment Number	Oxygen Partial Pressure (atm)	Time[a] (min)	$\frac{dCO}{dt}$ (mmol/min)	$\frac{dCO_2}{dt}$ (mmol/min)	$\frac{dCO + dCO_2}{dt \quad dt}$ (mmol/min)	T (°K)
51	0.021	25-40	0.695	0.231	0.926	1039
52	0.042	28-40	0.944	0.254	1.198	1032
53	0.105	20-30	2.214	0.951	3.165	1041
53	0.105	37-40	1.807	0.851	2.658	1041
54	0.021	20-30	0.831	0.305	1.136	1083
55	0.042	10-35	1.605	0.568	2.173	1083
56	0.105	12-22	3.647	1.274	4.921	1089
56	0.105	30-37	2.844	1.150	3.994	1089
47	0.021	12-28	1.135	0.216	1.351	1178
48	0.042	5-22	1.892	0.440	2.332	1181
50	0.105	6-12	4.575	1.733	6.308	1197

[a]The data acquisition program was started at time zero, usually 5 minutes prior to the time of O_2 addition.

Theoretical Analysis - Kinetic Model

A kinetic model was developed to determine whether carbon-sulfate kinetics adequately describe the char burning data. The basis for this model is the rate equation developed by Cameron for the carbon-sulfate reaction, given in Eq. (2).

$$-d[SO_4]/dt = \frac{k_1[C]\ [SO_4]}{1 + k_4[SO_4]} \exp \frac{(-Ea)}{RT} \qquad (2)$$

Assumptions

1. The carbon concentration of the reaction zone is constant. This zone is slowly moving downward into the unreacted subsurface char layer. If carbon-sulfate kinetics control the rate, then the carbon concentration should be rate controlling. In all experiments, the char burning rate was fairly constant after a 5-minute induction period. If the carbon concentration was changing, the rate of CO/CO_2 generation should have also been changing.

2. The carbon concentration of the reaction zone is 0.12 gram C/gram total. The calculation of this average concentration is based on Eq. (2) with constant temperature, steady-state conditions and a carbon concentration of 24% in the char and 0% in the smelt. See Appendix XIV for details.

3. The temperature of the reaction zone is constant. The temperature difference between the radial and center thermocouple varied less than 25°K for most all experiments.

4. The depth of the active zone is 1 mm. This is based on postrun morphological examinations of the surface and carbon concentration measurements.

5. The density of the active zone is 1.2 g/mL. (The char density is 0.35, smelt density is 2.0 g/mL.) This assumes that the reaction zone is comprised of equal amounts of smelt and char. This assumption should be valid if the reaction is occurring at the char/smelt interface and the char is not being completely enveloped by the smelt.

6. Sufficient sulfate is present so that $k_4[SO_4] >> 1$, therefore Eq. (2) can be reduced to Eq. (15).

$$-d[SO_4]/dt = \frac{k_1}{k_4} [C] \quad \exp\frac{(-Ea)}{RT} \tag{15}$$

7. CO is the only product gas of the carbon-sulfate reaction, therefore the rate of carbon oxidation is given by Eq. (16).

$$r = 4\ d[SO_4]/dt = 4 \frac{k_1}{k_4} [C] \exp\left(-\frac{Ea}{RT}\right) \tag{16}$$

Equation (15) will be subsequently referred to as the kinetic model of char burning.

At 1042°K, the maximum measured rate was 3.2×10^{-3} moles/min. This was for the 10.5% O_2 experiment. The kinetic model predicts a rate of 3.8×10^{-3} moles/min which is within 20% of the measured rate. See Appendix XV for the calculation. This calculation suggests that carbon-sulfate kinetics may limit the char burning rate at 1042°K. The rate predicted by this kinetic model at other temperatures can be calculated by adjusting the absolute temperature in Eq. (15). The range of uncertainty for the kinetic model is ± 50%, with the active layer depth and density being the primary contributors at ± 20% each.

The rates and ranges of uncertainty for the kinetic model are plotted in Fig. 21 along with the measured rates for the char burning experiments. The plot shows that the measured rates for the 4.2 and 10.5% O_2 experiments at lower temperatures are within the bounds of the kinetic model. For all the high temperature experiments and all the 2.1% O_2 experiments, the measured rates are significantly lower than the kinetic model. The ln (rate) data at constant oxygen partial pressure do not vary with 1/T as much as the kinetic model (Fig. 21). This suggests that the reaction has a low activation energy for these conditions.

Mass Transfer Model

The following Arrhenius equation describes the rate of a reaction that has a first-order oxygen concentration dependence:

$$r = k\ pO_2\ \exp(-Ea/RT)$$

or

$$\ln(r/pO_2) = \ln k - Ea/RT \qquad (17)$$

Levenspiel states:[20]

"One can fit Arrhenius-type temperature dependency to any process

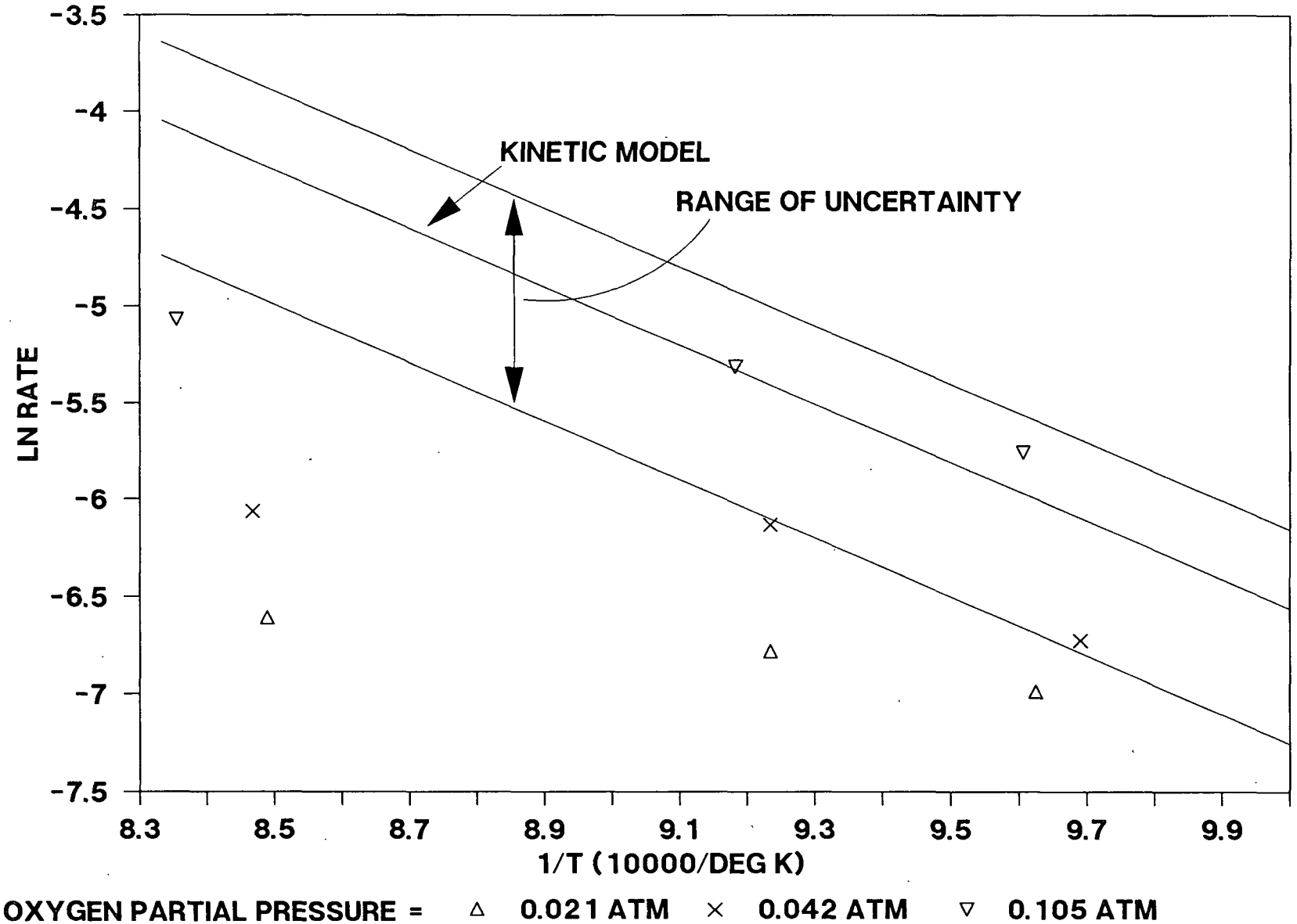

Figure 21. Char burning: experimental results and kinetic model.

as long as the temperature range is not too large. For the temperature ranges considered in reactions this type of fit for diffusional process causes no difficulties."

He also states that for gas diffusion at 1273°K, the Ea is small, approximately, 17 Kj/mole (4 kcal/mole). An activation energy of 84 to 418 kJ/mole (20 to 100 kcal/mole) suggests kinetic limitations.

Using Eq. (17) as the basis, the $\ln(r/pO_2)$ is plotted versus 1/T to determine the temperature dependence of the rate data (Fig. 22). An activation energy of 18.4 ± 3.0 kJ/mole (4.4 ± 0.7 kcal/mole) was determined from a linear regression analysis for the five data that were outside the range of uncertainty of the kinetically-limited model. The r^2 calculated was 0.77. For these conditions, the low activation energy suggests that the rate is oxygen mass transfer limited. The mass transfer model of Eq. (18) was determined from this linear regression analysis.

$$r = 0.391\ pO_2 \exp(-Ea/RT) \qquad (18)$$

with: Ea = 18.4 kJ/mole

Also included in Fig. 22 are the data that fit the kinetic model. At moderate temperatures, all the rate data agree with the mass transfer model. The 4.2% O_2 and the 10.5% O_2 data at low temperatures do not fit the mass transfer model.

Char Burning Rate - Results Summary

For high temperatures of about 1180°K (1664°F) the char burning reactions were oxygen mass transfer limited for the entire range of oxygen partial pressures. This is evidenced by:

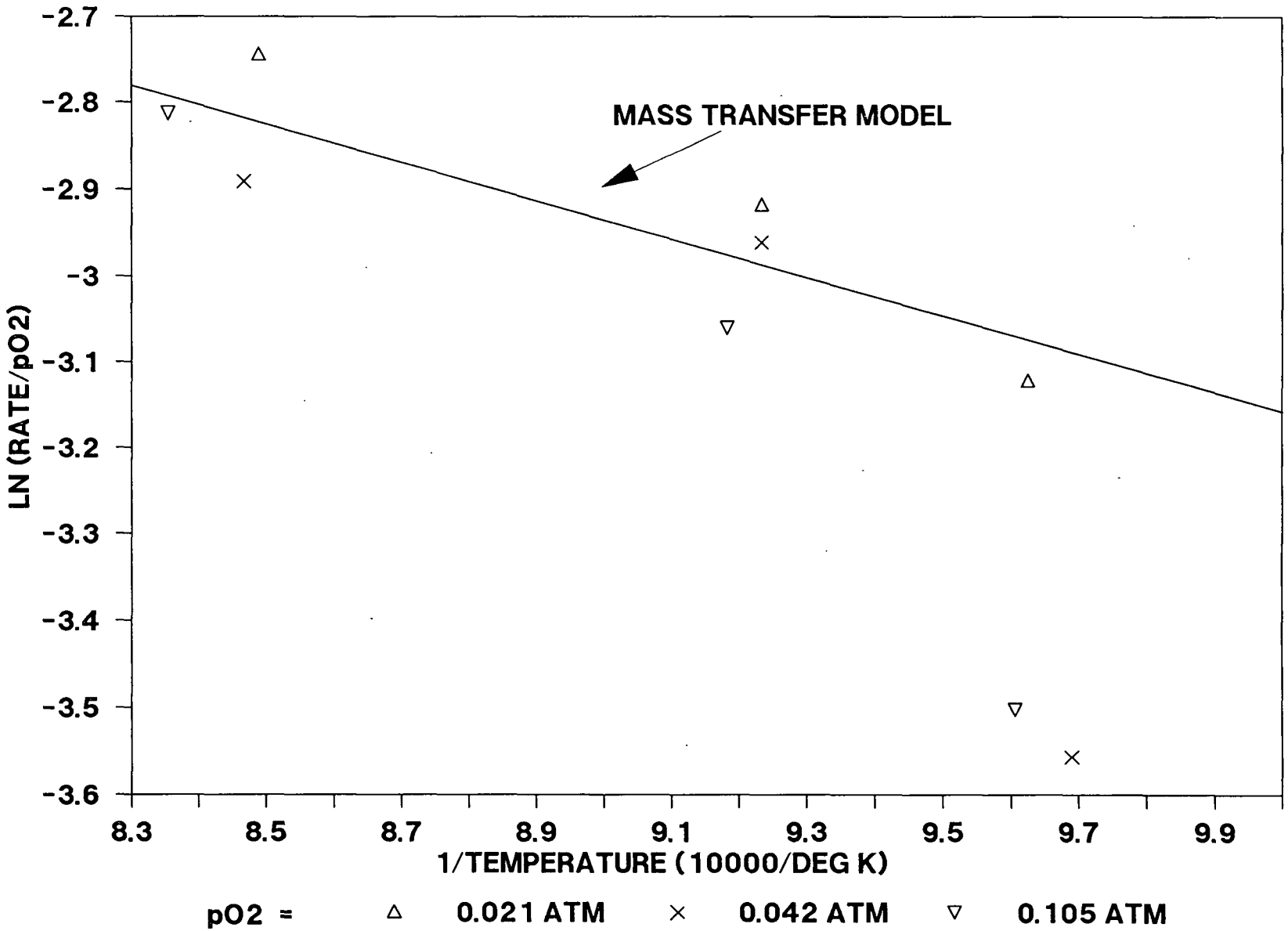

Figure 22. Char burning results: temperature dependence.

- Char burning rates are proportional to pO_2 and have a low Arrhenius activation energy.

- The measured char burning rate is well below the rate predicted by the kinetic model.

- The reduction ratio was greater than 0.95 for all sampling regions after the experiments.

For moderate temperatures of about 1085°K (1493°F), the char burning reactions are in the transitional regime, with oxygen mass transfer and carbon-sulfate kinetics both being significant. This is evidenced by:

- Char burning rates are proportional to pO_2 and have a low Arrhenius activation energy. This suggests that oxygen mass transfer is significant.

- The char burning rate with 2.1% O_2 does not fit the kinetic model. However with 4.2 and 10.5% O_2, the rates are within the range of uncertainty of the kinetic model.

- The sulfate concentrations in the impingement samples increase with increasing oxygen concentrations. This suggests that the char burning rate may be reaching kinetic limitations in the impingement region. The reduction ratio in the nonimpingement samples was greater than 0.91, suggesting that this region was mass transfer limited.

At low temperatures of about 1040°K (1412°F) the char burning reactions are in the transitional regime. This is evidenced by:

- The only rate data that fit the mass transfer model are with 2.1% O_2.
- The only rate data that do not fit the kinetic model are with 2.1% O_2. With 4.2 and 10.5% O_2, the measured rate is within the range of uncertainty of the kinetic model.
- Sulfate is present in increasing concentrations in the smelt samples which cover the entire char surface with increasing pO_2. This also suggests that the rate may be reaching kinetic limitations.

At temperatures greater than 1150°K (1610°F) char burning is controlled by the oxygen mass transfer rate for the conditions studied. The sulfur compounds present should be primarily sulfide, so the C/O ratio in the char should be very high.

The results of the CO/CO_2 product of the carbon-sulfate reaction suggest that at high C/O ratios, the CO/CO_2 product should be nearly exclusively CO. This was indeed the case, as evidenced by the results of the CO/CO_2 product of char burning studies. The $CO/(CO + CO_2)$ in the char pile gases ranged from 0.80 to 0.96 for all experimental conditions.

At temperatures less than 1100°K, both oxygen mass transfer and carbon-sulfate kinetics are significant. Oxygen mass transfer dominates with 2.1% O_2; with increasing pO_2, the carbon-sulfate kinetics become increasingly significant. Data analysis is further complicated at these temperatures by mixed-mode behavior. The rate-controlling factors change depending upon whether the impingement region or the nonimpingement surface region is being described.

CONCEPTUAL MODEL OF CHAR PILE BURNING

The conceptual model of kraft char burning was developed to explain the following apparently conflicting results of this investigation:

- At 10.5% O_2 and low temperatures of about 1040°K, the smelt covered the entire surface. The smelt's sulfate concentration was high and the carbon concentration was low, so the C/O ratio in the smelt was very low. The $CO/(CO + CO_2)$ of the off-char-pile gases were high, ranging from 0.80 to 0.86.

- For low C/O ratios, the results of the CO/CO_2 product of the carbon-sulfate reaction studies suggest that the CO/CO_2 ratio should be very low.

These conflicting results are explained by an interfacial char pile burning mechanism, shown in Fig. 23. The combustion air oxidizes the sulfide to sulfate. The sulfate of the smelt reacts with the fixed-carbon of the char at the char/smelt interface. The smelt layer on top of the char is in essence acting as an oxygen pump via the sulfate/sulfide cycle between the supply gas oxygen above and the char below.

To determine whether this model was reasonable, the C/O ratio required for the measured $CO/(CO + CO_2)$ was calculated and used to estimate the reduction ratio of the interface.

For the 10.5% O_2 experiment at low temperatures, the off-char-pile $CO/(CO + CO_2)$ values ranged from 0.80 to 0.86. A $CO/(CO + CO_2)$ of 0.80 is equal to a CO/CO_2 of 4/1. The C/O calculated from this CO/CO_2, using Eq. (12) of the carbon-sulfate studies, is 9. If all of the oxygen is present as sulfate, the

carbon/sulfate ratio is 36. The average carbon concentration of the interface is 12% by weight, as determined previously. If the sulfidity is assumed to be 30%, and the remainder of the interfacial material is assumed to be sulfate, sulfide and carbonate, the reduction ratio calculated is 0.77 (see Appendix XVI).

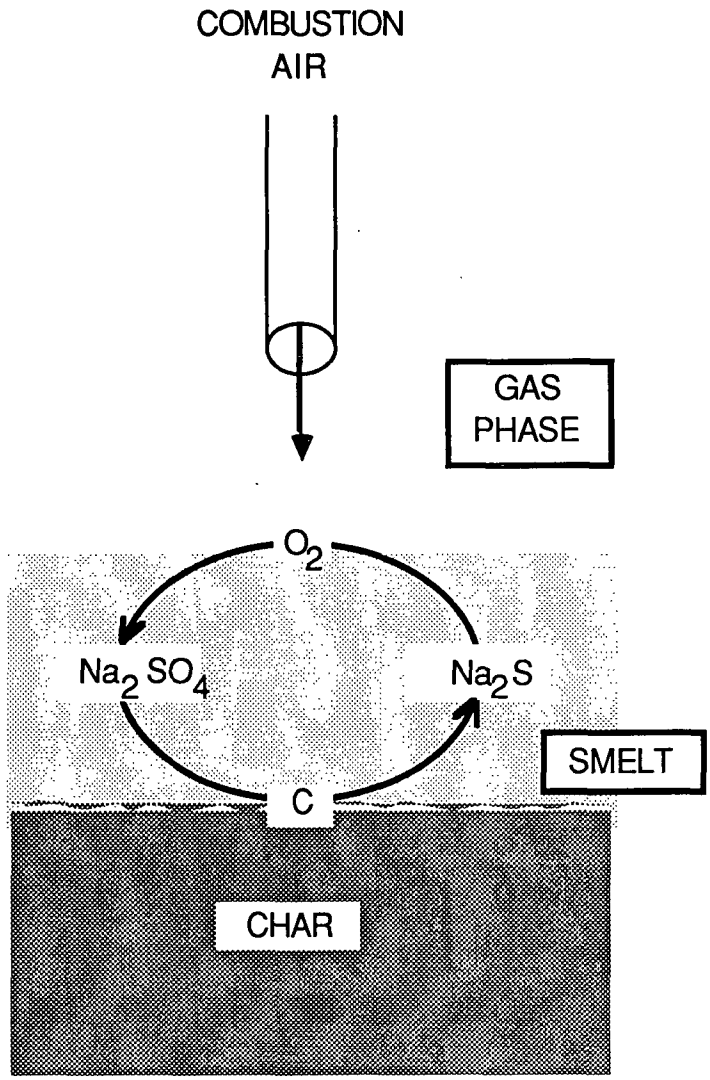

Figure 23. Interfacial mechanism of char burning.

The reduction ratio at the smelt/char interface calculated for the CO/CO_2 in the char pile gases is 0.77. The predicted interfacial sulfur-species composition is between the measured high sulfate of the smelt and the measured high sulfide of the char. The interfacial reaction mechanism explains the apparent contradiction and is consistent with experimental results.

IMPLICATIONS

The results of this thesis were obtained for a specific set of experimental conditions. The CO/CO_2 product results are easily translated to general characteristics of char burning and the carbon-sulfate reaction. The char burning rate studies are a bit more restricted in their applicability to char bed burning. The implications can be summarized as follows:

- The results of all investigations are consistent with the sulfate/sulfide cycle theory of char burning.

- The CO/CO_2 product of the carbon-sulfate reaction is given by:

$$CO/CO_2 = 0.403\ C/O$$

  The C/O is the elemental carbon/oxygen ratio. For the temperature range investigated, 1033 to 1113°K, the CO/CO_2 product was independent of temperature. At higher temperatures of up to 1500°K which are more representative of char bed burning conditions, the CO/CO_2 at a given C/O may be slightly higher. The CO/CO_2 product of coal char burning increases with increasing temperature.[12]

- The CO/CO_2 product of char burning was 4 to 24 at 1000 to 1150° with 2.1 to 10.5% O_2. Again, at temperatures more representative of char

bed conditions of up to 1500°K, the CO/CO_2 should be higher. The CO/CO_2 product of char burning was not a function of the oxygen partial pressure. These data were obtained for the impingement of a laminar jet on the char surface. In a char bed, conditions would exist where a turbulent jet is directly impinged in the char bed. Since the CO/CO_2 product of char burning is independent of oxygen partial pressure for the laminar conditions studied, the CO/CO_2 product results should not change with turbulent jet conditions.

- The char burning rate data suggest that at temperatures greater than 1150°K, the rate is oxygen mass transfer limited with a laminar jet of 2.1 to 10.5% O_2 impinged on the char surface. At lower temperatures, the char burning rate is controlled by both oxygen mass transfer and carbon-sulfate kinetics. At temperatures more representative of char bed conditions of up to 1500°K, for the laminar conditions studied, the char burning rate should be oxygen mass transfer limited. Laminar flow should exist over a char bed, except in the region where the primary jets impinge directly on the side of the bed. The char burning rate data were obtained for only one set of impingement geometry conditions. Before one can claim that the 1150°K threshhold of oxygen mass transfer control applies for all char bed conditions, more investigations are required.

- The smelt product of char burning collected on the char surface; it did not percolate through the char pile. The contact angle calculated for smelt on char is greater than 90°. This shows that smelt does not wet char.

RECOMMENDATIONS

Char burning rate data should be obtained for the following experimental conditions in order to conclusively determine the factors affecting oxygen mass transfer versus carbon-sulfate kinetics control:

- for a similar reactor with various impingement velocities, temperatures and oxygen partial pressures.
- for a reactor where the supply gases are directed tangentially across the char surface. The effects of temperature, oxygen partial pressure and velocity should also be studied.

Another interesting study could be directed at determining the role of thiosulfate in char burning. Very limited data suggest that thiosulfate may be present during char burning. It was detected in the char samples only (not in the smelt samples) after some of the char burning experiments. It is possible that this thiosulfate formed during cooling. It is also possible that the thiosulfate formed upon dilution of the sample prior to ion chromatograph analysis.

CONCLUSIONS

1. The CO/CO_2 product of the carbon-sulfate reaction is a linear function of the elemental C/O:

$$CO/CO_2 = 0.403\ C/O$$

At 1033 to 1113°K, temperature did not affect the CO/CO_2. The oxygen of the sulfate supplied at least 88% of the elemental oxygen for carbon oxidation with the remainder supplied by oxygen sorbed by the char during sample preparation.

2. The CO/CO_2 product of char burning is principally CO for the impingement of a laminar, oxygen-containing jet on the char surface. The CO/CO_2 ranged from 4 to 24 at 1000 to 1150°K and 2.1 to 10.5% oxygen. The significance of the homogeneous, gas-phase oxidation of CO to CO_2 was quantified by terminating the O_2 and simultaneously increasing the N_2 flow to the reactor. The CO/CO_2 product of the heterogeneous reaction was calculated when O_2 was no longer detected in the exhaust gases. The CO/CO_2 was not a function of oxygen partial pressure. A turbulent jet would reduce the boundary layer thickness and thus increase the oxygen concentration at the surface. Since pO_2 did not affect the CO/CO_2, CO should be the principal product for turbulent conditions.

3. The char burning rate is controlled by the oxygen mass transfer rate at temperatures greater than 1150°K. At lower temperatures, both oxygen mass transfer and carbon-sulfate kinetics are important. These generalizations are for the impingement of a laminar jet of 2.1 to 10.5% oxygen on the char surface. For turbulent conditions, more data are required to determine the effect of jet velocity on the rate-controlling mechanism.

4. The smelt product of char burning collected on the char surface; it did not percolate through the char pile. The contact angle calculated for smelt on char is greater than 90°, showing that smelt does not wet the char.

5. Oxygen is readily sorbed by kraft char at room temperature. This oxygen is released as CO and CO_2 upon heating. $1.82 * 10^{-2}$ grams of O_2 were sorbed per gram of char.

6. The results of this thesis are consistent with the sulfate/sulfide theory of kraft char burning.

ACKNOWLEDGMENTS

I would like to thank The Institute of Paper Chemistry and its member companies for their support throughout my tenure. I would also like to thank the following Institute staff and faculty members whose guidance and assistance is sincerely appreciated: Mr. Don Sachs, Mr. Orlie Kuehl, Ms. Connie Weber, Dr. David Clay, Dr. Thomas Grace, Dr. Peter Parker, and Dr. John Cameron.

LITERATURE CITED

1. Richardson, D. L.; Merriam, R. L. Study of cooling and smelt solidification in black liquor recovery boilers. Phase I Report, Arthur D. Little, Inc., Cambridge, MA, Feb., 1977.

2. Richardson, D. L.; Merriam, R. L. A study of black liquor recovery furnace firing conditions, char bed characteristics and performance. Phase II Report, Arthur D. Little, Inc., Cambridge, MA, Dec., 1978.

3. Borg, A.; Teder, A.; Warnquist, B., Tappi 57(1):126-9(1974).

4. Cameron, J. H.; Grace, T. M.; Malcolm, E. W. A kinetic study of sulfate reduction with carbon. Project 3473-1, Report Two, The Institute of Paper Chemistry, Appleton, WI, June, 1983.

5. Grace, T. M.; Cameron, J. H.; Clay, D. T. Char burning. Project 3473-6, The Institute of Paper Chemistry, Appleton, WI, Feb., 1985.

6. Grace, T. M.; Cameron, J. H.; Clay, D. T., Tappi 69(10):108-13(Oct., 1986).

7. Cameron, J. H.; Grace, T. M. A kinetic study of sulfate reduction with carbon. Project 3473-1, Report Three, The Institute of Paper Chemistry, Appleton, WI, Jan., 1985.

8. Thorman, R. P.; Macur, T. S. 1985 TAPPI International Recovery Conf. Proc., Book IV, TAPPI Press, Atlanta, GA, 1985:451-8.

9. Cameron, J. H.; Grace, T. M. A kinetic study of sulfate reduction with carbon. Project 3473-1, Report One, The Institute of Paper Chemistry, Appleton, WI, June, 1981.

10. Sjoberg, M.; Cameron, J. H. A kinetic study of sulfate reduction by carbon monoxide. Denver, AIChE Meeting, Sept., 1983.

11. Atomics International. Development of a molten carbonate process for removal of sulfur dioxide from power plant stack gases. Progress Report Two, Part 1. Process Chemistry - Reduction, Atomics International, North American Rockwell, Oct., 1968.

12. Laurendeau, N. M., Prog. Energy Combust. Sci. 4:221-70(1978).

13. Goerg, K. A.; Cameron, J. H. A kinetic study of kraft char gasification with CO_2. AIChE Meeting, Boston, MA, Aug., 1986.

14. Hupa, M.; Solin, P. Combustion behavior of black liquor droplets. 1985 TAPPI International Chemical Recovery Conf. Proc., Book IV, TAPPI Press, Atlanta, GA, May, 1985:335-44.

15. Perry, R. H.; Chilton, C. H., Chemical Engineers' Handbook, 5th ed., McGraw-Hill, Inc., St. Louis, 1976:5-19-20.

16. TAPPI Test Method T 699 pm-83, Atlanta, GA.

17. National Council of the Paper Industry for Air and Stream Improvement, Atmosphere Quality Improvement Technical Bulletin No. 68, Oct., 1983.

18. Adamson, A. W., Physical Chemistry of Surfaces, 3rd ed., John Wiley & Sons, New York, 1976:459-62.

19. Krause, H. H.; Simon, R.; Levy, A. Smelt-water explosions. Final report to Fourdrinier Kraft Board Institute, Battelle, Columbus, OH, Jan. 31, 1973.

20. Levenspiel, O., Chemical Reaction Engineering, 2nd ed., John Wiley & Sons, New York, 1972:489-91.

21. McCabe, W. L.; Smith, J. C., Unit Operations of Chemical Engineering, 3rd ed., McGraw-Hill, Inc., St. Louis, 1976:995-6.

22. Kreith, F., Principles of Heat Transfer, 3rd ed., Harper & Row Publishers, Inc., New York, 1973:236-7.

APPENDIX I

MOLAR BALANCE OF CHAR COMBUSTION

A molar balance of char combustion was calculated to determine the percentage of the oxygen required by kraft char combustion that is supplied by the carbon-sulfate reaction versus the percentage supplied by the combustion air.

ASSUMPTIONS

- The Na_2CO_3 is inert.
- The CO/CO_2 of the product gases is 50/50.
- The simplified char and smelt compositions suggested by Grace are representative.
- The reduction ratio is 0.50 in the char and 0.95 in the smelt.

Basis: 30 moles of char initially

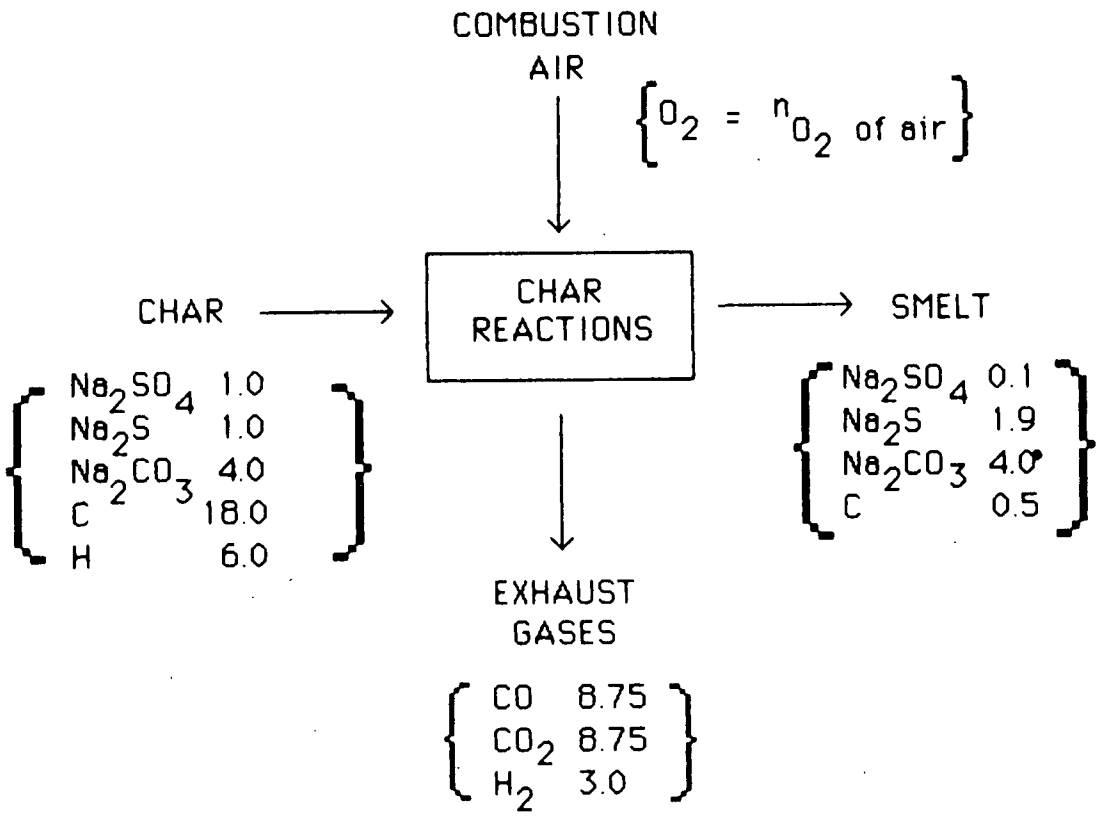

The moles of O_2 supplied by the combustion air is therefore:

$$n_{O_2,air} = \Sigma\, n_{O_2,exhaust\ gas} - \Sigma\, n_{O_2,sulfate}$$

$$= 1/2\, n_{CO} + n_{CO_2} - 2\,(n_{SO_4,char} - n_{SO_4,smelt})$$

$$= 11.33 \text{ moles } O_2$$

and the percentage of the required oxygen supplied by the combustion air is:

$$\%\ O_{2,combustion\ air} = \frac{n_{O_2,air}}{n_{O_2,air} + n_{O_2,S_{O_4}}}$$

$$= \frac{11.33}{11.33 + 2(1-0.1)} = 86\%$$

APPENDIX II

CALCULATION OF THE RELATIVE SIGNIFICANCE OF CO_2 REDUCTION BY CARBON

The relative significance of CO_2 reduction by C was determined by comparing its rate of reaction to that of the carbon-sulfate reaction using the following assumptions.

ASSUMPTIONS

1. The partial pressure of CO (pCO) = 0.05 atm.

2. The partial pressure of CO_2 (pCO_2) = 0.05 atm.

3. Temperature (T) = 1200°K.

4. Cameron's sulfate reduction by kraft char rate equation is representative:

$$-\frac{d[SO_4]}{dt} = \frac{k_1[C][SO_4]}{1 + k_4[SO_4]} \exp\left(-\frac{Ea}{RT}\right) \qquad (2)$$

5. Sufficient sulfate is present so that $k_4[SO_4] \gg 1$, therefore the rate equation becomes:

$$-\frac{d[SO_4]}{dt} = \frac{k_1}{k_4}[C] \exp\left(-\frac{Ea}{RT}\right) \qquad (14)$$

6. The CO/CO_2 product of the carbon-sulfate reaction is 1:1, therefore the rate of carbon consumption is 8/3 times the rate of sulfate consumption.

The rate of carbon consumption via CO_2 reduction ($-dC^*/dt$) is:

$$-\frac{d[C^*]}{dt} = \frac{k_1^*[pCO_2][C]}{1 + k_2,[pCO_2], + k_3,[pCO]} \exp -\frac{Ea^*}{RT} \qquad (5)$$

The rate of carbon consumption via sulfate reduction by carbon (-dC/dt) is:

$$-\frac{d[C]}{dt} = \frac{8}{3} \cdot \frac{k_1}{k_4} [C] \exp\left(-\frac{Ea}{RT}\right) \qquad (19)$$

The relative rate of CO_2 reduction by C is obtained by dividing Eq. (5) by Eq. (19):

with: $k_1 = 5.96 \cdot 10^4 \frac{L}{\text{mole-sec}}$ $\qquad$ $k_1^* = 6.26 \times 10^9 \frac{atm}{min}$

$k_4 = 45.6 \frac{L}{\text{mole}}$ $\qquad$ $k_2^* = 29.0\ atm^{-1}$

$\qquad\qquad\qquad\qquad\qquad\quad$ $k_3^* = 45.6\ atm^{-1}$

$Ea = 29.2 \frac{kcal}{\text{mole}}$ $\qquad$ $Ea = 54.3$ kcal/mole

so:
$$\frac{d[C^*]}{d[C]} = 0.0085 \qquad (20)$$

APPENDIX III

EXPERIMENTAL APPARATUS SPECIFICATIONS

Description	Manufacturer - Specifications
Induction furnace	Lepel Model T-20-3-KC-HB
Stainless steel retort	height = 15.2 cm, diam. = 5.08 cm 310 SS pipe (std. 2 inch)
Hastelloy retort	height = 12.7 cm, diam. = 6.35 cm, (std. 2.5-inch pipe)
Alumina crucible	McDanel refractory - 1 7/8-inch o.d. * 1 5/8-inch i.d. * 4 inches long
CO/CO_2 analyzer	Infrared Industries IR 702 gas analyzer
O_2 analyzer	Teledyne O_2 analyzer
Supply gas flowmeters	Hastings Mass Flowmeter Model NALL

APPENDIX IV

REYNOLDS NUMBER CALCULATION

Density Calculation, ρ

from the ideal gas law:

$$\rho = \frac{n}{v} = \frac{P}{RT}$$

$$\rho = (1 \text{ atm}) \left(\frac{\text{mole-°K}}{0.08205 \text{ L-atm}}\right) \left(\frac{29 \text{ g}}{\text{mole}}\right) \left(\frac{1}{1190°\text{K}}\right)$$

$$\rho = 0.297 \text{ g/L}$$

Effective Diameter Calculation

$$D_{tube} = 4.5 \text{ mm}$$

$$D_{thermocouple} = 1.6 \text{ mm}$$

$$\text{Open Area} = \left[\left(\frac{4.5}{2}\right)^2 - \left(\frac{1.6}{2}\right)^2\right] \pi = 4.42 \pi$$

$$D_{effective} = 2 \sqrt{4.42 \text{ mm}^2} = 0.42 \text{ cm}$$

Velocity Calculation

from ideal gas law

$$\frac{V_o}{T_o} = \frac{V_A}{T_A}$$

where: V_o, T_o = standard conditions

or

$$V_A = V_o \frac{T_A}{T_o}$$

and: V_A, T_A = actual conditions

so

$$\frac{q_o}{A} = v_o$$

$$v_A = v_o \left(\frac{T_A}{T_o}\right)$$

$$v_A = \left(\frac{1\ L}{min}\right)\left(\frac{1000\ cm^3}{L}\right)\left(\frac{1}{4.42 \cdot \pi\ mm^2}\right)\left(\frac{100\ mm^2}{cm^2}\right)\left(\frac{1190°K}{273°K}\right)\left(\frac{1\ min}{60\ sec}\right)$$

$$v_A = 523\ cm/s$$

Viscosity Estimation, μ:[21]

for N_2 at 1190°K,

$$\mu = 4.6 \times 10^{-4}\ poise$$

Reynolds Number Calculation, Re:

$$Re = \frac{\rho D v}{\mu}$$

$$= \left(\frac{0.297\ g}{1000\ cm^3}\right)(0.42\ cm)\left(\frac{523\ cm}{s}\right)\left(\frac{cm\text{-}s}{4.6 \times 10^{-4}\ g}\right)$$

$$= 142$$

APPENDIX V

RADIATION-SHIELDED THERMOCOUPLE

A radiation-shielded thermocouple was constructed, as diagrammed in Fig. 24, and placed in the exhaust gas port. The thermocouple performs an energy balance on the system. The radiation from the walls to the thermocouple must be insignificant compared to the convection heat transfer from the exhaust gases. The stainless steel tubing shields the radiation contribution because of its low emittance, $\varepsilon = 0.20$.[18] The walls of the reactor have an ε of approximately 0.85. With the shield in place, the thermocouple no longer "sees" the reactor walls but sees the stainless steel tubing. To determine whether the radiative contribution was significant, the gas flow was decreased from 1.0 to 0.6 L/min, then increased to 1.5 L/min. The temperature reading did not change. If the temperature had changed, then radiation from the tube to the thermocouple would have been affecting the temperature reading. Since it did not, the thermocouple was being effectively shielded.

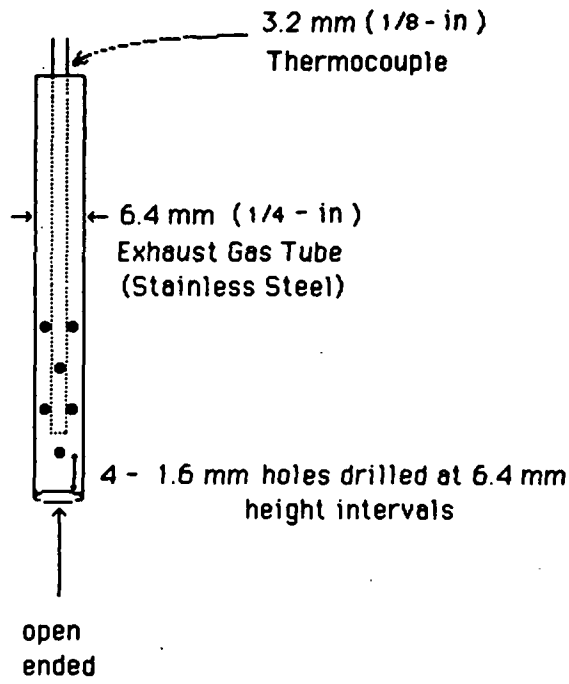

Figure 24. Radiation-shielded thermocouple.

APPENDIX VI

RESPONSE TIMES OF GAS ANALYZERS

The apparatus used to check the response times of the gas analyzer was identical to that of the char burning experiments except the 40 mL of char was replaced with 40 mL of ignited sand. Three different experiments were run, one with a supply gas of 6.2% CO_2, a second with a supply gas of 6.3% CO, and a third with a supply gas of 5.0% O_2. The supply gas valve for the CO, CO_2 or O_2 was cut and a flow rate of about 1.0 L/min maintained by increasing the N_2 flow at time t_o. The delay time between the time the meters first reacted to the termination of CO, CO_2, or O_2 flow and t_o was 25 seconds for CO and CO_2 and 31 seconds for O_2.

Once this delay time was taken into account, a linear regression analysis indicated that all three gas concentrations could be expressed as:

for $t_o \leq t \leq t_o + t_d$

$$X(t) = X_o \tag{21}$$

for $t > t_o + t_d$

$$X(t) = X_o \exp(-0.0832\ t_x) \tag{22}$$

where: t_o = time of air flow termination

t_d = delay time

$X(t)$ = gas concentration at time t

X_o = gas concentration at time t_o

$t_x = t - (t_o + t_d)$

This model is shown versus experimental results in Fig. 25, 26, and 27. The model fits the data well.

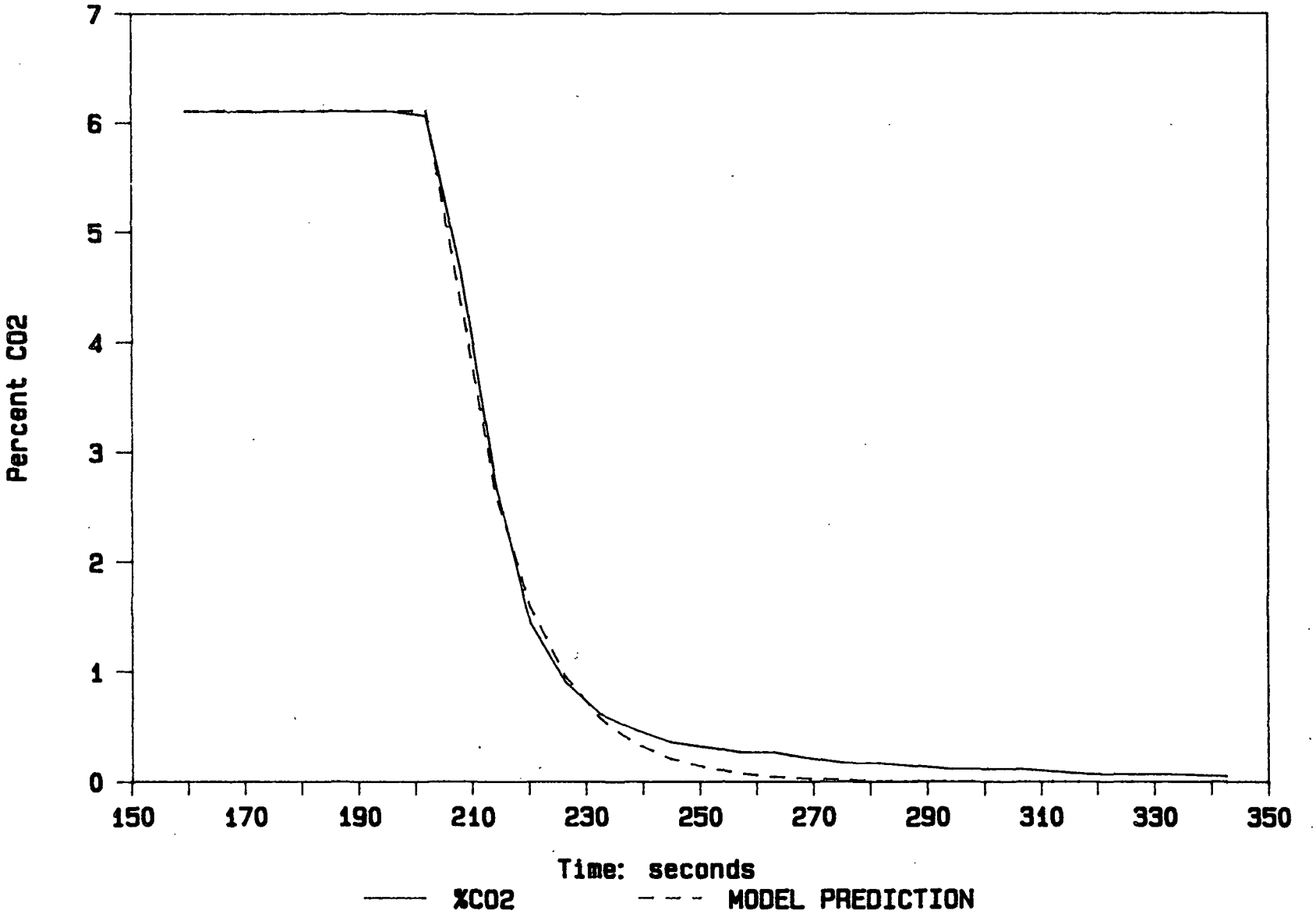

Figure 25. CO_2 analyzer response.

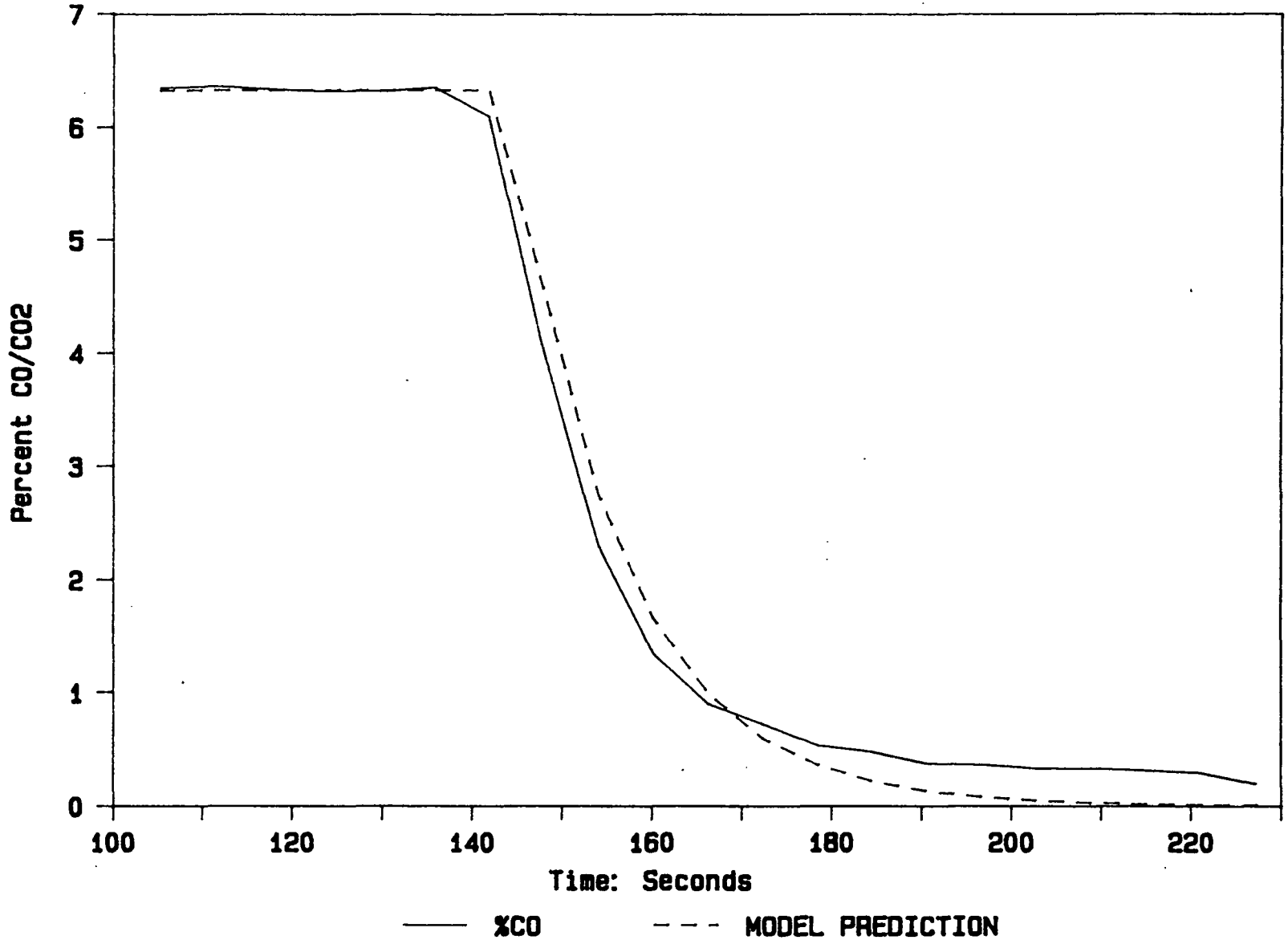

Figure 26. CO analyzer response.

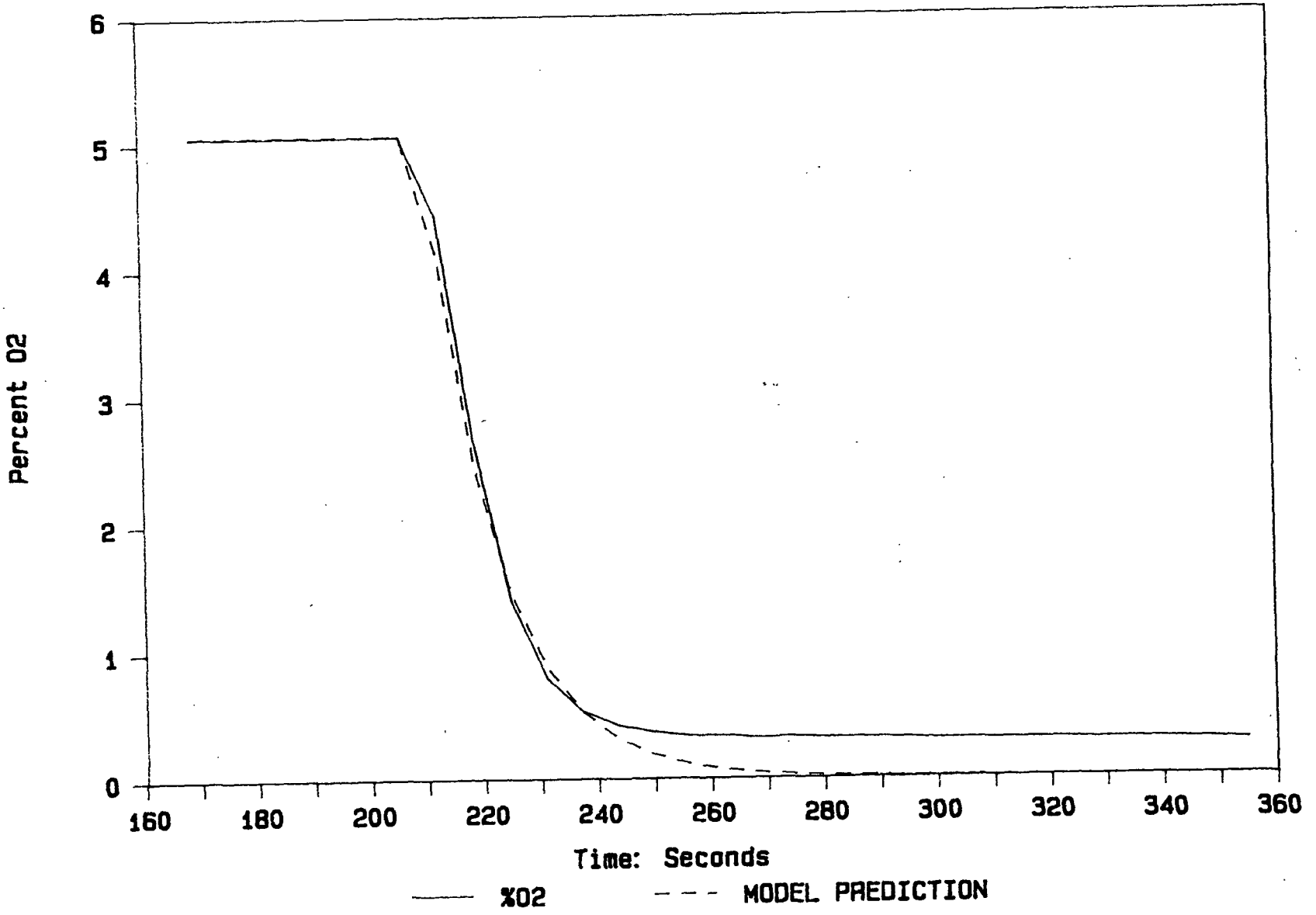

Figure 27. O_2 analyzer response.

APPENDIX VII

SUPPLY GAS SYSTEM

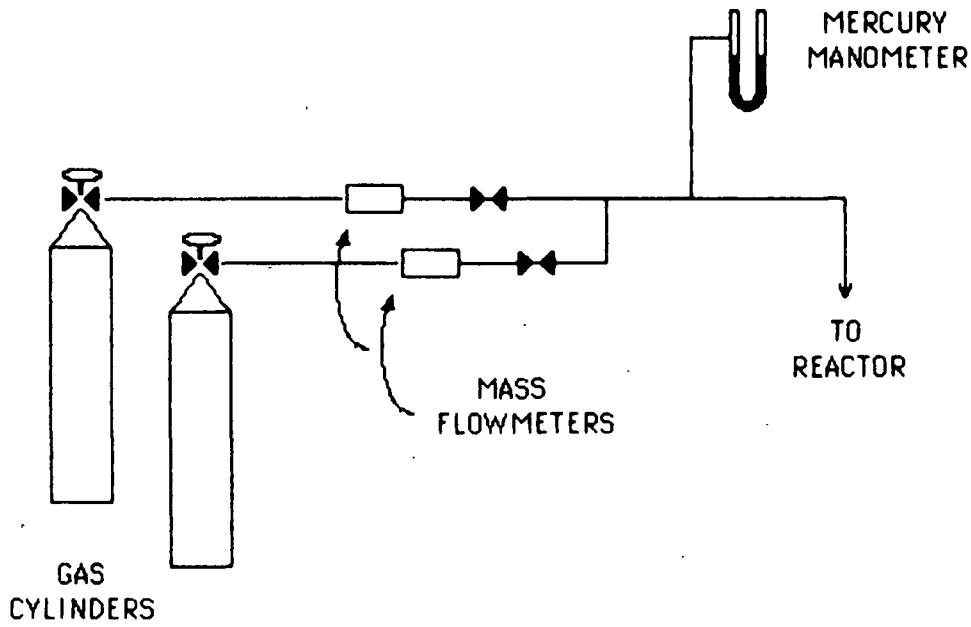

Figure 28. Supply gas system.

APPENDIX VIII

MASS FLOWMETER CALIBRATIONS

The apparatus sketched in Fig. 29 was used to measure the actual flow rate. The bubble flowmeter measured flow rate, q_B, was adjusted by a factor from the ideal gas law that accounts for actual pressure and temperature conditions. This adjusted bubble flowmeter reading, q_A, was divided by the mass flowmeter reading, q_M, to obtain the calibration factor used in the data acquisition program.

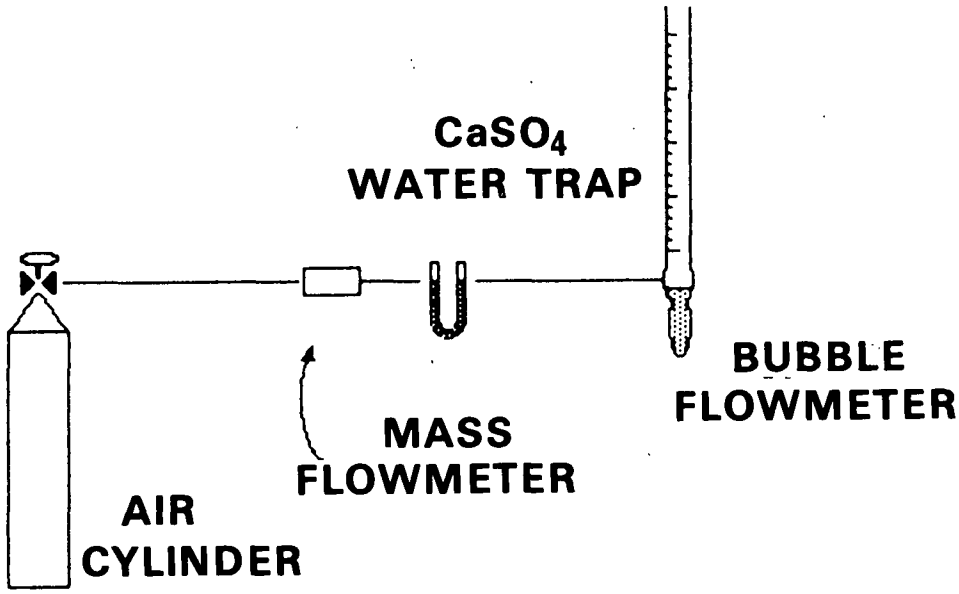

Figure 29. Mass flowmeter calibration apparatus.

From the ideal gas law:

$$q_A = q_B \left(\frac{T_o}{T_A}\right)\left(\frac{p_A}{p_o}\right) \qquad (23)$$

where T_A = measured temperature (°K)

T_o = standard conditions (273°K)

p_A = measured pressure (atm)

p_o = standard conditions (1 atm)

and the calibration factor, k_1, used in the data acquisition program was:

$$k_1 = \frac{q_A}{q_M} \tag{24}$$

where q_A = adjusted bubble meter flow rate

q_B = measured bubble meter flow rate

q_M = mass flowmeter reading.

Gas-Specific Calibration Factors

The following gas-specific calibration factors, k_2, were used to correct the mass flowmeter readings if gases other than air were used:

$$k_2 = \frac{q_c}{q_M} \tag{25}$$

where q_c = corrected flowmeter reading

q_M = flowmeter reading

Gas	k_2
Air	1.00
CO_2	0.73
CO	1.00
N_2	1.02

APPENDIX IX

DATA MANIPULATION FOR PYROLYSIS EXPERIMENTS 8 AND 15

In Pyrolysis Experiment 8, the char was handled in air whereas in Pyrolysis Experiment 15, the char was handled in nitrogen. Table 21 lists the data and calculations used to determine the % O_2 due to sulfate reduction, the % O_2 due to incomplete pyrolysis and the moles O_2 sorbed per gram of char.

Definitions for Table 21

(1) Cut-off time = the time at which the pyrolysis was determined to be complete. This was the time where the rate of CO generation leveled at a constant value.

(2) Moles of O generated = the total amount of CO and CO_2 generated in the exhaust gases, summed as moles of O, from the beginning of the experiment to the cut-off time.

(4) Mass of CO/CO_2 = total mass of CO plus CO_2 generated throughout the entire experiment.

(5) Final char mass = (3)-(4).

(8) Initial $S^{=}$ mass = (6)*(3).

(9) Final $S^{=}$ mass = (7)*(5).

(10) Δmoles $S^{=}$ = [(9)-(8)]/32. Sulfide was the sulfur-species used to determine the amount of sulfate consumed via the carbon-sulfate reaction. Sulfide was chosen because there was always a greater change in sulfide during the experiments than a change in sulfate. The initial amount of sulfate does

not include other sulfur-oxygen compounds that could contribute to the reaction.

(11) Δmoles due to C/SO_4 reaction = 2 x (10)

(12) % O due to C/SO_4 reaction = (11)/(2) x 100

(13) unaccountable O = (2) - (11)

(14) moles of O sorbed by char = $\frac{(13) \text{ of EXP } 8}{(3) \text{ of EXP } 8} - \frac{(13) \text{ of EXP } 15}{(3) \text{ of EXP } 15}$

(15) moles of O sorbed = (14) x (3)

(16) % O due to sorbed O = (15)/(2) x 100

(17) % O due to incomplete pyrolysis = 100 - (12) - (16)

Table 21. Data manipulation for Experiments 8 and 15

		EXP 8	EXP 15
(1)	cut-off time (min)	16.88	17.92
(2)	moles of O generated	2.556×10^{-2}	8.39×10^{-3}
(3)	initial mass of char (9)	6.0701	7.1097
(4)	mass of CO/CO_2 (g)	0.7061	0.8957
(5)	final mass of char	5.3640	6.2140
(6)	initial % $S^{=}$ (wt.%)	0.50	3.0
(7)	final % $S^{=}$	2.74	3.9
(8)	initial $S^{=}$ mass (g)	0.0304	0.2133
(9)	final $S^{=}$ mass	0.1465	0.2424
(10)	Δmoles $S^{=}$	3.64×10^{-3}	9.08×10^{-4}
(11)	Δmoles O due to C/SO_4 reaction	1.45×10^{-2}	3.64×10^{-3}
(12)	% O due to C/SO_4 reaction	57%	43%
(13)	unaccountable O (moles)	1.10×10^{-2}	4.75×10^{-3}
(14)	moles O sorbed/gram of char	1.14×10^{-3}	
(15)	moles O sorbed	6.94×10^{-3}	
(16)	% O due to sorbed O	27%	
(17)	% O due to incomplete pyrolysis	16%	57%

APPENDIX X

CALCULATION OF INITIAL C/SO_4 OF EXPERIMENT 17

The carbon content of the source char was not measured for Experiment 17, the sulfate-loaded liquor experiment. In order to estimate this carbon concentration so that the C/SO_4 could be calculated, the following assumptions were required.

ASSUMPTIONS

- the char consists of three components: fixed carbon (C), sulfur (S), and the remainder of the char (R).
- the ratio of R/C was identical for the sulfate-loaded liquor char (Experiment 14) and a char similarly produced with no sulfate added (Experiment 5C2).

Basis: 100 g of char

Given:

	Total S, %	Wt.% C	% SO_4 (as wt.% S)
EXP 5C2	3.2	25.7	--
EXP 14	8.7	X	1.77

Mass Balance for EXP 14 Char

Total mass = C + S + R

$100 = X + 8.7 + (71.1/25.7) \times X$

Molar Ratio of C/SO_4

$$\text{moles of C} = \frac{24.2 \text{ g}}{12 \text{ g mole}} = 2.02$$

$$\text{moles of } SO_4 = \frac{1.77 \text{ g } SO_4}{32 \text{ g mole}} = 0.0553$$

$$C/SO_4 = 2.02/0.0553 = 37/1$$

APPENDIX XI

CALCULATION OF INITIAL C/O FOR CO/CO_2 PRODUCT OF THE CARBON-SULFATE REACTION STUDIES

The initial C/O ratio for the CO/CO_2 product of the carbon-sulfate reaction must include the oxygen content of the sulfate plus the sorbed oxygen of the char. An estimate of the moles of oxygen sorbed can be made from the sulfate-limited experiments where all of the oxygen was quantified in the exhaust gases. Two such experiments were run, Experiments 77 and 78. The calculations are listed in Table 22.

Table 22. Determining the amount of oxygen sorbed by the char in the sulfate-limited, carbon-sulfate reaction studies.

		EXP 77	EXP 78
(1)	Total CO/CO_2 generated (as moles O)	0.0852	0.0688
(2)	Na_2SO_4 added (as moles O)	0.0748	0.0630
(3)	O content of char = (1) - (2)	0.0104	0.0058
(4)	Ratio of O supplied by Na_2SO_4 to total = (2)/(1) x 100	88%	92%
(5)	Total CO/CO_2 generated (as moles C)	0.0758	0.0956
(6)	O/C (moles/mole) = (3)/(5)	0.1372	0.0607
(7)	Mass of char (g)	3.790	4.780
(8)	Moles O/g-char = (3)/(7)	2.74×10^{-3}	1.21×10^{-3}

The results of the O/C calculation in Table 19, line (6), can be averaged to obtain an average value for Experiments 77 and 78 of 0.0989 moles O per mole C. This ratio was used in Table 23 to determine whether the initial oxygen for the carbon-limited experiments, Experiments 71 to 74, required adjustment for the sorbed O.

Table 23. Determination of the significance of the O sorbed by the char in the carbon-limited experiments.

		EXP 71	EXP 72	EXP 73	EXP 74
(9)	Na_2SO_4 added (moles O)	0.04544	0.04528	0.04528	0.09117
(10)	C added (moles C)	0.02300	0.02292	0.02292	0.04623
(11)	Sorbed O (moles)	0.00225	0.00225	0.00225	0.00457
(12)	Ratio of O supplied by SO_4 to total	0.95	0.95	0.95	0.95

where:

(11) Sorbed O moles = (10) x 0.0989

(12) Ratio of O supplied by SO_4 to total $= \frac{(9)}{(9) + (11)}$

The results show that the oxygen content of the char is insignificant for the carbon-limited experiments.

APPENDIX XII

ESTIMATION OF THE PORE SIZE FROM THE PARTICLE SIZE DISTRIBUTION

The minimum pore size can be estimated from the particle size distribution by assuming the smallest char particle governs the interparticular pore size. The smallest particle size fraction was the 62 to 74 μm fraction. If three of these particles form a tight pocket, the pocket can hold a cylinder 5/32 the size of the particle (Fig. 30). For a 68 μm particle, the pocket could hold a 10.6 μm cylinder. This 10.6 μm diameter was assumed to be the capillary diameter of the pore.

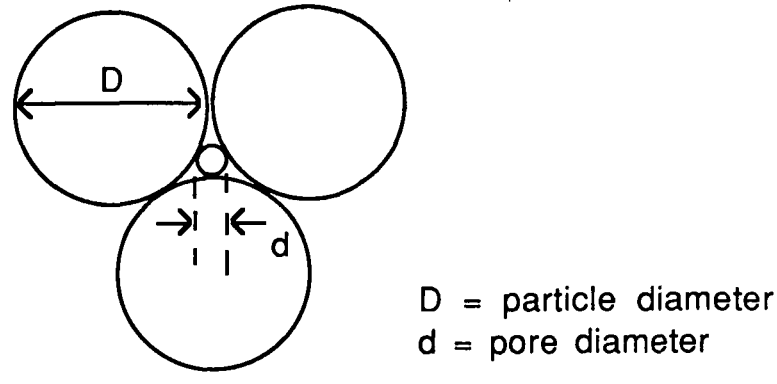

Figure 30. Estimation of interparticular pore size.

APPENDIX XIII

GRAPHIC RESULTS OF CHAR BURNING RATE EXPERIMENTS

Experiment 47

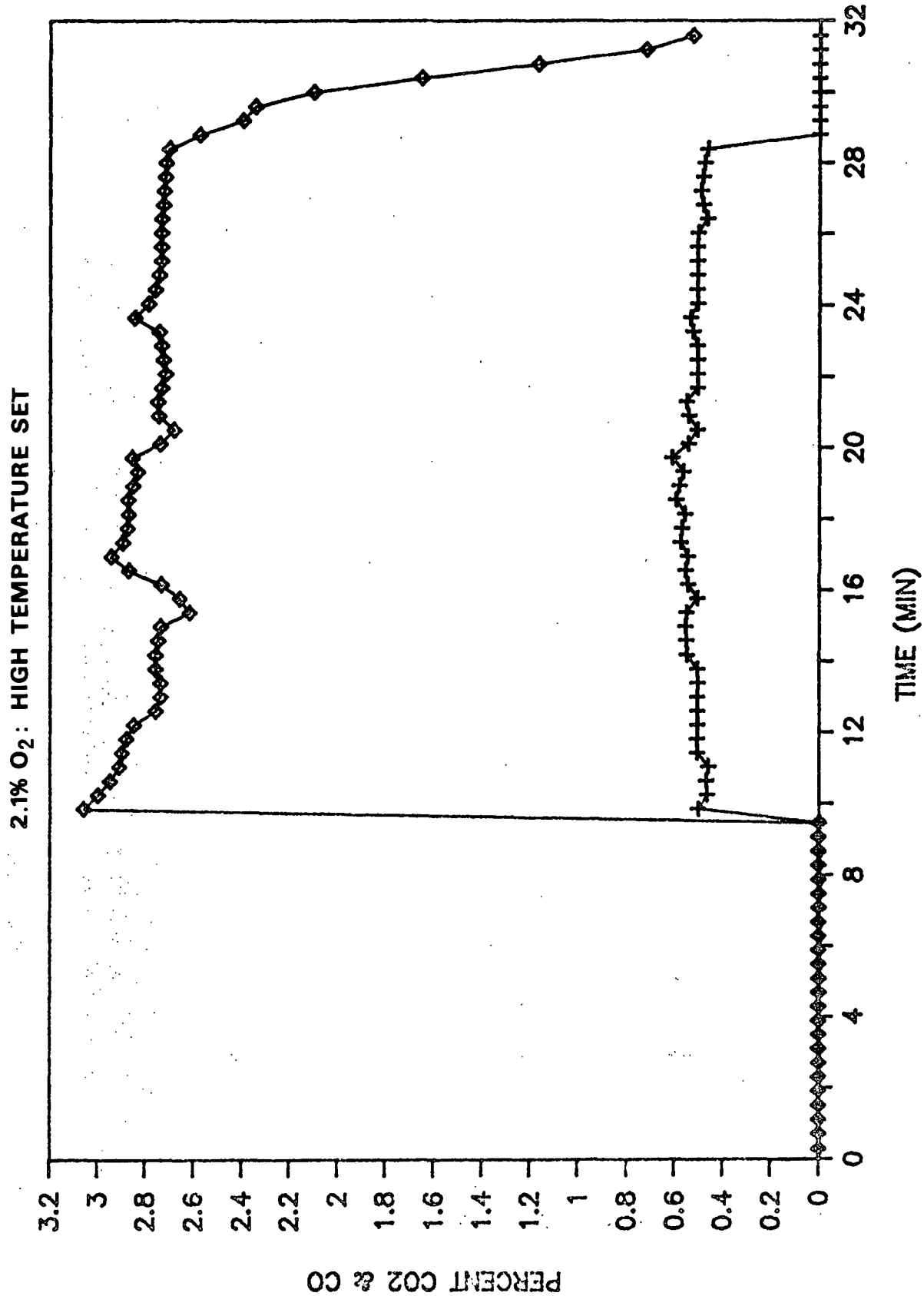

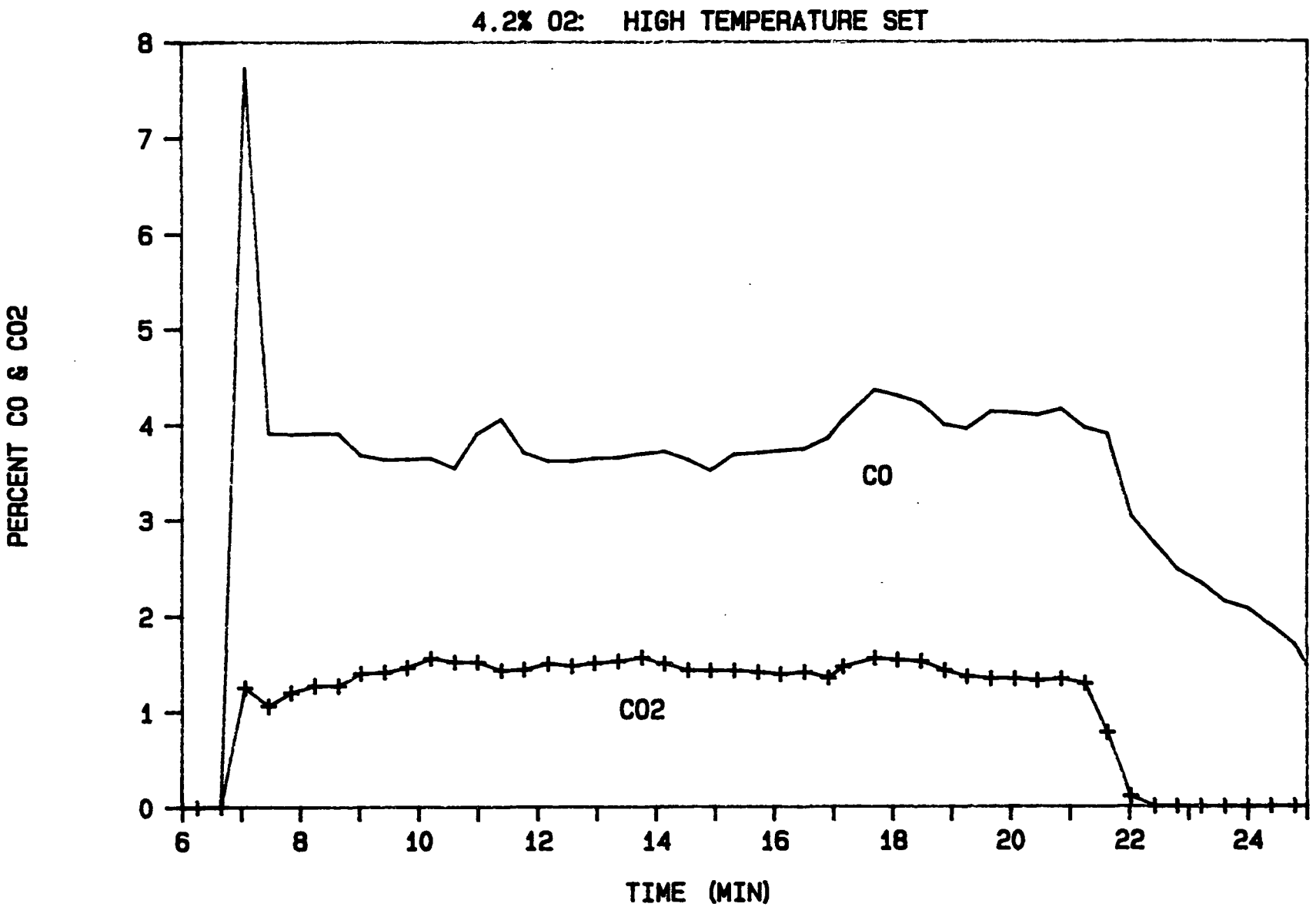

Experiment 49

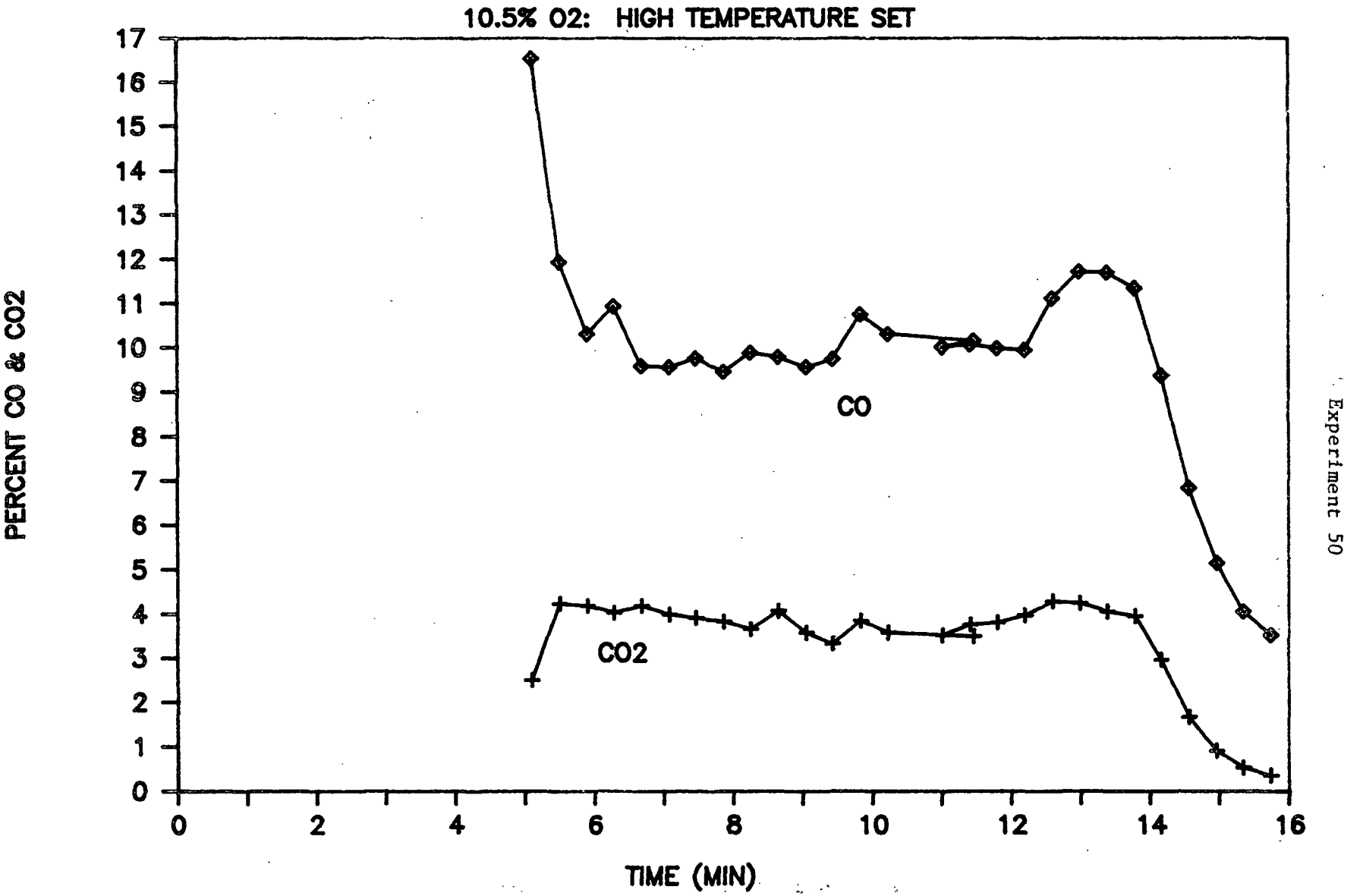

Experiment 50

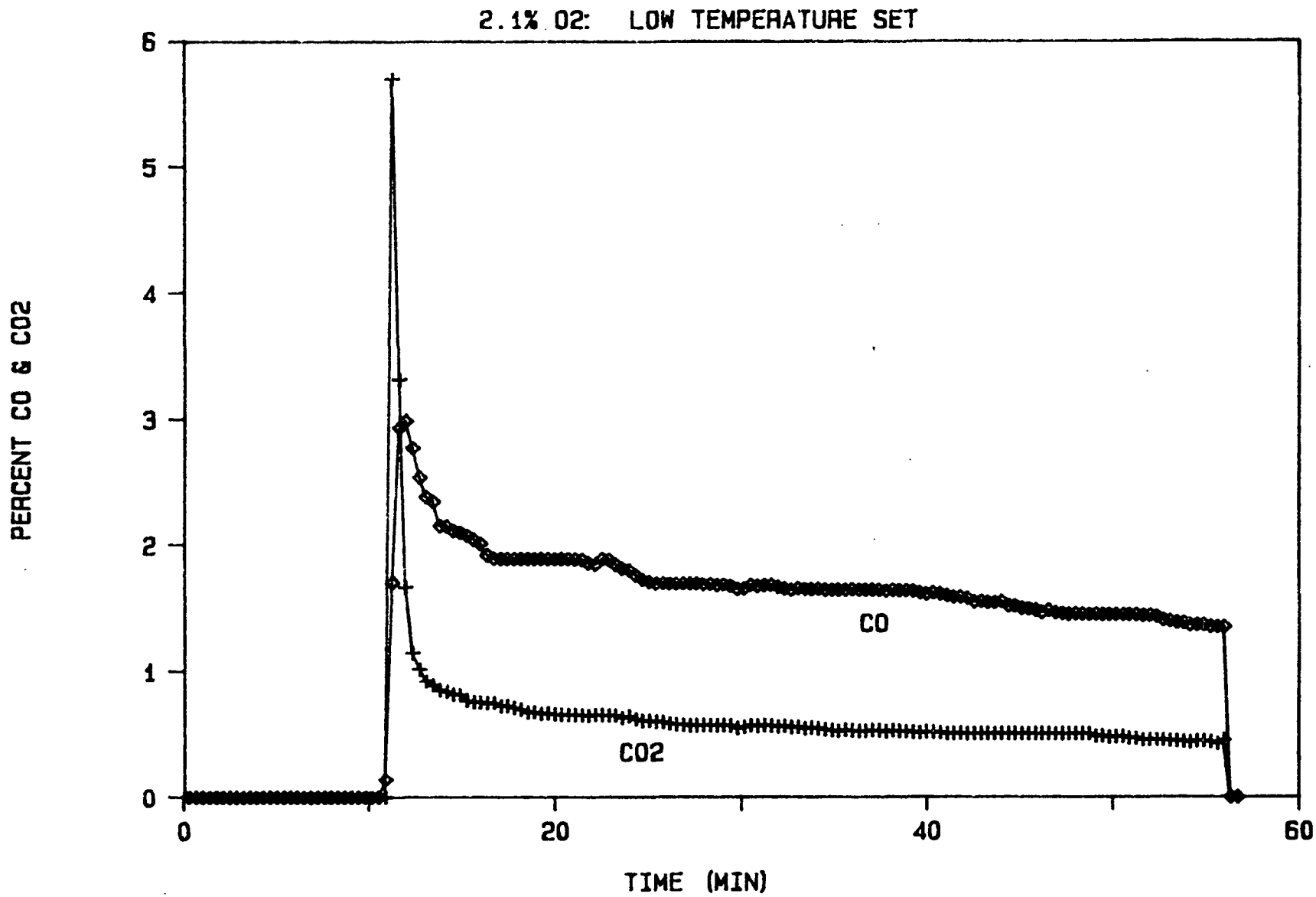

Experiment 51

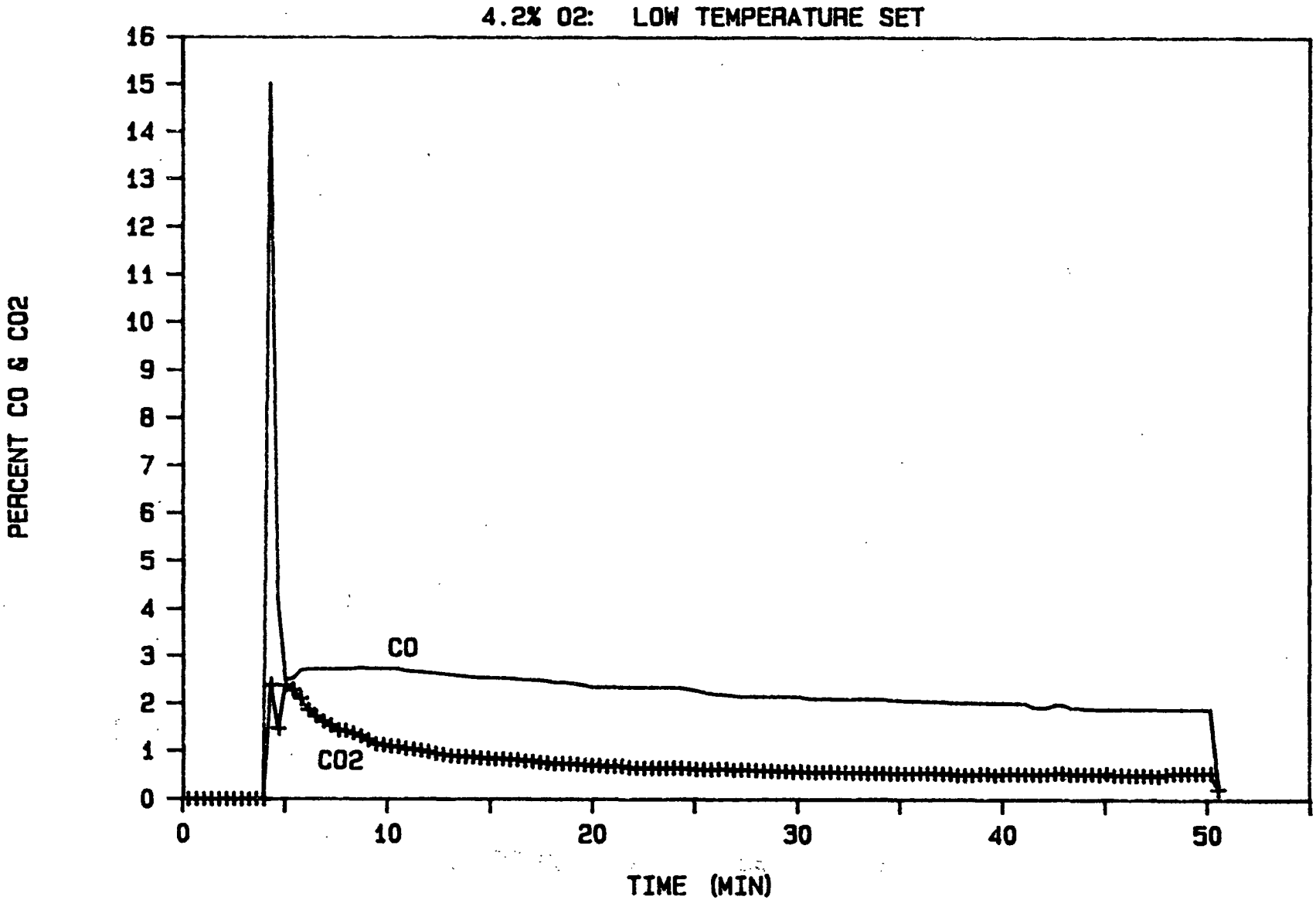

Experiment 52

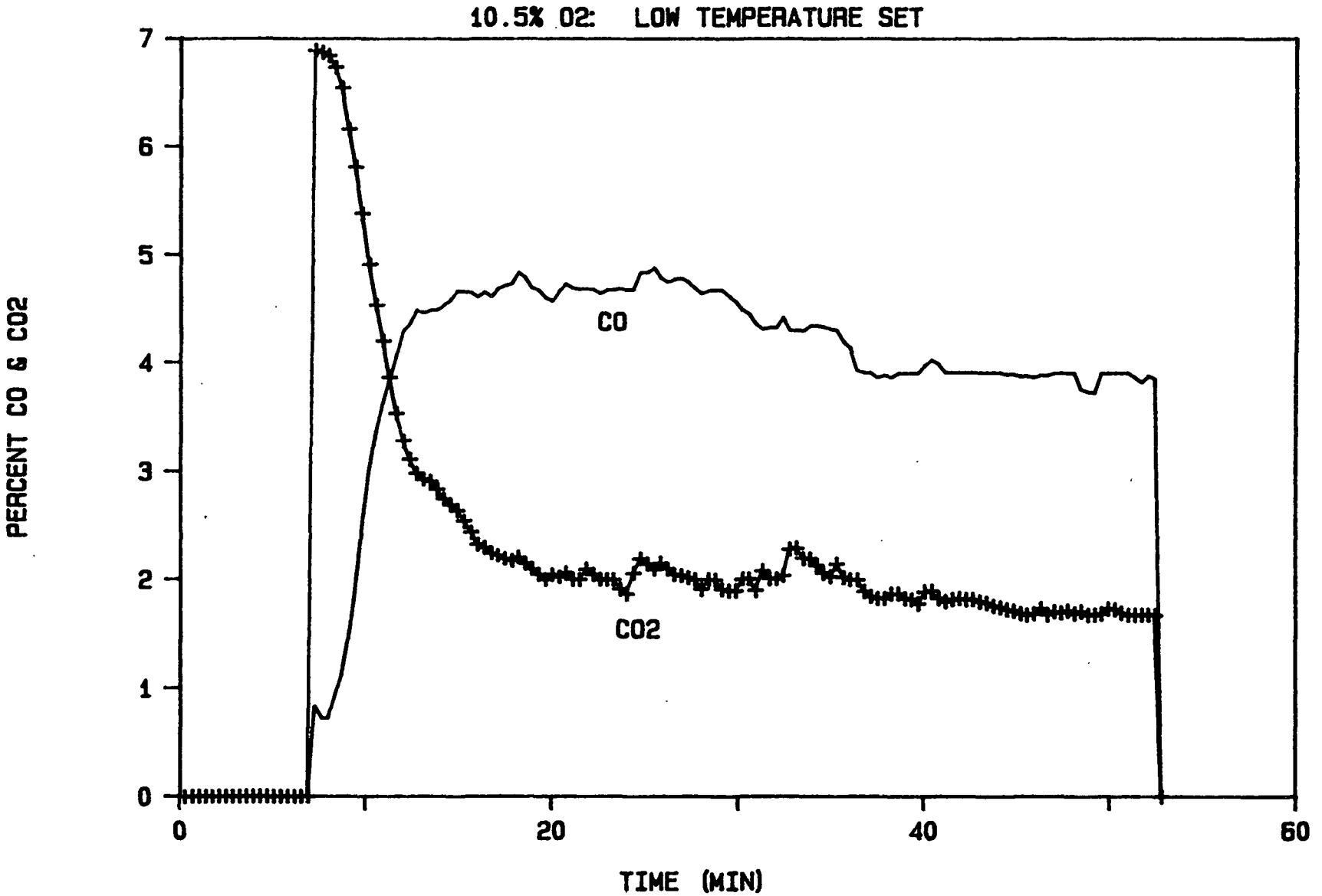

Experiment 53

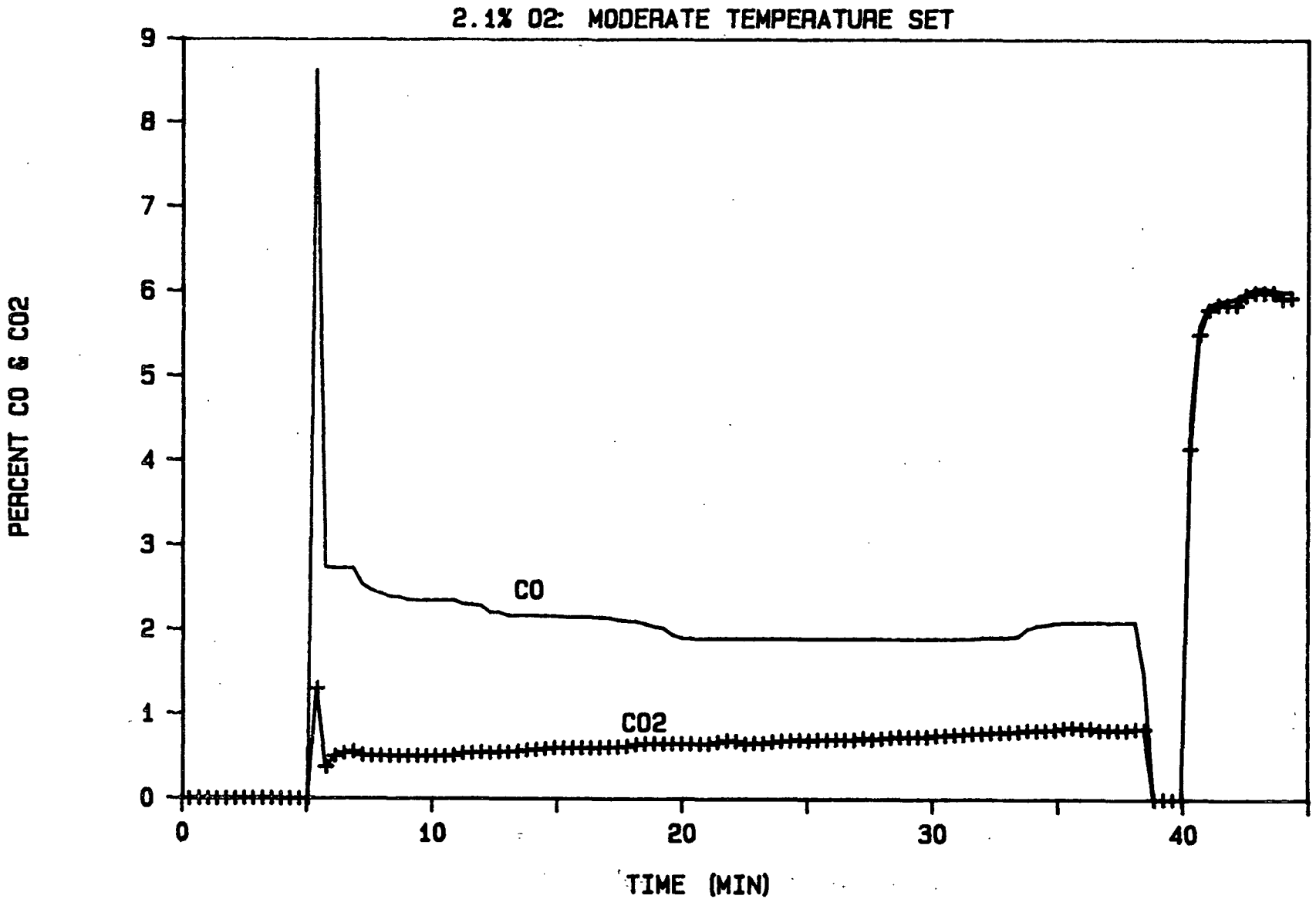

Experiment 54

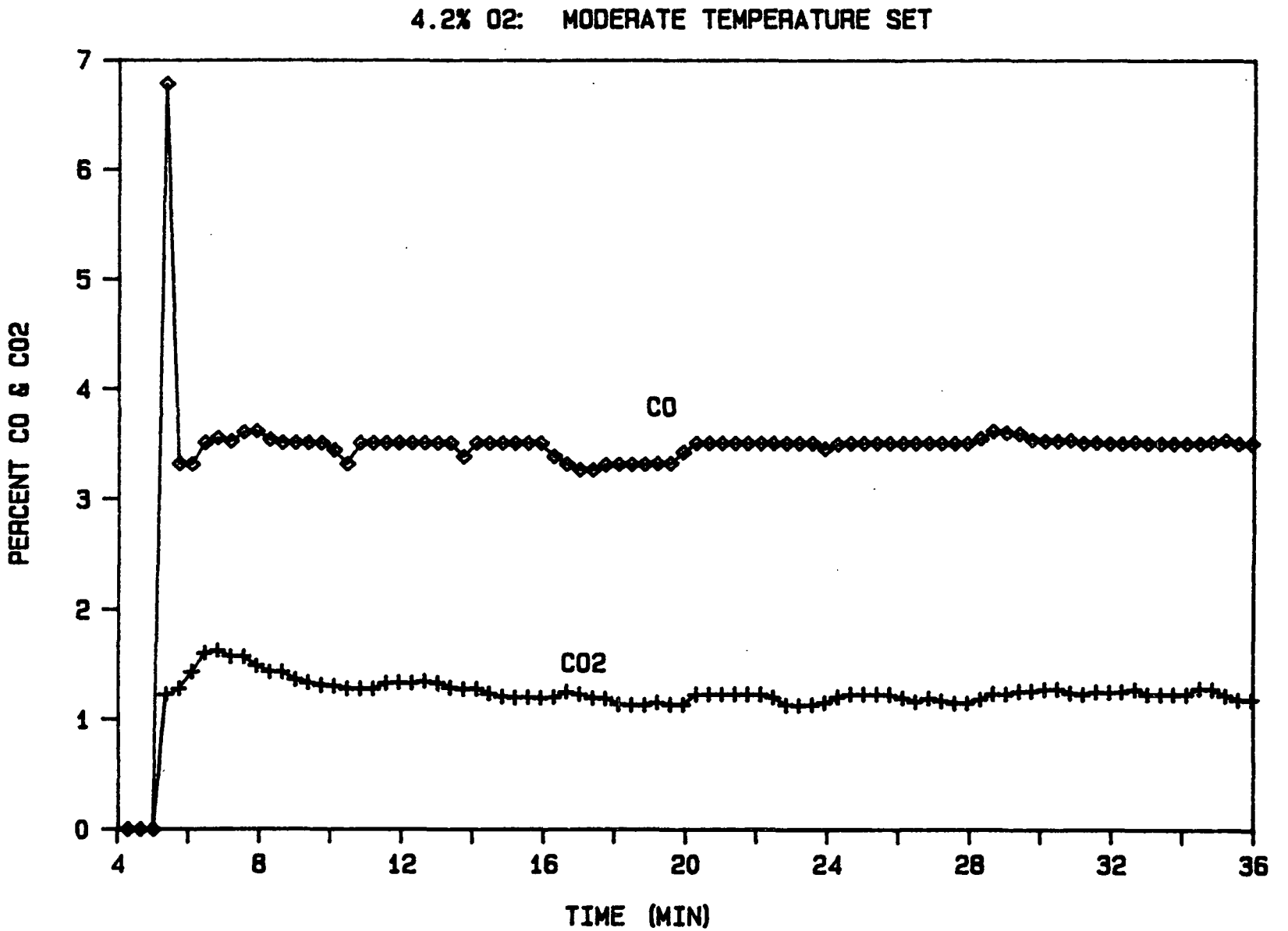

Experiment 55

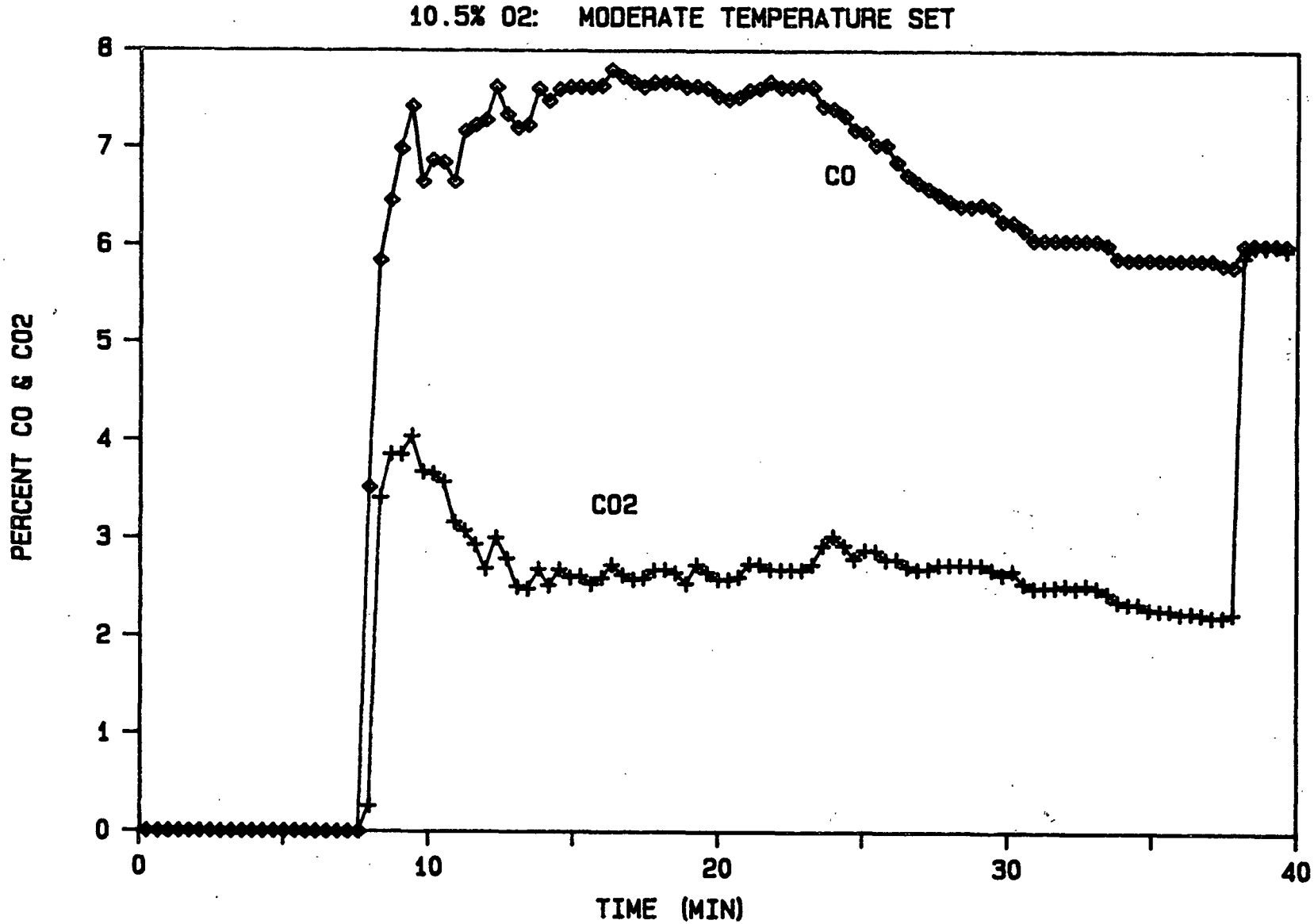

Experiment 56

APPENDIX XIV

DETERMINATION OF THE CARBON CONCENTRATION UPON WHICH TO BASE THE REACTION RATE CALCULATIONS FOR KINETICALLY-LIMITED CONDITIONS

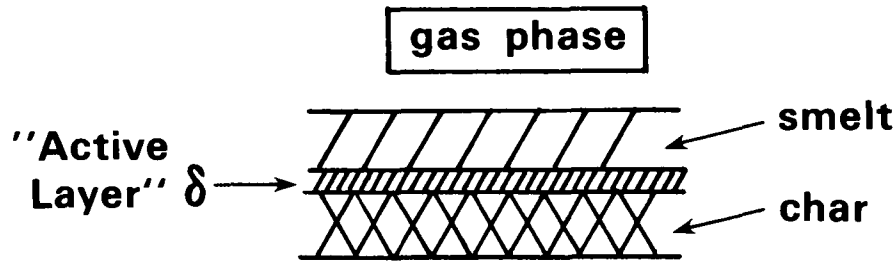

Boundary Conditions

1. The smelt carbon concentration = 0. This is based on measurements of less than 1% carbon for all smelt samples.

2. The char carbon concentration = 24%. This is based on carbon concentration measurements of char samples.

Assumptions

1. There is sufficient oxygen supplied to the system so that the carbon-sulfate reaction rate is controlled by carbon-sulfate kinetics, exclusive of the sulfate-dependent terms:

$$-\frac{d[SO_4]}{dt} = \frac{k_1}{k_4}[C]\ \exp\left(-\frac{Ea}{RT}\right) \qquad (14)$$

2. Temperature is constant throughout the active layer, δ.

$$-\frac{d[SO_4]}{dt} = k'[C]$$

3. Steady-state conditions are achieved - the char burning rate is constant. Therefore a constant relates the carbon-sulfate reaction rate to the char burning rate.

$$\frac{d[C]}{dt} = k''[C]$$

The average rate of reaction, $\hat{r}$, in the active layer is therefore:

$$\hat{r} = \frac{\int r dC}{\int dC} = \frac{\int k'' \, C \, dC}{\int dC}$$

$$= \frac{k''C^2}{2C} \Bigg|_0^{0.24} = k'' \, (0.12)$$

The carbon concentration to use in calculating the average rate of reaction is therefore 12%.

APPENDIX XV

KINETIC MODEL CALCULATIONS

Active layer volume, V:

$$V = \frac{\pi D^2}{4} h \tag{26}$$

where D = crucible diameter = 4.15 cm

h = depth of active layer = 0.1 cm

$V = 1.353 \times 10^{-3}$ L

Carbon concentration, [C]:

$$[C] = \frac{W_c \rho_T}{MW} \tag{27}$$

where W_c = wt.% C = 12%

ρ_T = active layer density = 12 moles/L

MW = molecular wt. of C = 12 g/mole

Therefore:

$$[C] = 12 \text{ moles/L}$$

Reaction rate at 1042°K, r, from Eq. (15):

$$r = 4V \frac{k_1}{k_4} [C] \exp\left(-\frac{Ea}{RT}\right) \tag{15}$$

with $k_1 = 5.96 \times 10^4 \frac{L}{\text{mole-sec}}$

$k_4 = 45.6$ L/mole

Ea = 30.0 kcal/mole

Therefore:

$$r = 3.82 \times 10^{-3} \text{ moles/min.}$$

APPENDIX XVI

CALCULATION OF THE REDUCTION RATIO AT THE CHAR/SMELT INTERFACE

The calculation of the reduction ratio at the char/smelt interface for the kinetically-limited conditions was based on the following assumptions.

1. The average carbon concentration of the interface was 12% (by weight). See Appendix XIV for this calculation.

2. The remaining 88% of the composition was inorganic salts.

3. Na_2CO_3, Na_2SO_4, and Na_2S were the only inorganic salts present.

4. The sulfidity, s, was 0.30.

$$s = \frac{Na_2S + Na_2SO_4}{Na_2S + Na_2SO_4 + Na_2CO_3} \tag{28}$$

5. The molar ratio of C/SO_4 was 36/1, as suggested by the CO/CO_2 product of the carbon-sulfate reaction studies.

Basis: 100 grams of interfacial material

	Weight Percent	Moles
C	12	1
Na_2S	X	X/78
Na_2SO_4	Y	Y/142
Na_2CO_3	Z	Z/106
Total	100	T

From Mass Balance: $X + Y + Z = 88$

or $X = 88 - Y - Z$ (29)

From Sulfidity = 0.30 $\quad \frac{T - 1 - Z/106}{T - 1} = 0.30$

or $\quad Z = 0.7\ (106)\ (T-1) = 74.2\ (T-1)$ (30)

with $\quad T = X/78 + Y/142 + Z/106 + 1$ (31)

From the C/SO_4 of 36/1: $\quad Y/142 = 1/36$ or $Y = 3.94$

The solution of X = 13.56, Z = 70.50, T = 1.95 was obtained by iteration, guessing T, then calculating Z using Eq. (30), then calculating X using Eq. (29), then determining T using Eq. (31).

The reduction ratio calculated is then: $X/(X + Y) = 0.77$.